Synthesis and Characterization of Polymeric Pore Former Microspheres using Modified Polymer Resin

Ransford Damptey

North Carolina A&T State University

A dissertation submitted to the graduate faculty

In partial fulfillment of the requirements for the degree of

DOCTOR OF PHILOSOPHY

Department: Joint School of Nanoscience and Nanoengineering

Major: Nanoengineering

Major Professor: Dr. Ram Mohan

Greensboro, North Carolina

2022

The Department of Energy's Kansas City National Security Campus is operated and managed by Honeywell Federal Manufacturing & Technologies, LLC under contract number DE-NA0002839

The Graduate College
North Carolina Agricultural and Technical State University

This is to certify that the Doctoral Dissertation of

Ransford Damptey

has met the dissertation requirements of
North Carolina Agricultural and Technical State University

Greensboro, North Carolina
2022

Approved by:

Dr. Ram Mohan
Major Professor

Dr. Sabrina Torres
Committee Member

Dr. Ajit Kelkar
Committee Member

Dr. Jeffrey Alston
Committee Member

Dr. Taher Abu-Lebdeh
Committee Member

Dr. Clay S. Gloster, Jr.
Dean, The Graduate College

Dr. Jingsheng Xu
Graduate Faculty Representative

Biographical Sketch

Ransford K. Damptey grew up in Accra, capital of Ghana, West Africa. Ransford had his primary education in Ghana (K through 12), before moving to the United States to join his family nd his education. Interested in pursuing a career in engineering academia, Ransford pursued a Chemical Engineering degree at North Carolina State University while actively involved in research. Ransford decided to take a gap year teaching Mathematics at Welborn Academy of Science and Technology before returning to graduate school at North Carolina Agricultural and Technical State University to pursue a Master's degree in Chemical Engineering. During his first year of graduate school with the Chemical Engineering department, Ransford was a teaching assistant and a research assistant during his second year as a graduate student with the Civil Engineering department. Ransford obtained his M.Sc. in Chemical engineering in 2018 and is currently pursuing his doctorate in Nanoengineering.

Dedication

Dedicating this to my mother. Love you!

Acknowledgments

I would like to acknowledge my advisors Dr. Ram Mohan and Dr. Sabrina Torres, whose wisdom, direction, and instruction have been invaluable. I would also like to thank Dr. Taher Abu-Lebdeh, my advisor for my Master's Thesis, who continues to be as supportive. Furthermore, Drs. Jeffrey Alston and Ajit Kelkar have been instrumental right from the proposal defense process. I am also grateful for my technical mentor at Kansas City National Security Campus (KCNSC), Laura Cummings, who has been helpful and supportive on multiple levels of my research journey. I am very grateful for having Dr. Thomas Robison from KCNSC who always provides a listening ear and offers technical advice whenever needed. I would also like to acknowledge my former manager at KCNSC, Dr. Jacqueline Rankin, for her contribution and the Ultrasonic Spray Pyrolysis work she pioneered. I thank my current manager, Dr. Marie LaGasse, who provided constant constructive feedback on my work during the summer of 2022. To Connor Pearson, Henry Pearson, Jackson Ham, John Daye, Steven Patterson, Zachery Peacock, and the entire D-896 department at KCNSC, I would like to thank you for allowing me to work with you. The Minority Serving Institutions Partnership Program (MSIPP) program has been instrumental in exposing me to national laboratories, renowned professionals, mentorship on several levels, and scholarships toward my master's and doctorate degrees. I am highly grateful for all of it. My colleagues at KCNSC and JSNN have been supportive, as we have encouraged each other to keep pushing through the setbacks of COVID-19. My friends, family and church family have all been a critical part of this process, as they have helped keep me sane and grounded through it all. Thank you!

The Department of Energy's Kansas City National Security Campus is operated and managed by Honeywell Federal Manufacturing & Technologies, LLC under contract number DE-NA0002839

Table of Contents

List of Figures

List of Tables

Abstract

Porosity in polymer parts is often desired to improve mechanical properties. Individual pores must be small enough that bulk mechanical properties are retained but significant enough to reduce the density of the material. Filler materials can be incorporated into polymer matrices and subsequently removed to create voids. The materials used to create the voids are known as pore-formers. The present research aims to create spherical pores in a silicone matrix by inserting and removing core materials or fillers post-cure. A method was developed to incorporate pore formers into an uncured polymer resin and remove the materials from the matrix. Polyethylene Glycol (PEG) and Polylactic Acid (PLA) microspheres are created and incorporated into silicone matrices as pore formers. Microspheres with controllable size distributions are formed via ultrasonic spray pyrolysis and emulsion formation. Microspheres are removed from the matrix by solvent extraction and calcination. PLA microspheres were modified by hydroxyl addition to the surface to study their solubility in water. PEG-PLA block copolymers are also synthesized and investigated, comparing their physical and chemical properties to the monomers to identify whether the block copolymer microspheres will be more easily removable than their monomeric microspheres. Moreover, other properties including thermal stability, rheology, and mechanical response are studied. The present dissertation provides a comprehensive understanding of the synthesis and characterization of PEG and PLA-based pore formers, toward the future development of feedstock for additive manufacturing porous structures.

CHAPTER 1

Introduction

Polymers are a class of macromolecules that have existed from the inception of life on the planet (e.g., carbohydrates) and continue to evolve into more complex forms [1]. Polymers exist in natural and synthetic forms, primarily characterized by long-chain repeat units of monomers. Over the last century, polymers have evolved from cheap plastics to key manufacturing components across various fields, from the automotive industry to pharmaceuticals [2, 3]. Polymers can be synthesized and controlled to have the desired properties for specific applications while exhibiting properties superior to that of classical materials such as glass, wood, and metals [4, 5]. Among the various forms of polymers, the present work focuses on polymeric foams.

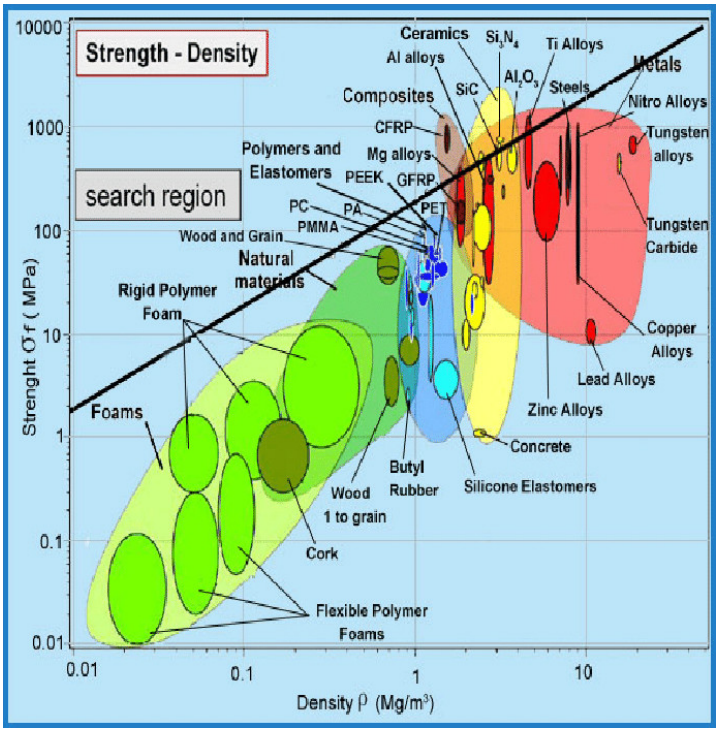

Figure 1. Strength vs. Density of various material classes [6].

Polymeric foam materials are prevalent in several applications and serve various functions notably in machine systems including the distribution and relieving of stress, mitigating effects of shock and vibration, accommodating dimensional changes caused by thermal variations, and maintaining the position of surrounding parts by applying the appropriate spring force [7-10]. Foams made from polysiloxanes are particularly interesting due to their relatively high thermal stability and chemical resistivity. Traditionally, siloxane pads and cushion materials have been molded similarly to many other materials [11, 12]. However, there has recently been shift to additive manufacturing to control mechanical properties. Even with the varied options for direct ink write lattice structures, the desired density and stiffness are not always achievable by changing the print structure alone. With the shift to additive manufacturing processes where 3-D structures are built layer by layer with each layer being 200 microns or less [13], there is a need for pore formers with average sizes in the range of 5-100 microns. This size range is consistent with the strand size and small enough not to contribute to clogging issues during printing. Polymeric spheres on the micron scale (otherwise known as microspheres) are potential candidates for this objective. Another requirement is suitable matrix materials compatible with the pore formers. Polymer matrix materials are being considered to embed the pore formers in a compatible polymer matrix and remove the pore formers during processing, thus resulting in porous structures. A fundamental material and process understanding of the pore former and polymeric matrix materials is needed and is focused on the present work. A polymer matrix of interest is polydimethylsiloxane (PDMS). PDMS is a commonly used polymer in several applications. It possesses unique properties such as thermal stability, low glass transition temperature and high chemical resistance [14], making it a choice material for direct ink-write applications.

1.1 Research Problem – Significance and Relevance

Pore former materials can be embedded in polymer matrices and removed during post-processing, resulting in the formation of porous structures. Pores in polymeric foams control the physical and mechanical properties such as the density and yield stress. Chemical blowing agents are typically used for creating irregularly shaped cellular structures. There are applications, however, that require well-defined pore structures, in which case pore formation via chemical blowing agents may not be ideal. Removable polymeric microspheres as pore formers, unlike chemical blowing agents, provide the option of having good control over the size, shape, and porosity of polymer parts, with the added benefit of repeatability in pore formation. However, polymeric microspheres are not readily available, and methods to prepare them are not always intuitive. A repeatable method for making microspheres that fall within the desired size range must be developed to ensure that the process for synthesizing microspheres can be scaled successfully. Developing a process for making polymeric microspheres that act as pore formers in a polymer matrix would allow for porous structures that are more controllable in the porosity distribution. The density reduction of materials from void creation can be predicted more quantitatively by identifying the mass fraction of pore formers to incorporate into the polymer matrix before curing. Pores created in this manner can be more evenly distributed, each with similar morphology. The pore former microspheres can also be loaded into a direct ink-write polymer ink for 3-D printing applications, given that the microsphere sizes will be smaller than the thickness of each printed layer.

Polylactic acid (PLA) and polyethylene glycol (PEG) emerge as forerunners among polymers that can be used to form microspheres. Polylactic acid and polyethylene glycol are biocompatible and used in various biologically related applications, notably drug delivery and

drug encapsulation. Such characteristics makes PLA and PEG biologically inert. PLA is also biodegradable, and PEG is chemically inert. PLA and PEG can be dissolved easily in organic solvents, and bulk PLA and PEG can be converted into particles with varying morphologies (microspheres, nanoparticles, etc.). Physical properties of PLA and PEG, such as melting temperature, can also be altered, given the appropriate chemistries. PLA and PEG can also form amphiphiles since they are hydrophobic and hydrophilic respectively. Diblock and triblock copolymers consisting of PLA and PEG can be formed, further allowing for other applications that benefit from the hydrophilic and hydrophobic block(s) [15].

1.2 Research and Dissertation Focus

The present research and dissertation focus on synthesizing and characterizing PLA and PEG-based pore formers. Key contributions and findings include:

- Developed a method of modifying PLA to make it easily removable from a matrix. Investigations focused on:
    - Surface modification
    - Block Copolymerization
- Demonstrated synthesizing solid and core-shell microspheres with a narrow size distribution efficiently using methods such as Ultrasonic Spray Pyrolysis, bulk emulsion process, etc. The present research focused on the following:
    - Solid Polylactic acid (PLA) microspheres
    - Solid modified PLA microspheres
    - Solid PEG microspheres

- Creating porosity in a silicone matrix and porous silicon material structures through
    - Pore formers:
        - Solid PEG microspheres
        - Solid PLA microspheres
        - Modified PLA
    - Pore removal
        - Calcination
        - Water bath Sonication
        - Solvent extraction
- Analysis and Characterization of Synthesized Materials:

Research investigations studied extensively material characteristics, and their analysis, including before and after microstructures after the removal of pore-formers through characterization techniques including:

- Imaging: Optical Microscope, scanning electron microscope (SEM), to obtain information on morphology and size of particles.
- Particle Size Analysis with the Malvern Instrument and/or microscopy images to analyze the particle size distribution of pore former materials.
- Fourier Transform Infrared Spectroscopy (FTIR) and Nuclear Magnetic Resonance (NMR) for chemical identification

- Thermal Analysis (Thermogravimetric Analysis (TGA), Differential Scanning Calorimetry (DSC)) to assess particles' decomposition profile and heat flow profile respectively.
- Rheology characterization to analyze changes when adding microspheres to uncured resin is an essential consideration for feedstock in additive manufacturing porous structures.
- Dynamic Mechanical Analysis (DMA) studied the changes in mechanical properties of cured materials, with and without porosity.

1.3 Microsphere Formation

This section addresses the methods used for polymer microsphere formation including the factors that inform each synthesis pathway. The polymer must be dissolved in a solvent prior to the microsphere process, and as such, solvent selection is the first step to making microspheres. Microspheres were prepared primarily by two methods, namely Ultrasonic Spray Pyrolysis (USP) and Single Emulsion method.

1.3.1 Polymer Solubility

The solubility of precursor solution is very crucial to any synthesis process. Uniform dispersion of the precursor molecules ensures that similar properties of the microparticles are formed after the curing process. The precursor solution comprises the material (in our case, polymer) we wish to synthesize microparticles out of and the solvent. This solution is atomized at ultrasonic frequencies in the Ultrasonic Spray Pyrolysis process. As a result, the choice of solvent for this process is important. The precursor solution's atomization depends on its

concentration and chosen solvent. In a multiphase system with more than one precursor, a solvent that selectively dissolves each precursor material must be identified and selected for solubilizing each component of the system. For example, researchers identified toluene as a solvent that can dissolve both polydimethylsiloxane (PDMS) and polyethylene glycol (PEG) and, as such, can be used as the solvent of choice in making PDMS-PEG core-shell microspheres [14, 16]. In Currie et al., it was discovered that in a di-block copolymer system, when the solvent chosen dissolves only one polymer and not the other, the polymer tends to form micelles, resulting in very inhomogeneous structures [17].

Following the prior literature, the present research investigated potential solvents that can observably solubilize the precursors and were selected as the media for the microsphere formation process. These solvents are identified by conducting a simple solubility test. Small amounts of the candidate precursor are added to small amounts of various solvents to determine whether they will dissolve. Tabulated results from these studies are included and discussed in Chapter 3 of this document.

1.3.2 Emulsion Formation

An emulsion is achieved by mixing two immiscible liquids in equilibrium, most commonly an oil and water phase [18]. These systems are not spontaneous and are thermodynamically unstable. The system separates into two phases when two immiscible liquids are added together. The lighter-density oil phase remains above the settled higher density water phase for water and oil. These systems can be engineered and varied to have various properties. High shear mechanical mixing, for instance, can be introduced into the system to break up the phases, but upon reaching thermodynamic equilibrium, the phases separate once more. However,

a third phase (amphiphile) can be introduced into the system to stabilize it. The amphiphiles (known as emulsifiers) may significantly decrease the interfacial tension of the two liquids, leading to mixing and ultimately stabilizing the system [18]. For a stabilized emulsion system, there is always a bulk and a dispersed phase. The dispersed phase is always distributed "in" the bulk phase. Emulsions can also be categorized as macroemulsions or microemulsions based on the size of the droplets formed.

1.3.2.1 Single Emulsions

Emulsions, whereby only two phases exist, are called Single Emulsions. There are generally two types of single emulsions: water-in-oil (W/O) and oil-in-water (O/W). "Single emulsions" are so termed because the systems comprise a single dispersion and bulk phases. Single emulsion systems can be created in a straightforward approach that has been implemented in various applications, from pharmaceuticals to drug delivery applications. Figure 2 below is a graphical depiction of a single emulsion process.

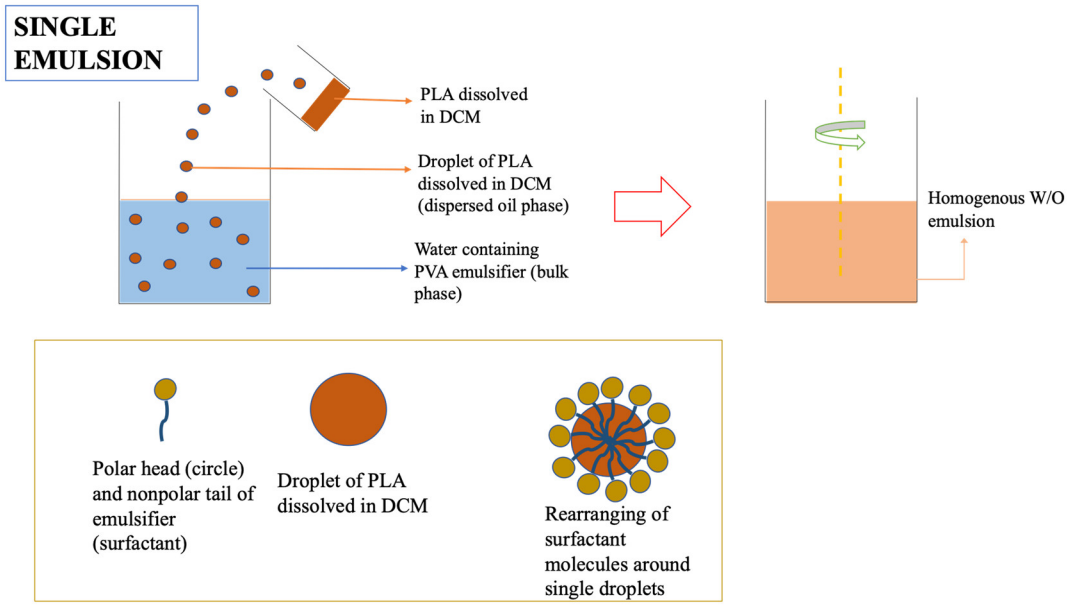

Figure 2. Single Emulsion Formation

The present work focused on the formation of macro- and microemulsions. For microemulsions, emulsifiers are generally used as surfactants [18]. Figure 3 highlights some examples of microemulsions. The parameter *g* is a geometric parameter, describing the size of the polar region of the stabilizing amphiphile. When $g>1$, the micelles present are reverse micelles.

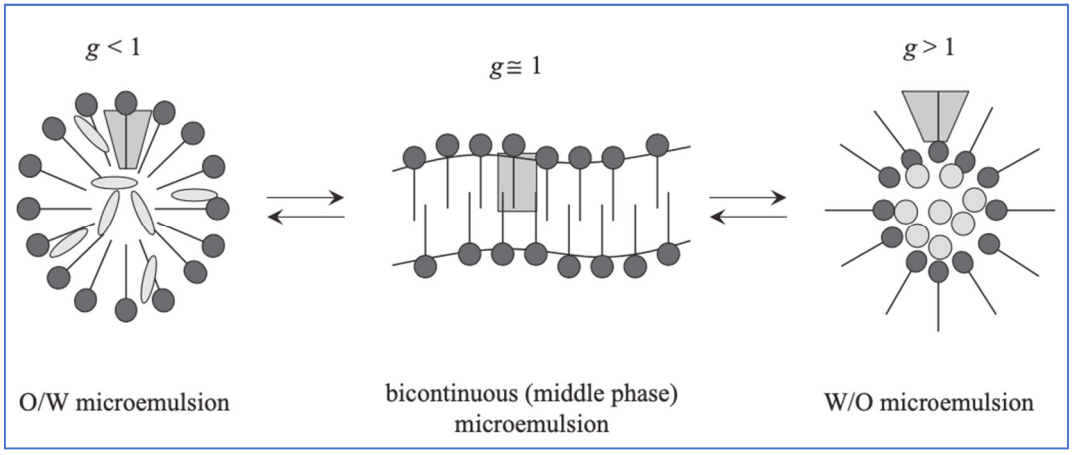

Figure 3. Consideration of packing geometry for the formation of microemulsions. [18]

Emulsions (particularly O/W emulsions) have been used to form polymeric micro- and nanoparticles [18-20]. The oil phase typically consists of the polymer(s) dissolved in the appropriate solvent, and the aqueous phase contains the emulsifier. In the case of drug delivery, the oil phase also contains the drug to be encapsulated. The oil phase is then dispersed into the aqueous phase and stirred. The mixture is then heated to evaporate the solvent, and the micro- or nanoparticles are formed. As a general rule of thumb, the solvent of the polymer has to be immiscible with the emulsion solvent, and its boiling point has to be lower than that of the emulsion solvent to ensure complete evaporation [21]. This process is generally called the emulsification solvent evaporation method. Instead of evaporation, the solvent may be removed either by extraction [16] or dialysis [22]. The drug is encapsulated after the solvent has evaporated for drug delivery applications.

In some cases, the particles are obtained by freeze dehydration [22] or spray drying for large-scale processes [19]. In other instances, after evaporation of the solvent, more water may be added to the mixture under constant stirring to harden the particles being formed [21]. Particles may be separated from the mixture by filtration (for microparticles) or centrifugation (for both micro- and nanoparticles).

The emulsion solvent evaporation method has been used in making micro- and nanoparticles of PLA and copolymeric versions of PLA [20-22], mainly for drug delivery applications. In most of these applications, polyvinyl alcohol (PVA) is used as an emulsifier in the aqueous phase of the emulsion. However, it may be replaced with other materials to enhance the biocompatibility and efficiency of the drug delivery process [19]. This method was explored in the present work, as it appears to be straightforward, and materials are available.

1.3.2.3 General Synthesis Considerations

An essential aspect of emulsion formation is the mechanism of mixing. The bulk and dispersed phases are generally known beforehand. Depending on the system, the surfactant/emulsifier is also chosen [23]. The mixing mechanism chosen, however, is dependent on the mixing time, the desired particle size and size distribution, and the viscosity of the phases present. Higher mix speeds generally produce smaller particle sizes and narrower size distributions [24]. High shear mixing leads to the formation of microspheres within a matter of minutes [25]. Magnetic stirrers can generate relatively small particles but may not be as efficient in generating a narrow distribution and do not constitute a high amount of shear mixing. Overhead mixers provide high shear and mix speeds, but too high speeds may destroy the morphology of the formed particles in the emulsion. On the other hand, Planetary mixers can form emulsions within a short time with a

narrow size distribution and operate at high speeds without added shear that may deform the formed particles.

1.3.3 Ultrasonic Spray Pyrolysis

According to the International Union of Pure and Applied Chemistry (IUPAC) Compendium of Chemical Terminology, pyrolysis is the thermal decomposition of materials at elevated temperatures in an inert atmosphere. When the material undergoing thermal decomposition is an aerosol, the process is termed spray pyrolysis. Spray Pyrolysis can be a continual process, making it a preferred method for synthesizing nanoparticles and thin films [26]. Spray Pyrolysis is widely used in producing films and powders [27]. Several spray pyrolysis techniques vary by the nebulization method, as shown in table 1. Generally, for spray pyrolysis, the droplets are created from a precursor solution, which contains material(s) to be thermally decomposed. Spray pyrolysis has been used to synthesize porous, solid, and core-shell organic and inorganic materials [6]. (For more details on materials and compounds made via spray pyrolysis, please refer to [6] and the references therein). However, spray pyrolysis is not to be confused with ultrasonic spray pyrolysis (USP), where the materials, though also subjected to elevated temperatures, do not undergo thermal decomposition. The high-temperature environment in USP is used to cure the polymers, thereby solidifying them. In USP, ultrasonic nebulization is used for droplet creation due to the narrow distribution and droplet size. A direct correlation exists between the droplet size and particle size via the equation

$$D_p = \left(\frac{M D_d^3 C}{100 \rho_p}\right)^{\frac{1}{3}} \quad (1)$$

where D_p is the average particle diameter, D_d is the average droplet diameter, M is the molecular weight of the precursor, C is the concentration of the precursor, and ρ_p is the product density [28].

Ultrasonic Spray Pyrolysis (USP) is a novel method used to synthesize fine powders in the industry [29]. Compared with other manufacturing and synthesis approaches, such as chemical vapor deposition (CVD), USP is a more efficient and controllable way of producing micro and nanoparticles with a narrow size distribution. USP processes can also occur under ambient temperature conditions and do not require a vacuum.

Table 1.

Nebulization methods commonly used in spray pyrolysis. [14]

Nebulization Method	Average Droplet Diameter (µm)	Droplet Size Distribution	Gas Flow Rate	Droplet Delivery Rate
Jet	10-1000	Broad	Low	High
Air-assisted	<1000	Broad	High	High
Rotary	10-1000	Broad	Low	High
Electrostatic	0.01-1000	Very Narrow	Low	Low to High*
VOAG	20-400	Very Narrow	Low	Medium
Ultrasonic (Nozzle)	10-1000	Medium	Low	Medium
Ultrasonic (Submerged)	1-10	Narrow	Low	Medium

*Small size has low delivery rate, large size has high delivery rate
**VOAG: vibrating orifice aerosol generator

In USP, droplets from a precursor solution are created by ultrasonic atomization using a piezoelectric transducer. The precursor solution is usually prepared at < 20wt.% of precursor to solvent ratio. The ultrasonic nebulizer is submerged in the liquid, operating at frequencies

between 1.6MHz and 2.4MHz [14]. Figure 4 schematically illustrates a lab-scale USP setup employed in the present study.

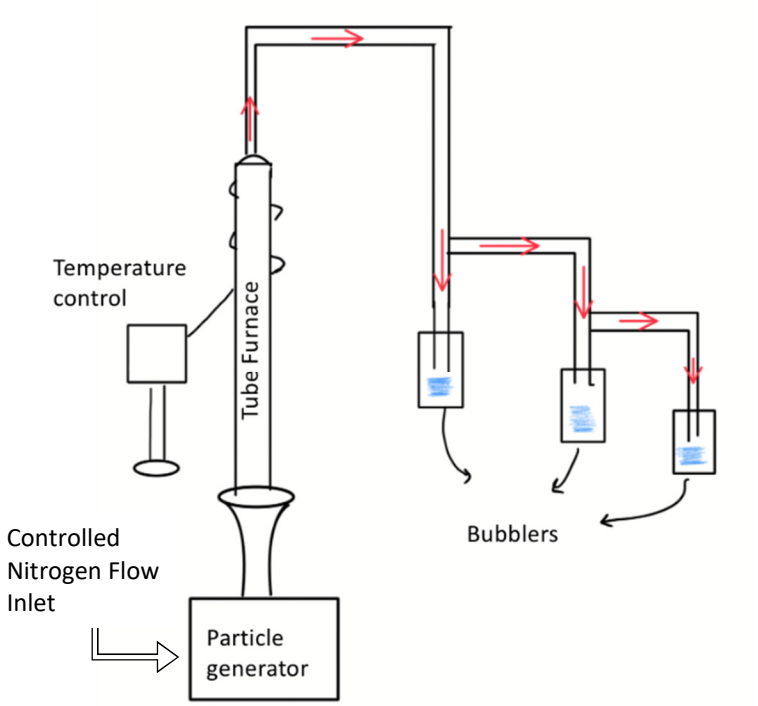

Figure 4. Ultrasonic Spray Pyrolysis – Lab setup.

In ultrasonic spray pyrolysis, the materials do not undergo decomposition in the furnace. The solvent in each droplet is evaporated, leaving the remaining solid polymer material. Each droplet acts as a reaction vessel, preventing agglomeration and coalescence. The droplets are cross-linked and densified in the furnace, forming cured solid particles [14]. The particles are then collected in bubbler tubes and later separated from the solution by centrifugation, filtration, or other separation mechanisms. Core-shell architectures can form when a nebulized solution contains more than one precursor and phase separation occurs [14].

Figure 5 illustrates a setup from the literature that employed a variation of USP setups to improve throughput and to create core-shell structures. A USP setup with two separate gas inlets and two furnaces was used by Košević et al. to reduce Platinum in forming Pt/TiO2 core-shell

powders [30]. In another research, two atomizers, each with its oxygen gas inlet, were incorporated into the ultrasonic spray pyrolysis setup to optimize the synthesis of TiO_2/RuO_2 core-shell particles [31].

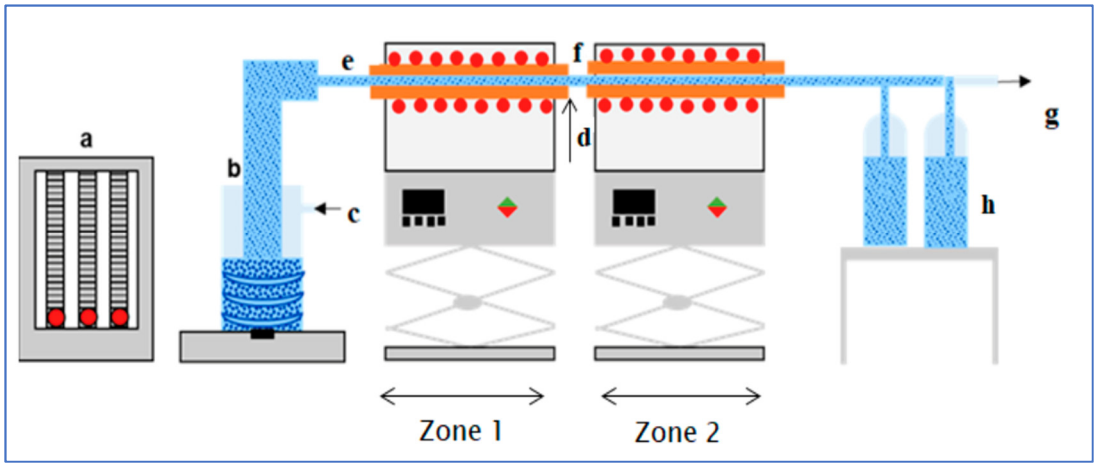

Figure 5. Experimental set-up used for ultrasonic spray syntheses (a) gas flow regulation of N_2 and H_2 (b) ultrasonic generator with precursor solution (c) gas inlet 1, N_2 (d) gas inlet 2, H_2, (e) furnace 1, (f) furnace 2, (g) gas outlet and (h) collection bottles [30].

1.4 Microsphere modification

In this section, we discuss how polymeric microspheres can be modified. The modifications alter properties such as hydrophobicity/hydrophilicity, crystallization temperature, decomposition temperature, immunotoxicity, and the mechanical properties of the synthesized polymer. The functional groups in polymers allow for surface modification, polymer grafting, and block copolymerization, among others. We will be focused on surface modification and block copolymerization.

1.4.1 Surface Modification

Polymers possess many excellent bulk properties making them suitable for many applications. In some cases, however, polymers may not possess the surface properties desired. Surface

modification becomes necessary then to make polymers entirely suitable for applications. Surface modification could be as straight forward as adding a coating to the surface. For instance, in Scanning Electron Microscope (SEM) applications, a metallic coating is applied to materials to improve the image's resolution. This coating does not affect the bulk properties of the material being imaged. Pores may also need to be created on the polymer surface to increase the material's surface area and/or make materials suitable for applications such as scaffolding [32] and drug delivery [33]. Notably, hydrophobic polymers can be surface modified to make them less hydrophobic. To achieve this, functional groups like a carboxylic group (-COOH), a hydroxyl group (-OH), or an amine group ($-NH_2$) are added to the surface of the polymer via polymer chemistry. Depending on the material, the surface of a given polymer material with a hydrophobic surface can be made hydrophilic in a few ways. Polyesters, for instance, can be surface modified by hydrolyzing the material with a base solution like sodium hydroxide to add hydroxyl groups to the surface [34]. Chen et al. surface-modified electrospun poly-l-lactic acid (PLLA) nanofibers by adding carboxylic groups to the surface plasma, in this case, for cartilage tissue engineering) [35].

Plasma treatment using oxygen gas is also an effective method to introduce oxygen-containing functional groups onto polymer surfaces [35]. In some applications, amine groups or other variations are added to the surface of materials to functionalize them via amination chemistry [36]. Amines may be used as a linkage in the formation of copolymers. In Yi et al., amines were used to link magnetic nanoparticles with glutaric dialdehydes and combined with lipase enzymes used as electrocatalysts for oxygen reduction reactions (ORR) [37], as shown in Figure 6. The reactivity of amines allows for a range of applications to be possible. In addition to

modifying a polymer's surface hydrophobicity/hydrophilicity, surface modification alters the surface charge of the polymers. Zeta potential allows us to ascertain this.

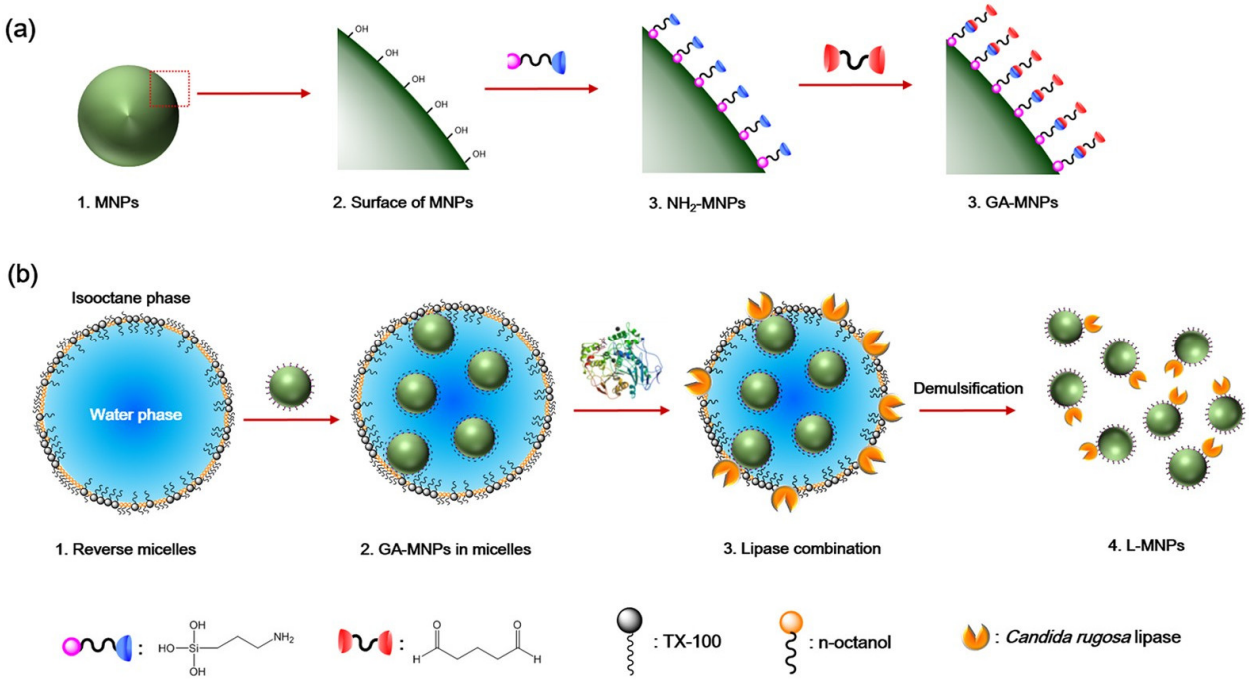

Figure 6. (a) Schematic showing the synthetic steps of the Glutaric Dialdehyde modified magnetic nanoparticles (GA-MNPs). (b) Synthesis of lipase-immobilized magnetic nanoparticles (L-MNPs) through the nonionic reverse micelle method. [37]

The Zeta potential of a particle in solution is a measure of the electric potential at the plane (slipping plane) that separates the mobile fluid from the fluid that remains static on the particle. Zeta potential values are either positive or negative, indicating the net charge on the surface of the particles. The higher the zeta potential, the more unstable the particle is; hence, the higher the possibility of flocculation or agglomeration. The zeta potential, therefore, allows us to study the changes in surface properties of the modified microspheres.

1.4.2 Block Copolymerization

A copolymer is a polymer formed when two (or more) different monomers are linked in the same polymer chain [38]. Homopolymers, however, are formed similarly but with just one monomer. Copolymers harness the properties of each monomer, producing a polymer that has superior properties to the constituent monomers. An example is the fluoropolymer ethylene-tetrafluoroethylene, which has better electrical, mechanical, and chemical properties than its constituent monomers, tetrafluoroethylene, and ethylene [39]. Several rubber derivatives such as acrylonitrile butadiene styrene (ABS), styrene-butadiene rubber, styrene-acrylonitrile, and styrene-isoprene-styrene are also copolymers that are widely used in several applications [40]. There are four types of copolymers stemming from the monomer arrangement: namely alternating (A-B-A-B-A-B-A-B), random (A-A-B-B-B-B-A-B-A-A-B-B), block (A-A-A-A-A-A-B-B-B-B-B-B), and graft copolymers (nonlinear block copolymers), with A and B as monomers. The focus of this section is block copolymers. Block copolymers are composed of two or more distinct homopolymers [41], arranged in a block-like manner, as described above.

Block copolymers can be fabricated in many ways. The most straight forward approach for making block copolymers is by the living or controlled polymerization of monomer A followed by the living or controlled polymerization of monomer B [42]. Free radical addition polymerization is a standard method for doing so. However, in some cases, the homopolymers already exist and need to be joined together to form the block copolymer. Functional groups at the end groups of the individual polymer chains allow for the covalent coupling of the homopolymers to form the block copolymer. Other methods employed in making block copolymers include ionic polymerization, metal-catalyzed polymerization, ring-opening polymerization, solution polymerization, change of mechanism polymerization, etc.

There are several reasons why researchers would want to join two or more distinct polymers, but a prominent among them is amphiphilicity. Amphiphilic block copolymers have been widely studied due to their ability to self-assemble as micelles. These structures interest researchers due to unique features such as their "nano size, core-shell architecture, and good thermodynamic stability in physiological conditions" [43]. In biomedical applications, the homopolymers forming the block copolymers are chosen such that the hydrophobic and hydrophilic constituent polymers are biodegradable and biocompatible, respectively [43]. The nanoscale hydrodynamic radii of block copolymers upon self-assembly make them ideal for nanoscale applications, such as forming block copolymer-based thin films and nanotubes [41].

PLA-PEG is an amphiphilic block copolymer synthesized in literature via ring-opening polymerization of lactide in the presence of PEG [22, 44]. In this diblock copolymer, PLA is the hydrophobic part, whereas the PEG is hydrophilic. The reaction is catalyzed by Tin (II) 2-ethyl hexanoate, stannous octoate ($Sn(Oct)_2$) [22], or by the less toxic acetic acid bismuth [45] at a temperature of 110°C, as shown in Figure 7.

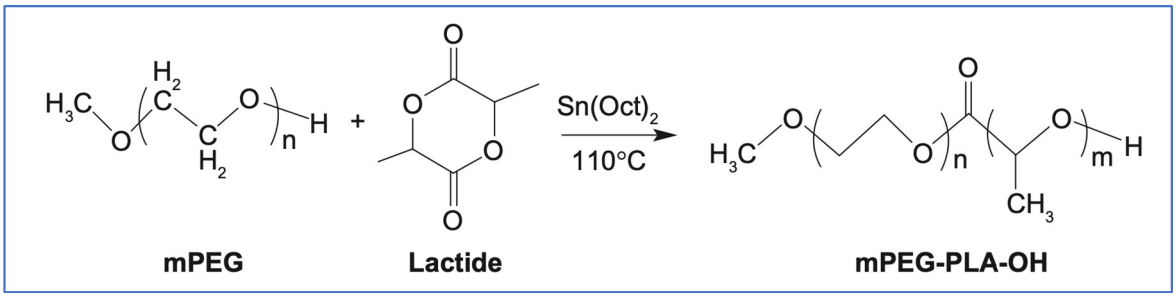

Figure 7. Synthesis scheme of mPEG-PLA. [44]

The block copolymer has also been synthesized, starting with glycol and lactic acid via anionic ring-opening polymerization, with 3,3-diethoxypropanol as an initiator [46]. The monomer: initiator: catalyst ratio (where applicable) can be modified in each case to create varying structures such as A-B-A triblock copolymers or star-shaped polymers [44-46]. These methods

were explored during the present work for the PEG-PLA system. In addition, the synthesis of PEG-PLA amphiphilic copolymers using PEG and PLA as the starting materials was explored. The proposed method is conjugating amine-functionalized PEG and PLA via click chemistry. Researchers have achieved significant success using click chemistry in the presence of an azide group to conjugate PEG with materials such as graphene oxide (GO) nanosheets [47-49]. The amine group will serve as the linkage between the two homopolymers. A conjugate process is a novel approach to forming PLA-PEG copolymers. Most methods in the literature, even those that involve click chemistry, form the diblock or triblock copolymers by ring-opening polymerization of D/L- lactide monomers [50-52]. This approach, if successful, will be helpful in applications where the constituent homopolymers already exist in polymer form.

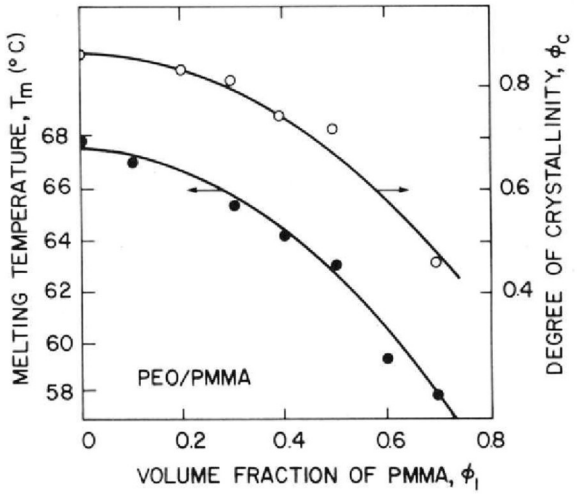

Figure 8. Dependence of melting point and degree of crystallinity of PEO/PMMA on the volume fraction of PMMA [53].

With block copolymer synthesis, it is feasible to achieve materials with different thermal properties and more suitable to a given process than homopolymers [54]. Figure 8 shows the decrease in the melting point of a polyethylene oxide – polymethylmethacrylate (PEO-PMMA) block copolymer as the volume fraction of PMMA is increased [53] from the literature. PEO has

a melting point of about 68ºC, whereas PMMA has a melting point of about 160ºC. Researchers have also found that the glass transition temperature and the melting point of a PLA/PEG block copolymer are lower than those of pure PLA [55]. Therefore, a PLA-based block copolymer used as a pore former could be more easily removed from a polymer matrix than PLA. The lower melting temperature corresponds to a lower calcination temperature of the pore former, implying a lower risk of degradation of the polymer matrix in the process.

1.5 Pore/Void Formation

Pore structures are often desired in materials to control their mechanical, electrical, and thermal properties [7-10]. In some cases, pores are avoided at all costs. For many mechanically intensive applications where malleability, ductility, and hardness are required, pores can initiate crack propagation, in which case pores are not ideal. The pores are often the case with builds that include metal parts in additive manufacturing. However, in other applications, voids are desired to engineer material properties. The materials are typically polymers and, in a few instances, ceramics.

1.5.1 Applications and Material Property Control

Research shows that controlling the number of voids in polymers directly impacts their density. Significant work has been done on generating porosity in epoxy rubber and foams with cell-like voids for various applications. Such applications include catalytic supports, lightweight structures, and biological scaffolds [7]. Silicone has shown much promise in being a viable candidate for creating voids in polymer matrices due to desirable properties such as flexibility, thermal stability, and mechanical versatility. Among the number of applications for which silicones are used, prosthetic materials remain dominant. Silicones, particularly

polydimethylsiloxanes (PDMS), are biocompatible and ideal for making prosthetics, which may be required to absorb saliva or other tissue fluids [56]. In Bernardo et al., silicones are used as a preceramic for creating porous bioceramics (wollastonite-hydroxyapatite) [10], where silicone polymers were loaded with micro-and nano-sized active and passive fillers, which were then selectively decomposed upon pyrolysis in the formation of the bioceramic material [9, 10]. Silicone polymers may also be used as pore fillers, as in [8], where they are used to create and study the distribution and stability of cellular voids in aluminum foam specimens [57]. Porous PDMS sponges have also been shown to have structural advantages compared to bulk PDMS that make them suitable for water/oil separation [58-60] and microfluidics [61, 62], among others.

1.5.2 Pore Creation Methods

The most common pore-creation methods include templating and gas nucleation. Gas nucleation is carried out by precipitation or by the use of chemical blowing agents [63]. Templating is an umbrella term that describes structures created as place holders to generate pores. The template is a part of the final structure of the part built, with the sole purpose of being removed to create porosity. This templating is referred to as sacrificial templating. Templating may be hard, soft, or self-templating [64]. Templating may be used to create hollow nanostructures for energy-related applications and bulk materials. Pores can also be formed by adding hollow spherical particles (micro balloons) to polymers. This method is prominent in direct ink-write additive manufacturing. In Alison et al., hierarchical porous structures are created via sacrificial templating with 3-D printing to produce cell-like structures in bulk, as shown in Figure 9 [7].

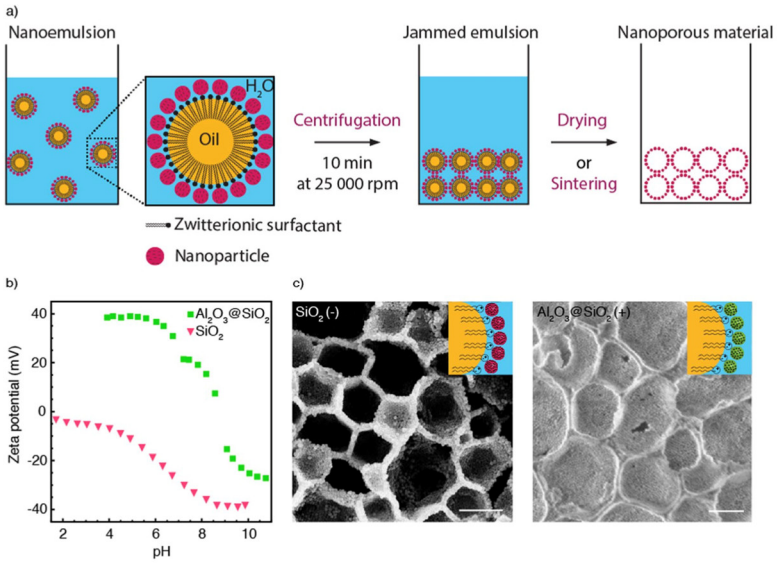

Figure 9. Sacrificial Templating [7].

Pore sizes may range from the macro to the microscale. The ease of pore former removal, size control, morphology control, and the impact the removal process has on the matrix material determine how efficient a material will be as a pore former. As a pore former, silicone has controllable size and morphology but has a relatively high decomposition temperature. As such, pore former removal by calcination may not be an ideal path if the matrix material is within the decomposition temperature range of silicone. Pore formers may also be removed by solvent extraction. The choice of solvent must be such that it selectively swells the polymer matrix and dissolves the pore former without dissolving the matrix or changing its mechanical, physical, or thermal properties.

1.6 Characterization Techniques

Analytical instruments have been developed over the years to help scientists identify the structural, physical, chemical, thermal, and mechanical changes that occur within a system after any given process. These devices are used to characterize the processes to confirm whether the intended purpose of an experiment was attained. The analytical tools described in this section

help confirm the formation of modified polymers, assessing their physical, chemical, mechanical, and thermal properties before and after incorporation into polymer matrices in the present work.

1.6.1 Microscopy

There are two primary microscopy forms, namely optical and electron microscopy. Optical microscopy is based on light, whereas electron microscopy is based on electrons. Scanning Electron Microscopy is a form of electron microscopy, whereas confocal imaging is optical microscopy.

1.6.1.2 Confocal Imaging – Keyence Microscope

Confocal imaging is a form of optical imaging whereby, unlike other optical spectroscopy approaches, multiple mirrors with similar foci and radii of curvature are employed [65, 66]. The Keyence Microscope uses confocal imaging. Marvin Minsky pioneered this method of imaging in 1957. Confocal microscopy involves using both reflected and transmitted light to produce an image. This increases the size range of materials that can be imaged via optical microscopy. Images generated are two-dimensional images. The Keyence microscope is connected to a computer with a graphic user interface and comes with lenses that have different magnification ranges. The range of magnification varies from 100-1000x. The Keyence microscope can image materials within a lower micron-size range, thus ideal for many biological specimens. However, the capability begins to fail for materials on the nanoscale.

1.6.1.1 Scanning Electron Microscope (SEM)

Scanning Electron Microscope (SEM) is used to investigate particles' morphology, size, and size distribution by using secondary and backscattered electrons [67]. Unlike confocal microscopy,

the principle of operation is electron-based. SEM can be used to obtain gray-scale three-dimensional views of particles. SEM has been revolutionary in microcopy, considering up to 30,000x magnifications can be obtained and can be used to observe structures in the nanometer range. The SEM generally comprises an electron source, lenses to focus the electron beam, scan coils, an electron detector, a sample chamber, and a computer with a desktop for viewing the sample chamber and the scanned images. The SEM allows the chamber pressure and voltage (extra high tension) to be controlled. The SEM operates under a vacuum to limit the interference of particles with the electrons.

In the next section we discuss techniques used to determine the chemical properties of a given sample.

1.6.2 Chemical Analysis

This section focuses on the chemical analysis methods used in the characterization of compounds. Poly-3-hydroxybutyrate (PHB) is used as an example chemical structure for the purposes of this discussion. We discuss Fourier Transform Infrared Spectroscopy (FTIR) and Nuclear Magnetic Resonance (NMR), and how each method provides specific information about PHB's chemical structure.

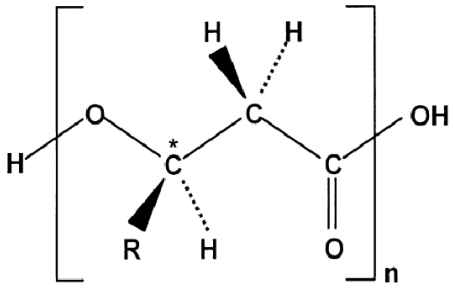

Figure 10. Chemical structure of poly-3-hydroxybutyrate.

1.6.2.1 Fourier Transform Infrared Spectroscopy

Fourier Transform Infrared spectroscopy (FTIR) provides information about the functional groups present in a sample based on the vibrational resonance of the bonds present [68] using radiations in the infrared spectrum. FTIR is used for chemical identification. When an infrared spectrum is passed through a sample, it absorbs a portion of the radiation and transmits the rest. An absorption or transmission spectrum can be generated based on the sample scan. Different chemicals absorb and transmit light based on the molecular structure and chemical bonding present. As such, FTIR provides a molecular "fingerprint" and as such, is effective for chemical identification [69].

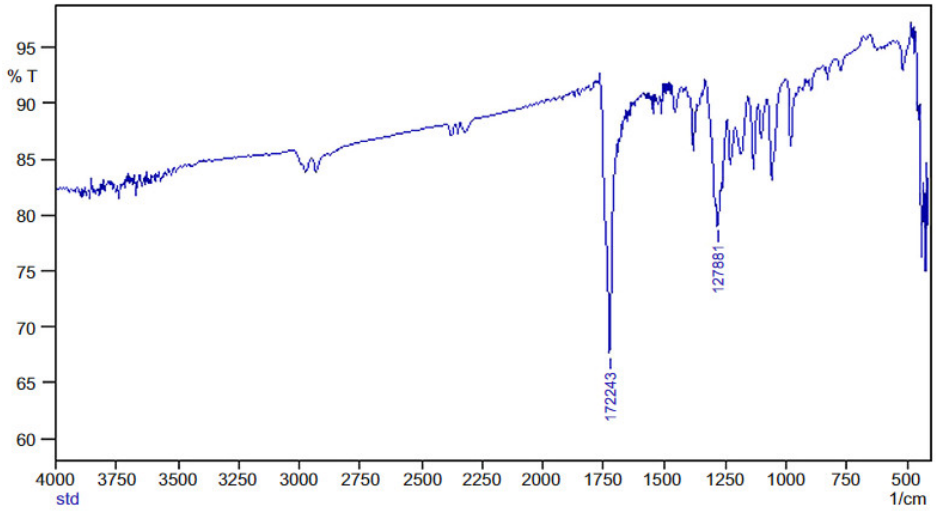

Figure 11. FTIR spectrum of poly-3-hydroxybutyrate [70].

Figure 11 shows the FTIR spectrum of poly-3-hydroxybutyrate. The y-axis represents the percent transmittance, and the x-axis represents the wave number. Two characteristic peaks for the above spectrum are observed, corresponding to specific rotations around carbon atoms. The peak at 1724 cm^{-1} corresponds to the C–O stretch of the ester group present in the molecular chain of a highly ordered structure, whereas the peak at 1279 cm^{-1} corresponds to the ester

bonding [70]. For chemical identification, there are tables that relate bond configurations (stretching, rotation, etc.) to absorption/transmission ranges.

1.6.2.2. Nuclear Magnetic Resonance

Nuclear Magnetic Resonance (NMR) spectroscopy is "the absorption of radiofrequency radiation by a nucleus in a strong magnetic field [71]." When a nucleus is brought into a magnetic field, the nucleus absorbs the radiation energy, spins in alignment with the field based on the atomic number and number of neutrons in the nucleus, remits the energy, and returns to a lower energy state. Molecules comprise atoms, each with its nuclear composition and bonding. NMR is therefore an efficient chemical identification tool. There are two common types of NMR, namely carbon-NMR or proton (^{1}H) NMR, and the chemical species to be observed may determine which approach will be expedient.

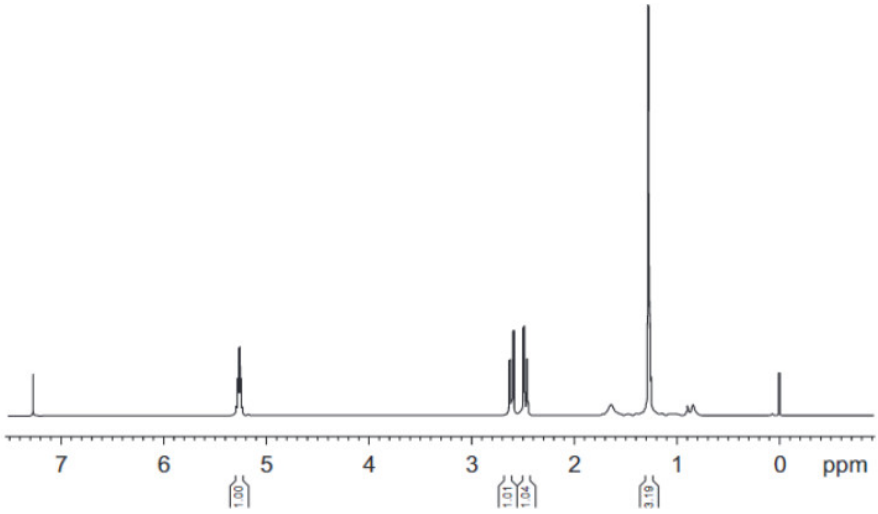

Figure 12. ^{1}H-NMR spectrum of poly-3-hydroxybutyrate [70].

Figure 12 shows the NMR spectrum of PHB. This spectrum shows three characteristic signals. The strong peak at 1.53 ppm represents the proton attached to the methyl group in the chemical. The double peak at 2.75 ppm corresponds to a methylene group adjacent to an asymmetric

carbon atom with a single proton. The third characteristic peak occurs at 5.52 ppm, corresponding to a methylene group.

1.6.3 Thermal Analysis

1.6.3.1 Thermogravimetric Analysis

Thermogravimetric Analysis (TGA) is another method used for sample characterization [72]. For any TGA operation, a sample's change in weight is observed as a function of temperature or time (isothermal condition) as the sample is subjected to a controlled temperature profile under a controlled atmosphere of nitrogen, air, or another gas [73]. In this document, all TGA analysis are done in air. TGA data can also help determine which substances are still present within a solid sample after an experiment to remove that component has been carried out. TGA can be used in core-shell materials to confirm the presence of both materials and the removal of either the core or shell material when heat is applied. This analytical characterization technique can also be used to study the decomposition of a given material under a temperature ramp or isothermal conditions over time.

1.6.3.2 Differential Scanning Calorimetry

Differential Scanning Calorimetry (DSC) shows any sample's heat absorption profile for a specified temperature range. It calculates the apparent heat capacity of a macromolecule or polymer as a function of temperature [74, 75]. Information such as the glass transition temperature, crystallization temperature, sublimation temperature, melting temperature, enthalpy change, entropy change, and change in material heat capacity can all be derived from the DSC by analyzing the heat flow profile [75]. This information helps us understand materials' thermal elasticity and plasticity, the various phases that can exist within a set temperature range, and the crystallinity of materials with recurring heating and cooling cycles.

1.6.4 Rheology

Rheology is a thermomechanical process used to study materials' flow and deformation [76]. These are translated as strain and strain rate measurements, analyzing the impact of an external force (stress) upon an object. The stress, strain, and strain rate can be used to make predictions about the mechanical behavior of the materials. A rheometer is used to perform rheology measurements in a controlled environment. Three factors that most impact rheology are an external force, internal structure, and environmental conditions such as temperature [77]. Rheology measurements are performed by placing the material between either two parallel plates or two cones, confined to a spacing of about 1mm [78]. Other fixtures may be available, suitable for a specific sample, depending on the instrument used to perform rheology. For a given polymer resin filled with pore fillers, rheology can be used to determine the extrudability of the resin at different loading percentages for 3D printing applications. Rheology and understanding the extrudability is the property of interest in the present work and has been investigated. Storage modulus, loss modulus, viscosity, and angular frequency, among other variables can be obtained from the rheometer.

1.6.5 Dynamic Mechanical Analysis

The Dynamic Mechanical Analysis (DMA) technique is a thermomechanical analysis tool used to analyze a material's properties and variations due to temperature, time, frequency, stress, etc. [79]. DMA studies a sample’s kinetic properties generated from its stress/strain relationship. This versatile method allows polymer materials to be tested under varying load stresses for compression, deflection, elongation, and tension. A DMA employs various deformation modes, such as dual cantilever bending, 3-point bending, tension/compression, and shear, using a sinusoidal source to study viscoelastic properties such as storage modulus, loss modulus, and

loss tangent. This device is connected to a computer that generates x-y plots for the various tests performed. The present work employed DMA to study the changes in the mechanical properties of polymer blends before and after the removal of the pore filler.

1.6.6 Particle Size Distribution

The particle size distribution of the particles formed will be analyzed using a Malvern Mastersizer 3000. Referred to as the "world's leading particle size analyzer," this analytical tool uses light scattering and diffraction to measure the angular deflection of suspensions, emulsions, and dry, dispersed powder samples [80]. The equipment is connected to a computer software that displays the measured data points into graphs, tables, and other forms. The particle size analyzer measures particle size and the particle size distribution of a given powder sample.

Figure 13. Malvern Mastersizer 3000 and its Accessories. [80]

From that information, powder properties such as flowability can be determined. The Malvern Mastersizer can analyze both dry powder samples and powder samples dispersed in a non-evasive solvent. In the case of the latter, accessories of the Mastersizer make that possible. When

a sample is introduced into the Mastersizer, a laser beam passes through it. The intensity of the scattered light varies depending on the size of the particles. The degree of refraction of each light ray in the refracted beam is proportional to the sizes of the particles. The equipment uses this knowledge to then compute the particle size and particle size distribution of the particles in the sample [80].

In the next chapter, we discuss the two primary methods for preparing microspheres, namely Ultrasonic Spray Pyrolysis (USP) and the Emulsion method. The methodology of microsphere preparation along with how the resulting microsphere properties from each method differ, will be examined.

CHAPTER 2

Microsphere Formation

2.1 Introduction

Polymeric microspheres are prevalent in several applications. They are used as absorbents, latex diagnostics, affinity bioseparators, pore formers, as well as drug and enzyme applications [81, 82]. The choice of polymer for microsphere formation is dependent on its intended purpose. In biologically related applications, for instance, the polymers must have a suitable biocompatibility, bioavailability, biodegradability, and non-immunogenicity [19]. In industrial packaging applications, properties such as gas permeability are desirable [83, 84]. Ideally, the polymers must be soluble and miscible in various solvents. In drug delivery applications, the drug to be encapsulated within the core of a polymer as well as the polymer itself must be soluble in the same precursor solvent, and hence, compatibility with more than a few solvents becomes a prime factor for consideration [85, 86]. Polymer microspheres must also possess the desirable thermal, mechanical, and chemical properties for the given application. Among the homopolymers that have been studied, polylactic acid (PLA) and polyethylene glycol (PEG) exhibit properties that make them preferable across several applications.

Polylactic acid (PLA) is a material of interest in this research. PLA is among a class of biopolyesters that are biodegradable and biocompatible [87, 88]. PLA has garnered significant attention in recent decades, particularly in biomedical applications [89], pharmaceutical applications, drug delivery applications [82, 90, 91] owing to its biodegradability and biocompatibility [87]. PLA was discovered by notable Swedish scientist Carl Scheele in the 1700's and used for the repair of mandibular fractures in dogs [92]. PLA has come a long way since then. PLA, being a thermoplastic, is also used in packaging for bottling, plastic films,

shrink wrapping, etc. [84]. PLA can be mass produced on a large scale, and is commercially available in a wide range of molecular weights [87]. This aliphatic polyester can be synthesized in several ways, using different precursors, but prominent among these is the ring-opening polymerization of lactide. Figure 14 shows the various stereoisomers of PLA that can exist.

PLA has two enantiomers namely poly (1-lactid) acid (PLLA) and poly (d-lactic) acid (PDLA), derived from the optical monomers l-lactide and d-lactide respectively. Another version of the polymer, poly (d, l-lactic) acid (PDLLA) also exists and is completely amorphous unlike PDLA and PLLA which are semi-crystalline and have similar physical and chemical properties [86, 92]. In most cases, the polymer consists of a mixture of poly-d-lactide/poly-l-lactide and poly-meso-lactide isomers [93]. The isomeric composition of the polymer provides variability in the crystallinity of the polymer [87]. As such, PLA can be manufactured as soft and elastic polymers or high strength polymers, depending on the intended application. In an amorphous state, PLA remains thermally crystallizable, exhibiting slow crystallization kinetics [87].

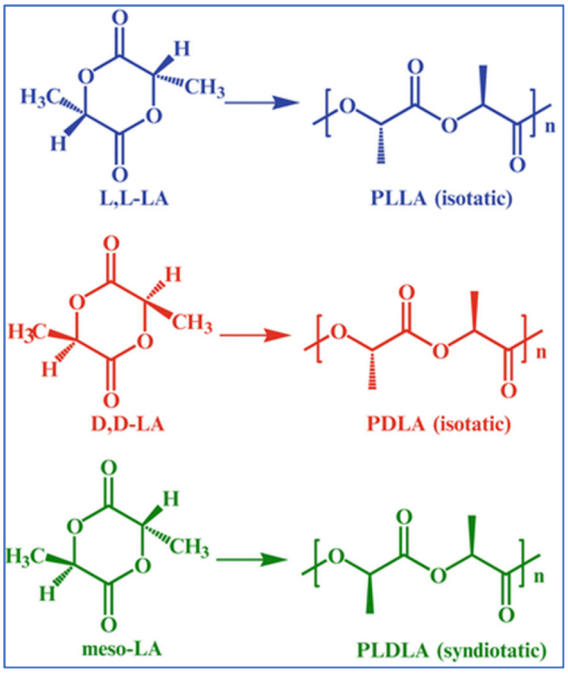

Figure 14. Stereoisomers of PLA and their corresponding precursor Lactide molecules. [93]

Table 2 shows PLA's typical thermal transition temperatures [87]. The thermal properties shown in the table indicate that PLA remains solid at room temperature. This is desired for the targeted applications. PLA has a relatively low thermal decomposition temperature, which can be explored in the generation of porosity in thermally stable materials (e.g., silicone) by calcination. PLA can also be degraded by hydrolysis or transesterification, owing to the presence of carboxylic and ester groups, respectively [87]. The presence of these bonds also suggests that PLA could either surface modified or conjoined chemically with other polymer chains to either alter the surface properties of pure PLA (such as degree of hydrophobicity) [34, 35] or to enhance its thermal and chemical properties [88, 94]. PLA is hydrophobic and can be copolymerized with hydrophilic polymers to form amphiphiles, which can be further converted to polymersomes [95], microspheres [96], and the like. In many drug delivery applications, micro- and nanoparticles of PLA and copolymers of PLA (common amongst them being PLA-PEG (polyethylene glycol), PLA-PEG-PLA, PLA-PLGA (polylactic-co-glycolic acid), PLA-PVA (polyvinyl alcohol), among others) are used for encapsulation [19, 88, 89]. Due to its moldability, PLA can also be fabricated as films, scaffolds, micelles, and micro- and nanoparticles [92].

Table 2

Temperature range for PLA thermal transitions [97, 98]

Temperature Transition	**Temperature range (°F)**
T_g; Glass transition temperature	50 - 80
T_m; Melt temperature	130 - 170
T_d; Decomposition Temperature	230 - 260

Polylactic acid can dissolve in various solvents that include chlorinated and fluorinated organic compounds, tetrahydrofuran (THF), acetone, dimethylformamide (DMF), benzene, pyrrolidine, benzylamine [99]. The choice of solvent for PLA may depend on the polymer's molecular weight, stereochemistry, and percent crystallinity. Amorphous PLA is easier to dissolve than crystalline PLA [99]. The flexibility of PLA makes it an attractive candidate for further research for several applications, including additive manufacturing and porous material formation [41].

Polyethylene Glycol (PEG), like PLA, is a biocompatible polymer with applications predominantly in the medical field and is synthesized by ring-opening polymerization [100]. Unlike PLA, PEG is highly hydrophilic and non-biodegradable. PEG is non-volatile, colorless, inert, and non-toxic and is soluble in polar organic solvents, including benzene and chloroform, as well as nonpolar solvents, such as carbon tetrachloride. Depending on the molecular weight, PEG can exist as a liquid or a solid. PEG can also functionalize owing to the presence of the hydroxyl group, thus allowing different chemistries like surface functionalization or block copolymerization to be performed. Researchers have determined, for instance, that PEG can be made degradable by functionalizing with PLA [101]. PEG has applications in two primary industries: the medical and chemical industries. The medical industry uses PEG to manufacture laxatives [102]. PEG, like PLA, is inactive in drug delivery applications. It is also used in protein analysis via PEGylation [103] and gene therapy [104]. PEG is used as a binding and dispersion agent in the chemical industry to prevent agglomeration [105]. PEG is also used as a hydrophilic coating [106]. PEG, like PLA, can also undergo top-down manufacturing procedures to form various micro- and nanostructures.

PEG and particularly PLA microspheres are generally not produced for off-the-shelf or commercial purchase. The thermal, mechanical, and biological properties of PLA and PEG discussed, however, make them choice pore former candidates in the formation of evenly distributed micropores in polymer matrices. As such, there is a need for readily available PLA and PEG microspheres for such applications. In this chapter, we discuss simple approaches for creating PLA and PEG microspheres.

Section 2.2 covers the formation of PLA and PEG microspheres using ultrasonic spray pyrolysis (USP) whereas section 2.3 covers the formation of PLA microspheres using the single emulsion method. Formation of PEG microspheres via the emulsion method is discussed in section 4.2.

2.2 Ultrasonic Spray Pyrolysis (USP)

In this section, we will examine the formation of PEG and PLA microspheres. The prospect of both PEG microspheres and PLA microspheres being formed via USP creates room for forming PEG-PLA core-shell microspheres, much like PDMS-PEG microspheres.

2.2.1 Methodology and Setup

The setup shown in Figure 15 was used to produce polymer microparticles. The USP setup comprises a bottle for the precursor solution, a quarter-inch tube connecting the precursor bottle to the particle generator, a temperature source and control unit, a nitrogen flow inlet, a tube furnace, and bubblers connected to the tube furnace by ¾-inch tubing.

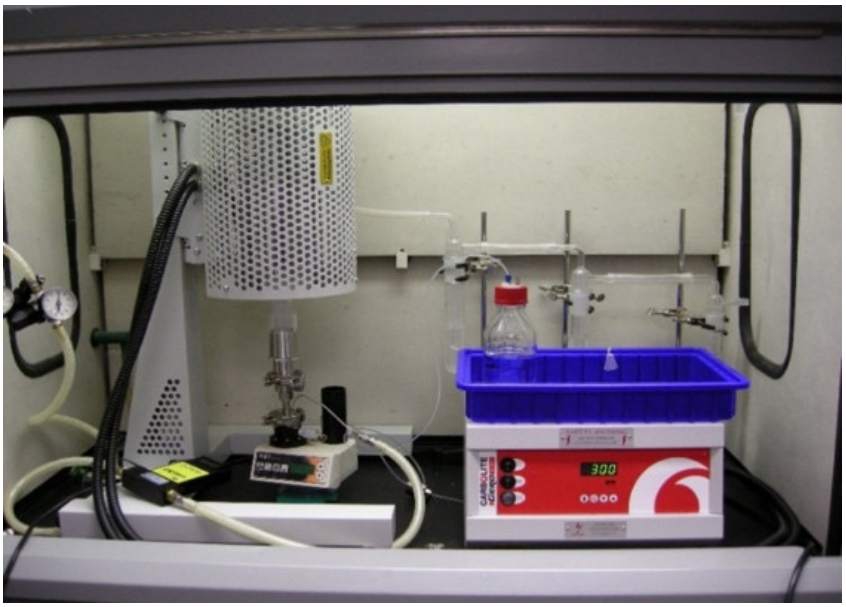

Figure 15. Typical USP Setup

Polymers used to prepare microparticles via USP include polylactic acid (PLA), polyethylene glycol (PEG), polydimethylsiloxane (PDMS), and polyvinylpyrrolidone (PVP).

Most of the polymers used in this process have molecular weights ranging from about 200 – 1200 g/mol, except for PLA, which has an average molecular weight of 100,000g/mol. In the case of PEG/PVP microspheres and PEG-PDMS core-shell microspheres, the starting solution for the USP process comprises a 1, 2, and 5 weight percent concentration of polymer in solvent. Due to the extremely high molecular weight of PLA, a starting solution is prepared with 41g of the PLA pellets first dissolved in 800mL of dichloromethane (DCM). The precursor solution for the USP process is prepared by diluting 20mL of the starting solution in 80mL of DCM to meet the dilution requirement for USP.

The precursor solution flows continuously into the particle generator's nebulizing chamber, which has a volume of 30mL. The solution is nebulized at 2.5MHz. The fine mist created from the nebulization is then carried upward by a nitrogen stream flowing at 0.6 *slpm* into the tube furnace, set at the curing temperature of the precursor polymer. The solvent

evaporates, leaving individual droplets acting like microreactors, which are then collected in test tubes half-filled with a solvent that does not dissolve the polymer (e.g., hexane for PEG and di-water for PLA). The microspheres are filtered out of the solution by centrifugation and afterward washed and dried.

2.2.2 Results and Discussion

2.2.2.1 Formation of PEG microspheres

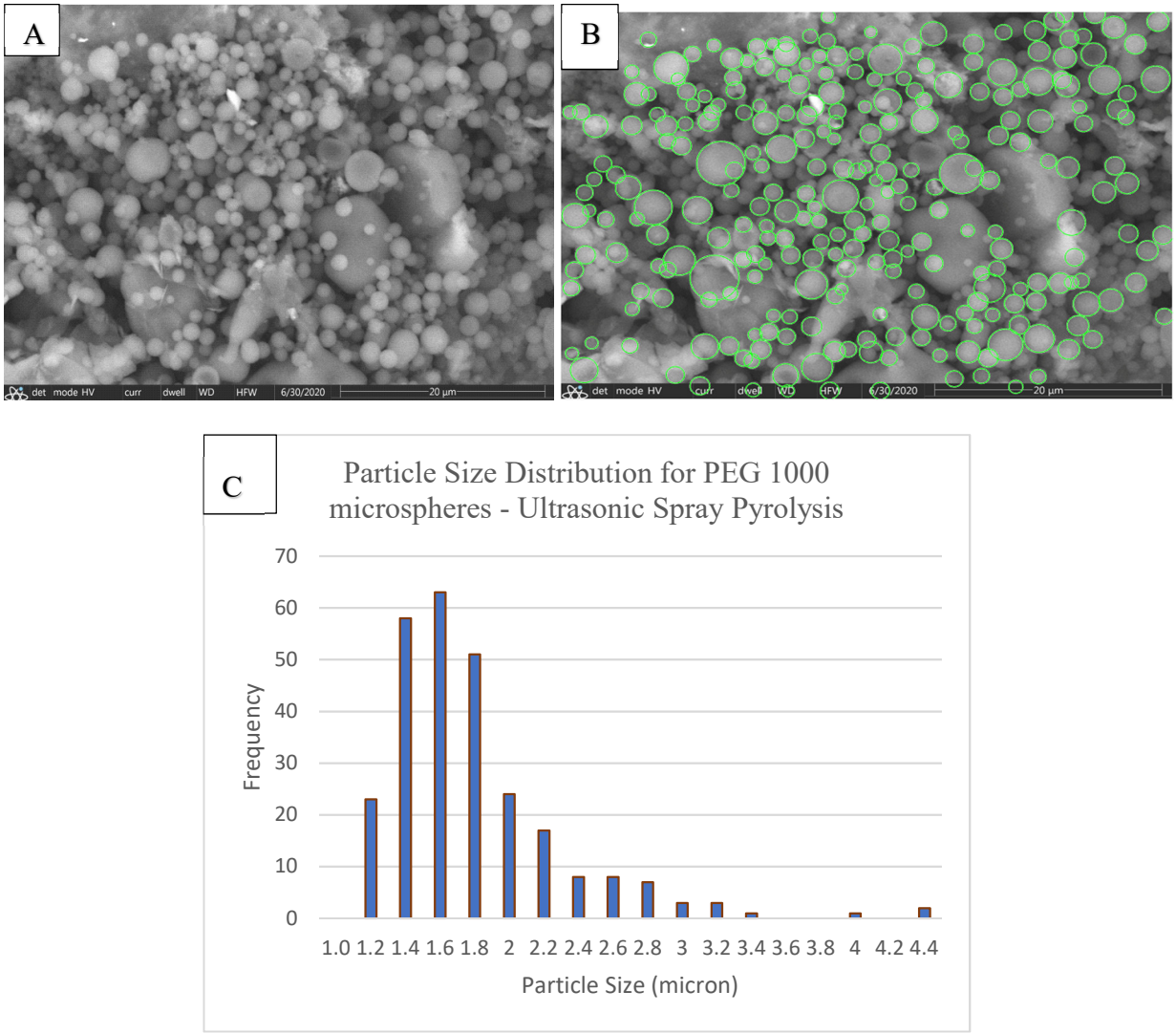

Figure 16. SEM image of Polyethylene Glycol (PEG) microspheres (A), the microsphere detection analysis of the SEM image of PEG 1000 microspheres via MATLAB (B) and the

Particle Size Distribution of the PEG 1000 microspheres (C) prepared using Ultrasonic Spray Pyrolysis.

Figure 16(A) shows the Scanning Electron Microscope image of PEG microspheres prepared by ultrasonic spray pyrolysis. The formed microspheres shown in the image are spherical. Figure 16(A) also shows that the particles retained the spherical morphology of droplets throughout the USP process. From this, we conclude that the USP method successfully produced spherical, monodisperse, PEG microparticles.

The sample collected from the USP process was limited in quantity and also slightly agglomerated, and as such it both would not have been ideal for a Malvern particle size analysis or a Dynamic Light Scattering (DLS) analysis. The SEM image, given that it is a 3-dimensional depiction of the particles formed, is used to calculate the particle size distribution using MATLAB.

To determine the size distribution of the PEG microspheres collected, a particle size analysis of the SEM image was performed using a MATLAB image processing script which detects and calculates the diameter of each particle. A graphical image of the result of the image analysis program is shown in Figure 16(B), where the detected microspheres are shown as green circles. A total of 269 spheres are detected, and the diameters of each of those microspheres are calculated. The particles measured had a mean diameter of 1.69 μm and a standard deviation of 0.51μm. The MATLAB functions "*imfindcircles*" and "*viscircles*" were used to find and calculate the diameter of the microspheres and circle the microspheres green, respectively.

The diameters calculated in MATLAB were exported to Microsoft Excel, and a frequency distribution chart was generated, as shown in Figure 16(C). The graph shows that the spheres are narrowly distributed within the size range of 1.1 - 4.3μm, as seen in Figure 16(C).

This depicts a relatively narrow distribution of uniform microspheres produced using ultrasonic spray pyrolysis.

The Ultrasonic Spray Pyrolysis process also produced microspheres at a very low efficiency. In the experiment described above, for 5g of PEG microspheres in the precursor, only about 0.5g of microspheres were collected, accounting for about 90% loss of material. This material loss is partly attributed to the rapid cooling of the topmost part of the heating chamber (not visible in Figure 14). Upon inspection of the heating chamber post-process, it was observed that some of the PEG microspheres clanged to the topmost part of the vertical heating chamber. This region is not in direct contact with the heating element, and for PEG microsphere synthesis, the chamber is set lower than 70^{o}C. The surroundings can quickly cool the topmost part of the vertical tube furnace and, as such, condenses the PEG droplets.

2.2.2.2 Formation of PLA microparticles

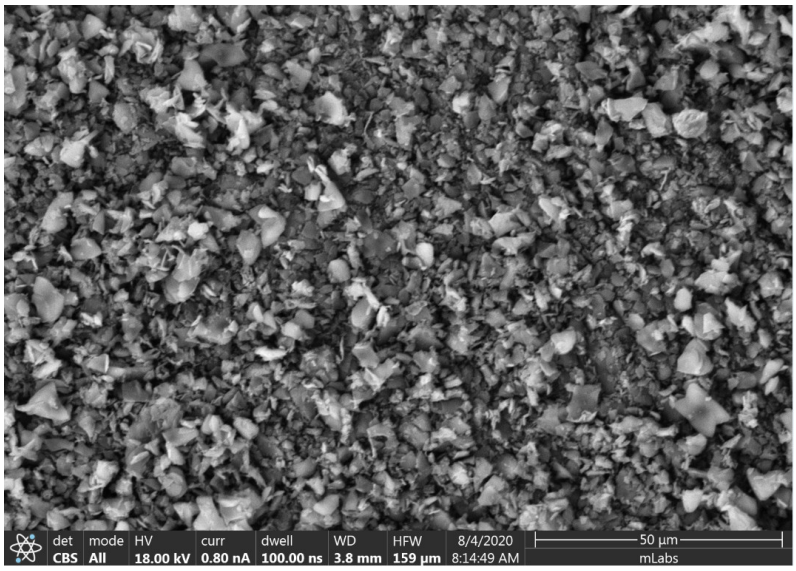

Figure 17. PLA particles obtained from failed Ultrasonic Spray Pyrolysis

Measuring particle size and particle size distribution of such a small powder sample is not feasible with the Malvern Mastersizer 3000 analytical tool, hence the need to use the MATLAB

script in calculating the particle sizes. Following the successful production of uniform PEG microspheres, we sought to produce PLA microspheres using the USP process. PLA was chosen due to its desirable chemical and thermal properties and affordability/accessibility. A successful USP synthesis with PLA would also pave the way for forming PEG-PLA core-shell microspheres comprising a hydrophilic core and a hydrophobic shell. PLA microsphere formation from the USP setup proved challenging, given that there is a concentration restraint on the precursor solution. The procedure described in section 2.2.1 above was unsuccessful. The starting solution did not form a mist like we would have expected. In the case of PLA, even with a further dilution of the starting material, the concentration of the PLA precursor solution could be above the maximum concentration of starting solution that the particle generator can nebulize at 2.5MHz. The PLA grade used in this experiment has an average molecular weight of about 100,000 g/mol. PLA dissolved in DCM flows with a similar consistency as oil. As such, it is feasible that PLA in DCM would only be atomized in a very dilute solution. In this case, producing PLA microspheres may not be as efficient using the Ultrasonic Spray Pyrolysis method. This needs to be investigated further. It could also be that for higher nebulization frequencies, the PLA solution would have formed a mist and, consequently, would have been able to prepare microspheres.

A successful, continuous USP production of PLA microspheres with a narrow distribution can benefit many applications. Careful process analysis revealed that at the end of the experiments, PLA particles were observed in the nebulization chamber of the USP after all the solvent had evaporated. If the particles were microspheres, this could mean that some of the precursor solution nebulized and, after solvent evaporation, fell back into the particle generator. If this were the case, the particles would most likely be spherical, and this would have been an

indication of whether the flow of the nitrogen through the vertical tube is laminar. SEM analysis of the PLA particles (Figure 17) shows no indication of the formation of spherical PLA particles. The absence of spherical particles in the SEM image in Figure 17 meant that the MATLAB script used to calculate the diameter of each particle could not be used to calculate the sizes and size distribution of the PLA microparticles.

The PLA samples collected were categorized as "starter" and "waste" microparticles. During experiments, when the solution in the particle generator did not nebulize, the particle generator was emptied, and the material was categorized as "waste." It was then replaced with a new, lower-concentration PLA-in-DCM solution. When this solution failed in the USP process, it was collected and categorized as a "starter." The DCM solvent in the waste and starter samples evaporated, leaving behind powdered PLA particles. The starter sample was measured to obtain the SEM image in Figure 17. There was enough powder material from starter and waste samples to conduct wet and dry particle size analyses using the Malvern Mastersizer 3000 analytical tool.

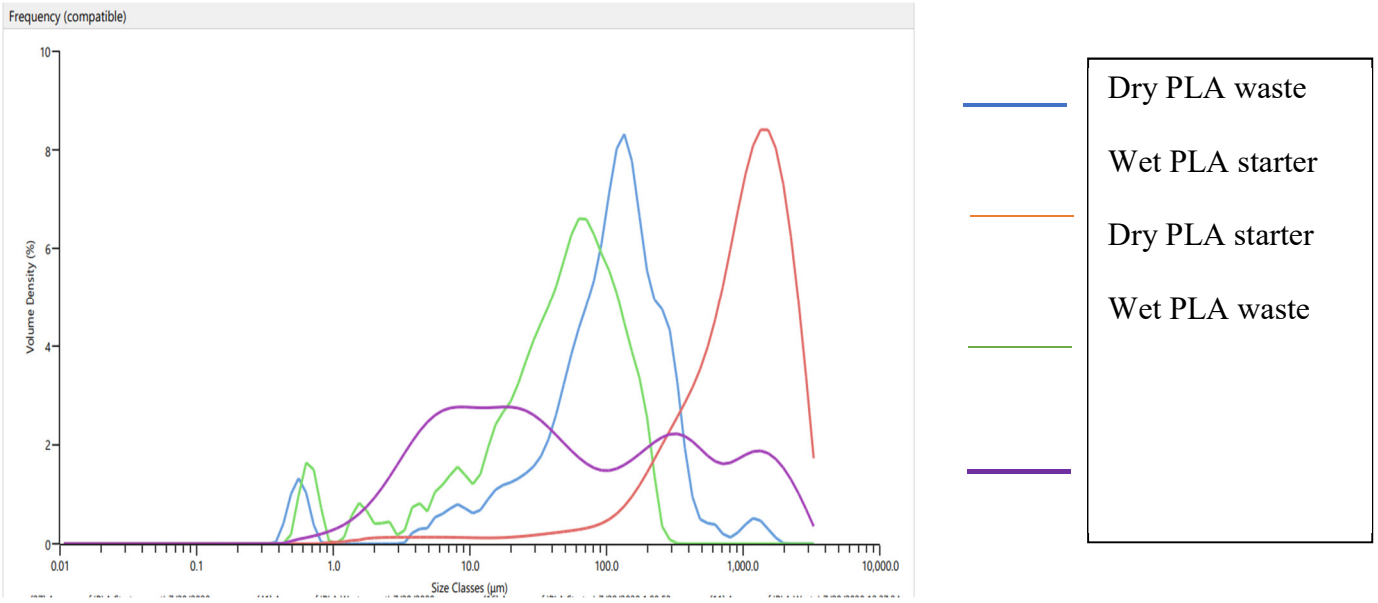

Figure 18. Particle Size Distribution of the "starter" and "waste" PLA microparticles collected during the USP process.

Figure 18 shows the results of the particle size analysis of PLA microparticles using the Malvern Mastersizer 3000. The wet analysis of the powder sample involves dispersing the powder sample in a solvent that does not dissolve the material for the particle size analysis. In contrast, for a dry analysis, the particle sizes of the particles are directly measured in the device. The gas flow rate and the nebulization frequency used in producing PEG microspheres were also used for PLA, so we expected to see particles in the lower micron range if microspheres are indeed formed. This is, however, not the case as observed in Figure 18. USP creates particles with a narrow distribution of sizes, but Figure 18 shows multimodal size distributions even for the same sample. There was no evidence of significant microsphere formation from the Particle Size Distribution data.

2.2.3 Conclusions

The ultrasonic spray pyrolysis method described above can successfully be used in creating PEG microspheres, among others, with a spherical morphology and a narrow size distribution. This method is, however, not efficient for mass production. Parameters such as the gas flow rate and the nebulization nozzle type can be altered to optimize the conversion rate of the polymer precursors into microspheres. Through this work, we also concluded that polymers with molecular weights on the order of 10^4 or higher are not ideal for use as precursor polymers in the formation of microspheres via USP.

Future work on the Ultrasonic Spray Pyrolysis setup would involve performing a parametric study to investigate the impact of precursor concentration on atomization. The goal would be to identify the threshold frequency above which the starting solution will fail to nebulize. The impact of the nitrogen flow rate and the flow direction on the percent conversion of starting material must also be fully understood.

2.3 Single Emulsion

This section focuses on the formation of PLA microspheres using the oil-in-water (O/W) single emulsion method. (A different approach is used to disperse PEG microspheres in a PDMS matrix, and this is discussed in Chapter 4). PLA microspheres were prepared in a manner that the experiments could be repeatable. Microspheres were prepared one batch at a time. PLA grade 4043D was used respectively in the production of microspheres.

2.3.1 Methodology and Experiment

The starting solution is prepared to make the PLA microspheres by dissolving about 40g of the PLA pellets in 800mL of DCM to form oil-in-water (O/W) single emulsions. The oil-in-water emulsion was prepared by dispersing 5mL of the starting solution for every 200mL DCM. The dispersion of the oil phase in the water phase was carried out by (1) using a magnetic stir plate, (2) using an overhead mixer, as well as (3) stirring with a planetary (Thinky) mixer. In each case, the microspheres were formed at room temperature.

Figure 19. The solvent removal process for Emulsion Formation

The microspheres prepared by mixing with the magnetic plate were stirred at 1200 revolutions per minute (rpm) for 60 minutes. The microspheres prepared by mixing with the overhead mixer were stirred at the highest setting on the Hamilton Beach overhead mixer for 4 minutes per every 200mL emulsion system. The microspheres prepared using the planetary vacuum mixer were prepared by mixing at 2000 rpm for 4 minutes under no vacuum. After dispersion, the microspheres prepared are obtained by eliminating the organic phase. This is done by pouring the 200mL emulsion into a 1L beaker filled with distilled water (shown in Figure 19) and chilled 2 hours. (In the absence of distilled water, deionized water can be used). The cold jar of water extracts the solvent from the emulsion whiles solidifying the liquid microsphere droplets formed. The microspheres are then obtained by vacuum filtration. After washing with deionized water, the microspheres dried in a fume hood.

2.3.2 Results and Discussions

Figure 20 shows the flowchart used for the determination of the optimal operational parameters that yield narrowly distributed microspheres with an average size of about 30 microns. The five tunable parameters were namely surfactant type, surfactant concentration, mixing method, mixing time, and mixing speed. To determine the optimal surfactant for our oil-in-water PLA emulsion system, the mixing method was held constant (stir plate), whiles the surfactants shown were dispersed in the bulk phase of the emulsion at the different concentrations shown. Among the three surfactants, PVA was the only one that formed a stable, uniform emulsion system, leading to the formation of microspheres. From literature, it was discovered that a 1% surfactant-to-bulk solvent volume ratio would be ideal for the PLA microsphere emulsion system [107]. With the ideal surfactant and surfactant concentration determined, different methods of mixing were employed, each with unique mixing parameters (time and speed).

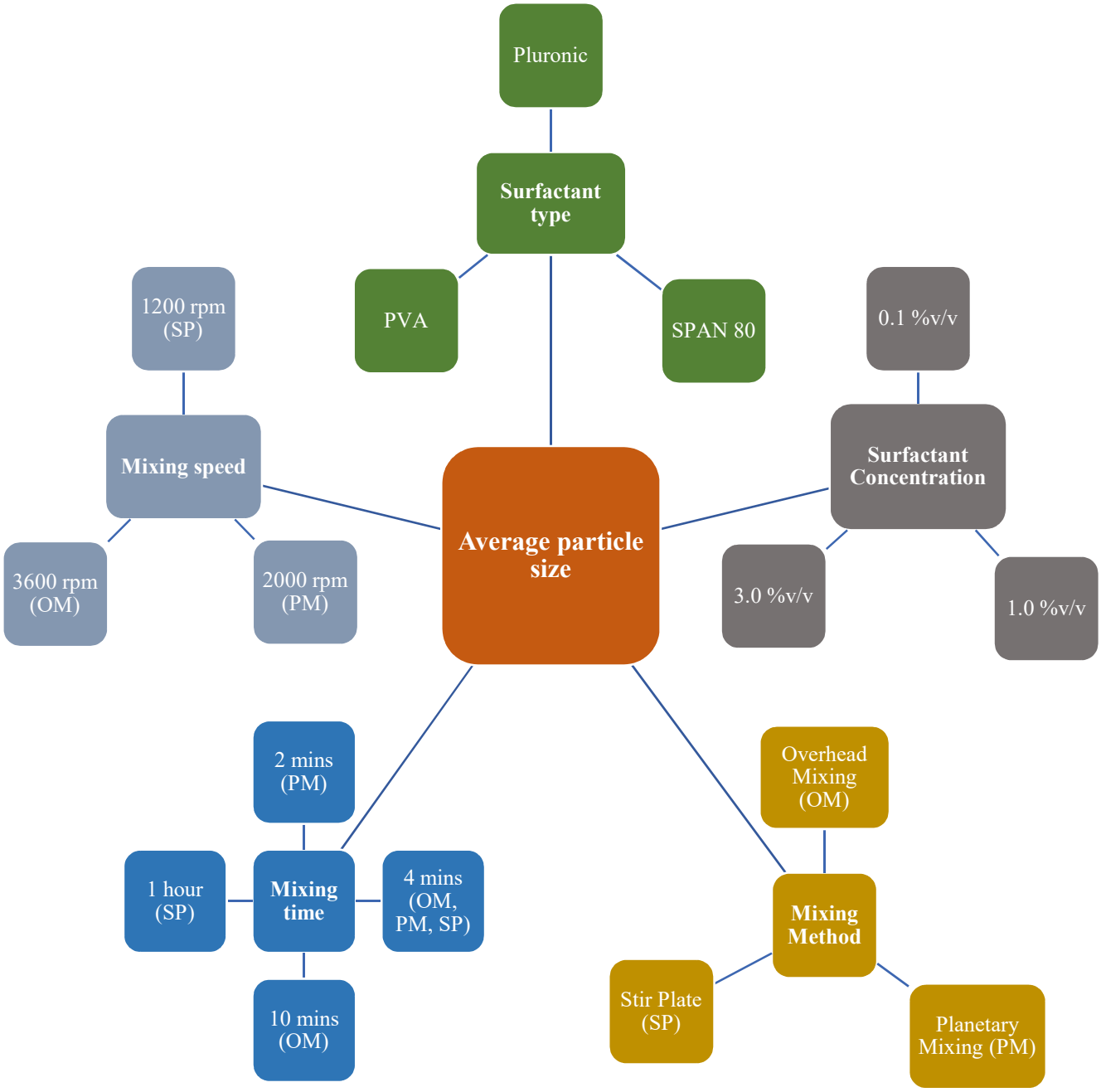

Figure 20. Process Parameter Flow Chart for PLA Microspheres Production

The analysis of how mix speed and mixing time impact the size and size distribution of the PLA microspheres is discussed later in this sub-section.

Different methods were explored for separating the microspheres from solution. After the emulsion was formed, two approaches were employed with the aim of removing the organic solvent (i.e. dichloromethane (DCM)) from the system, one at room temperature and the other at an elevated temperature. The room temperature approach for removing the organic solvent consisted of stirring the emulsion system overnight. The elevated temperature approach involved using a rotary evaporator (Rotavap) set to 50ºC to evaporate the DCM from the emulsion system, since DCM has a significantly higher vapor pressure than water and boils at 39ºC. Upon filtration, the PLA microspheres formed during the emulsion process could not be retained. There was also evidence of DCM traces in the filtrate. The PLA microspheres collected in both cases were also not in solid powder form as was expected. As such, another separation method was needed. A thermodynamic approach whereby a temperature drop was used to enhance separation of the DCM from the rest of the mixture. The water bath shown in Figure 19 was used to accomplish this. After emulsion formation, each 200mL emulsion was slowly poured into a 1L beaker filled with 800mL of chilled deionized water. The cold water was used to extract the DCM from the emulsion as well as solidify the PLA microspheres, which were apparently still in liquid droplet form when we implemented the previous solvent removal methods. This process took place for two hours, after which the liquid phase was decanted, and the PLA microspheres at the bottom of each 1L beaker filtered via vacuum filtration and washed. The dried product yielded powders with desired flowability. The high percent yields of PLA microspheres obtained was an indication that the organic solvent was sufficiently separated from the rest of the system.

Figure 21 shows the Scanning Electron Microscope (SEM) images of the emulsion microspheres prepared with the planetary mixer (A), a stir plate (B), and an overhead mixer (C). SEM data is preferred for this data given that it is a sure way to determine whether or not

microspheres were formed in the emulsion process. In each case, it appears the particles formed are microspheres. TEM is also ideal for particle sizes that tend to the sub-micron range, which is not the case with our data set. The ultimate goal of creating the microspheres is to remove them from a polymer matrix, and as such, the only physical criterion for microsphere production is that they are small enough for layer-by-layer direct ink-writing applications.

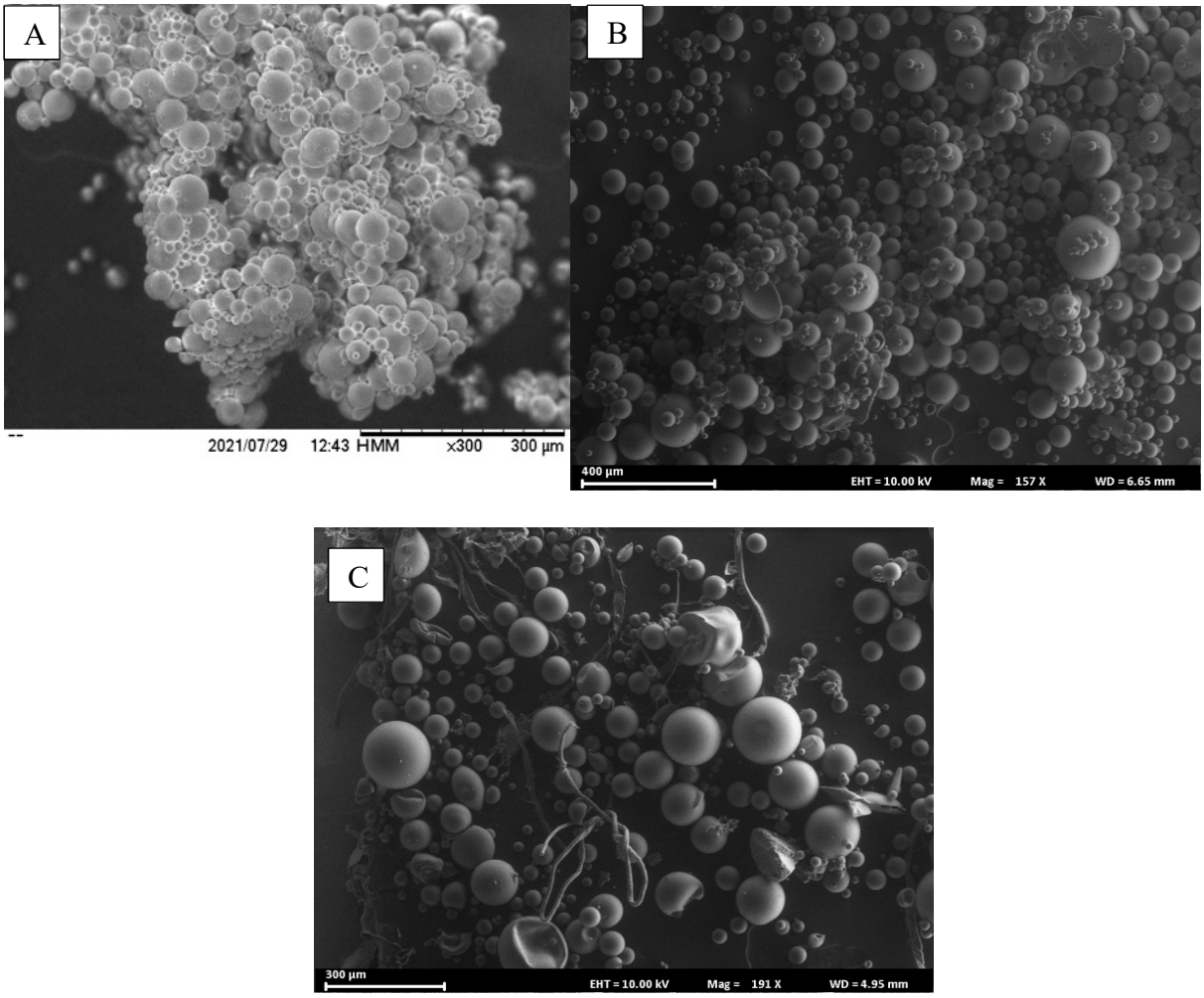

Figure 21. SEM images of (A) Thinky Mixer microspheres, (B) Stir plate microspheres and (C) Overhead mixer microspheres.

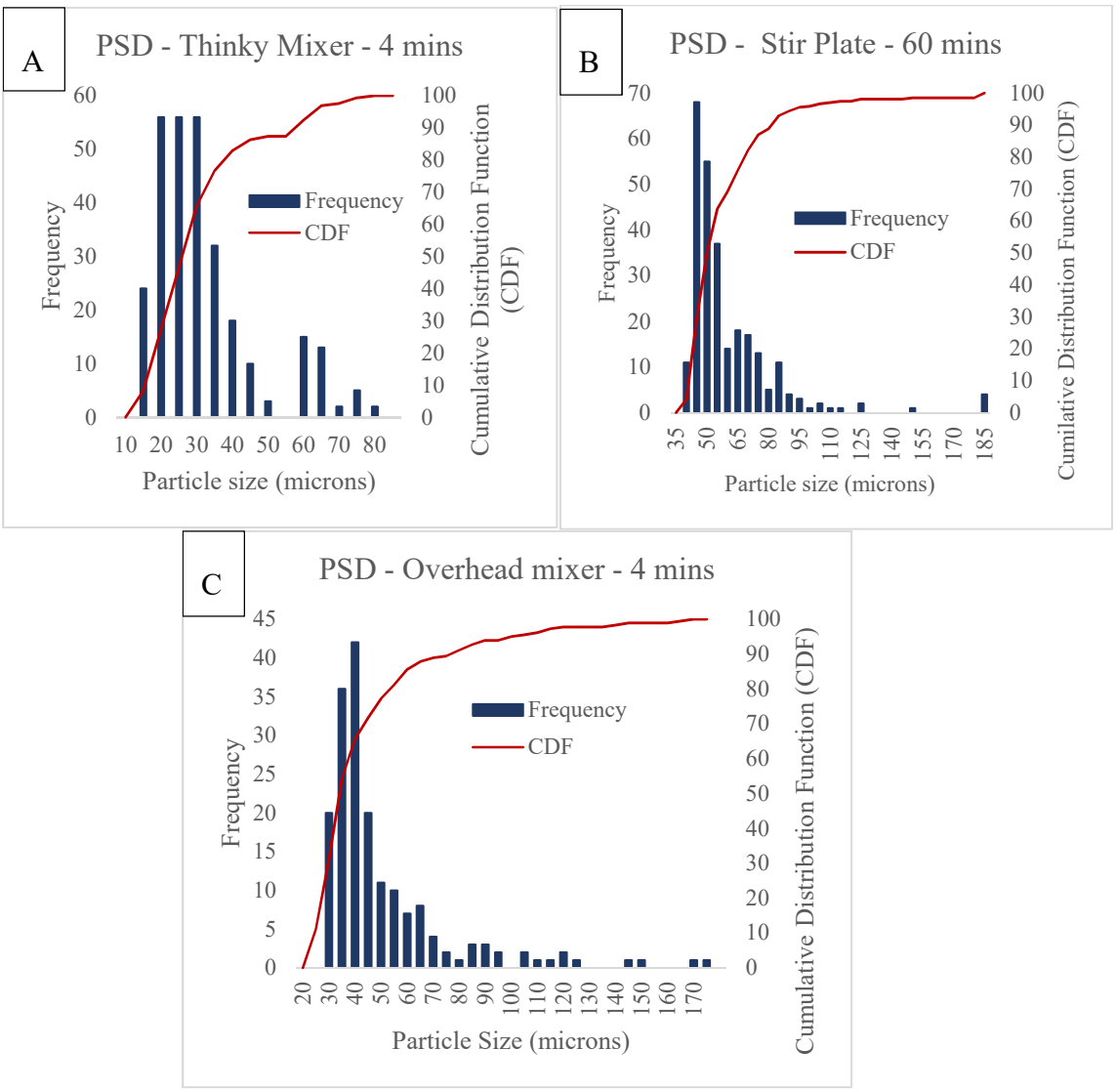

Figure 22. Particle Size Distribution of PLA Microspheres made with the Thinky Mixer (A) stir plate (B) and an overhead mixer (C).

Microspheres are formed in each single emulsion process and have sizes in the micron range. The sizes of the microspheres prepared via the single emulsion methods have diameters one magnitude higher than those prepared via ultrasonic spray pyrolysis. In the emulsion process, we can obtain up to 95% conversion of our polymers into microspheres.

A comparison of the three mixing methods reveals a correlation between mix speed and particle size. The speed of mixing for each of these methods also differs significantly. The smaller spheres are mixed for a much shorter time in the planetary than the larger spheres prepared on the stir plate.

The emulsion system takes longer to form on the stir plate. In addition, the planetary mixer introduces a substantial amount of shear force, which directly impacts the size of the microspheres, irrespective of the short mixing time. In each of these events, microspheres are prepared one batch at a time.

Figure 22 shows the particle size distribution data for the PLA microspheres prepared with the planetary (Thinky) mixer (A), stir plate (B) and the overhead mixer (C). This data was generated using a MATLAB program according to what is described in section 2.2.2.1. A comparison of the graphs in Figure 23 reveals that the microspheres prepared using the planetary mixer are relatively more narrowly distributed than those prepared using the stir plate and the overhead mixer.

In the emulsion processes, about 0.23g of PLA is collected for every 5mL of the starting solution. This represents over a 95% conversion of our starting PLA material into microspheres. Whereas this represents a large number, we can only make as many PLA microspheres as possible on a lab scale, given the amount of water needed to disperse even a small amount of PLA/DCM from the starting solution. Figure 23 compares microspheres prepared on a stir plate, mixed for 10, 30, and 60 minutes, all stirred at 1200rpm. The graph shows that the mixing speed and particle size distribution are not strongly correlated. Each mixing speed shows similar distributions across the particle size range shown. At longer mix times, however, more particles are seen in the lower micron size range. The Hamilton Beach mixer used had three-speed

settings. Microspheres were prepared with the highest mixing speeds, introducing the most shear into the emulsions. When the emulsion is stirred for longer than 4 minutes, the formed microspheres deform under the continuous shear applied. Mixing at the highest speed setting on the overhead mixer for 4 minutes was the optimum mixing criteria for the overhead mixer.

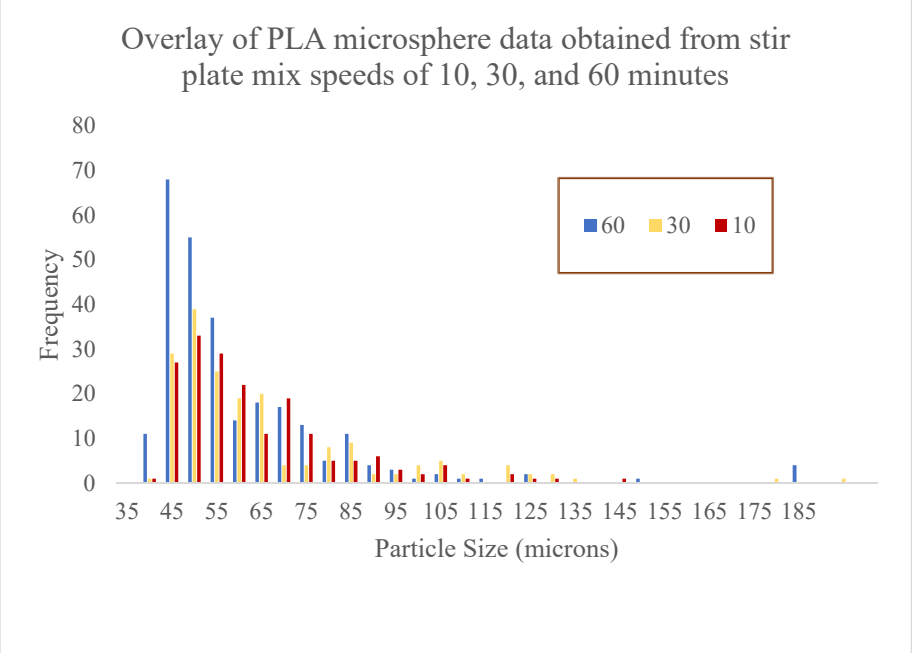

Figure 23. Overlay of PLA microspheres stirred at 10, 30, and 60 minutes on a stir plate.

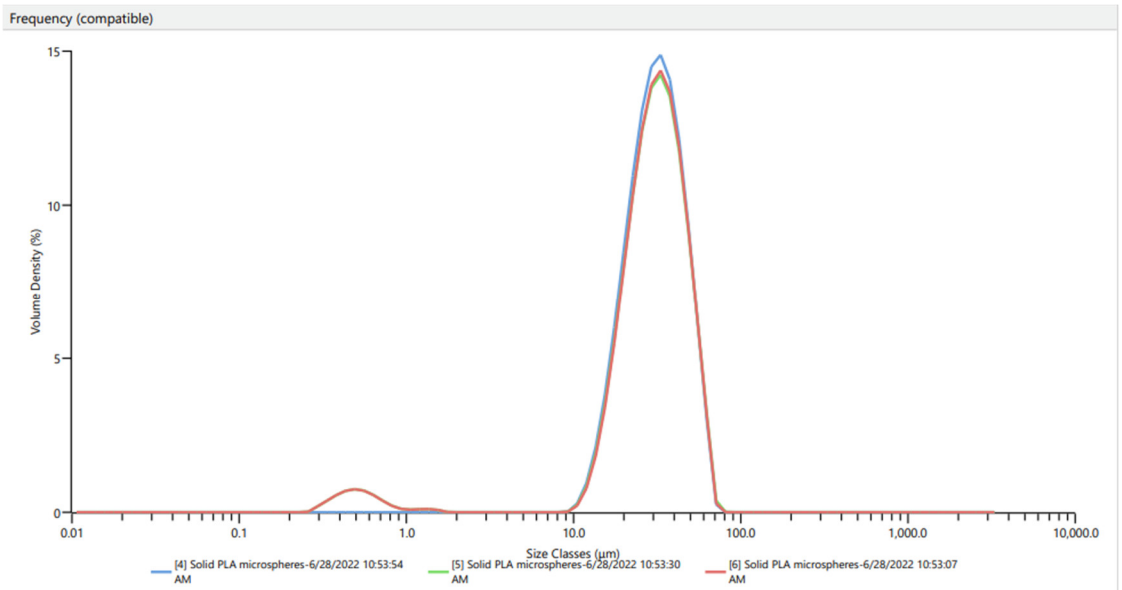

Record number	Sample Name	Dx(10) microns	Dx(50) microns	Dx(100) microns
4	Solid PLA microspheres	18.3	31.0	49.8
5	Solid PLA microspheres	16.7	30.7	50
6	Solid PLA microspheres	16.8	30.8	49.9
Mean		**17.3**	**30.8**	**49.9**
1x Std Dev		**0.877**	**0.205**	**0.110**
1xRSD (%)		**5.08**	**0.666**	**0.220**

Figure 24. Particle Size Analysis of solid PLA microspheres stirred in a Planetary Mixer for 5 minutes.

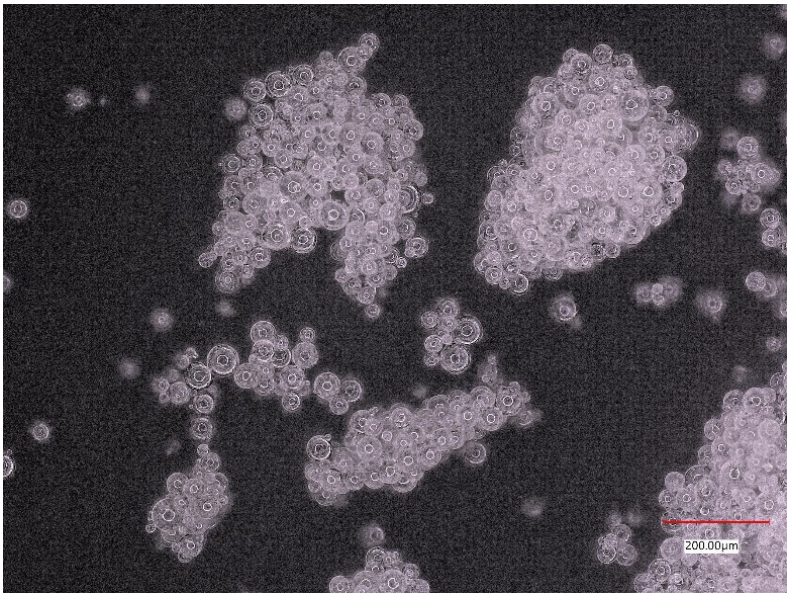

Figure 25. Optical Microscope image of PLA microspheres stirred with a planetary mixer for 5 minutes.

Figure 24 shows the particle size distribution of microspheres prepared using a planetary vacuum (Thinky) mixer. The Malvern Mastersizer generated the particle size distribution shown. The difference between Figure 24 and the one shown in Figure 22C is that the microspheres in Figure 24 were stirred in the Thinky mixer for five minutes as opposed to 4 minutes of mixing for the microspheres shown in Figure 22C. A comparison between the two distributions revealed no significant impact of an increased period of mixing on the size distributions. Figure 24 is an optical image of the microspheres prepared by stirring emulsion mixture for five minutes, captured with a Keyence Microscope. This further shows that the particle size distribution changes slowly with increased mixing time for a given mixing speed. The size range of the particles would also suggest that a dynamic light scattering (DLS) approach would not be ideal, since the microparticles are relatively large. Figure 26 compares the three different methods used to prepare single emulsions. Out of these three methods, the overhead mixer appears to be the best method for creating micron-sized spherical particles in a repeatable, efficient way.

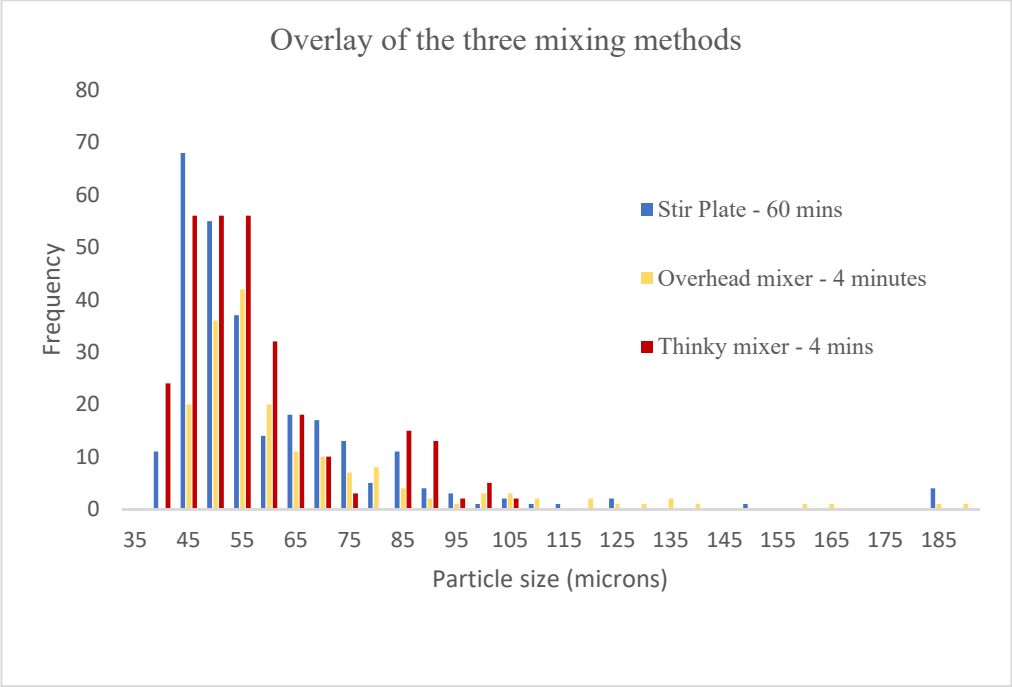

Figure 26. Overlay of the optimal size distributions obtained from the three mixing methods (Stir plate, overhead mixing, and planetary mixer)

Table 3 compares all three mixing methods by comparing their process times, particle size range, and particle size distributions. We deduce from the above results that planetary mixing is the most efficient way to prepare small, monodisperse PLA microspheres. The table, along with the particle size distribution graphs in Figure 20, further reveal that for each of these processes, there are tunable parameters that directly impact the sizes and size distribution of the microspheres. Mixing speed, length of mixing, the concentration of the starting solution, and even the concentration of the precursor are all parameters that can be tuned to obtain a narrower distribution of microspheres. This might take longer for mixing methods such as the stir plate, but a narrower size distribution is theoretically attainable. Following the results, an emulsion was prepared using the planetary mixer with all parameters remaining the same, except the mixing time.

Figure

Table 3. Comparison of Methods Used for Microsphere Synthesis

	Stir Plate			**Overhead Mixer**		**Planetary Mixer**
Mixing/Process time (mins)	10	30	60	4	10	3
Mixing speed (rpm)	1200			"III"	"III"	2000
Particle Size Range (microns)	30-130	34-129	37-124	25-125	n/a	11-77
Particle Size Distribution	polydisperse			polydisperse		monodisperse
Overall Comments	All PLA in the emulsion is converted into microspheres; sizes are the largest among all other mixing methods.			Not all the PLA in the solution become microspheres. The sizes of the spheres are smaller than those prepared on the stir plate		Microspheres are smaller, well-defined, and monodisperse.

2.4 Conclusions

The results show that both ultrasonic spray pyrolysis and the emulsion processes consistently produce spherical microparticles. It was determined that mixing time, the desired particle size, the desired size distribution, as well as the viscosity of the phases present may influence the method that is chosen to prepare microspheres. Of the methods discussed, Ultrasonic Spray Pyrolysis is best for producing particles less than 10 microns, given the appropriate concentration of the starting solution. In general, the single emulsion processes are ideal for producing microspheres at high conversion rates for applications where a narrow particle size distribution is not be a stringent requirement. The overhead mixer has the highest speed of the methods chosen and is ideal for systems with at least one highly viscous phase, when the time of mixing is constrained such that the formed microspheres are not destroyed, as was seen in Figure 22C. Planetary mixers can form emulsions within a short time, producing microspheres with a narrow size distribution. They can also operate at relatively high speeds (up to 2000 rpm) without added shear from a blade that may deform the formed particles, which is the case for overhead mixers.

Higher mix speeds generally correlate to smaller particle sizes and narrow size distributions. High shear mixing leads to the formation of microspheres within a matter of minutes. Emulsions by magnetic stirring can generate relatively small particles but may not be as efficient in generating a narrow distribution and do not constitute a high amount of shear mixing. When the phases are uniform and have a low viscosity, however, uniform particles with a narrow size distribution can be generated with this stirring method.

Planetary mixing proved to be most efficient of the three emulsion methods discussed for emulsion preparation, given that it can be carried out in a short time, mixed with little to no filming/crystallization of the PLA, while producing microspheres with a relatively narrow size

distribution. The only downside to this method, along with the other methods described in this chapter, is that each method is a batch process. A straightforward, scalable, continuous approach for narrowly distributed microsphere production will be the focus of any future work.

Further studies can be done to determine precisely how various PVA surfactant ratios, duration of mixing and speed of mixing impact the size of PLA microspheres. With enough data, a factorial analysis method such as ANOVA (analysis of variance) or another statistical tool can be used to determine which parameter or combination of parameters has the most impact on the particle size and particle size distribution of PLA microspheres.

CHAPTER 3

Polymer Modification

3.1 Introduction

In this chapter, we will discuss how polymeric microspheres can be modified. Such modification may be desired to alter properties such as hydrophobicity/hydrophilicity, crystallization temperature, decomposition temperature, and the mechanical properties of the polymer. The functional groups in polymers allow for surface modification, polymer grafting, and block copolymerization, among others. PLA is an asymmetric aliphatic ester with functional groups that can be modified. The ring-opening polymerization of lactide to form PLA is also a reversible process. As with esters, PLA can undergo hydrolysis to form an acid and an alcohol. Due to PLA's asymmetry, other variations of the polymer can be formed, namely PDLA, PLLA, and PDLLA. This makes PLA highly functionalizable. PLA generally ranges from semi-crystalline to amorphous, depending on the fraction of stereoisomers existing within the compound. In this section, we will focus on click chemistry, surface modification, and block copolymerization of PLA.

3.2 Click Chemistry/Polymer Grafting

Upon condensation, polynucleotides, polypeptides, and polysaccharides reversibly produce smaller unit oligomers. The reverse reactions from the oligomers to polysaccharides/polypeptides/polynucleotides occur in nature through the linking of smaller unit molecules by way of carbon-heteroatom-carbon bonds [108, 109]. The term coined to represent reactions that produce larger molecules by carbon-heteroatom connections among smaller molecules is known as Click Chemistry. In the past two decades, researchers have found great utility in this simple, straightforward synthesis approach that mimics reactions in nature for

applications, mainly in drug delivery, where the molecules involved are complex. Click chemistry reactions also occur at room temperature. Not every molecule with heteroatomic bonds can be conjugated to form larger molecules by click chemistry. The Nobel prize for Chemistry in 2022 was awarded to three scientists for discovering and pioneering Click Chemistry reactions around the world [110]. Click chemistry reactions are energetic, and reactions are limited to "spring-loaded" reactants [111]. In addition, reactions following the click chemistry principle must be modular, broad in scope, give very high yields, be stereospecific, involve benign reactants, and produce benign byproducts that are easily removable and insensitive to oxygen and water [111]. The azide group is generally used in click chemistry reactions as a linkage between two molecules. Cycloadditions of unsaturated species, nucleophilic substitution, and non-aldol carbonyl chemistry are examples of reaction syntheses that occur via click chemistry [111].

This section discusses a polymer-polymer reaction that mimics a typical click chemistry reaction. This reaction involves a polymer grafting between PLA and PEG. To do this, we obtained amine-terminated PEG to be reacted with PLA. The reaction between these two homopolymers occurs through an amine linkage, including the formation of heteroatomic bonds, as a candidate for a click chemistry reaction synthesis. The reaction discussed in this section occurs at room temperature and is as such not energy intensive. *N*,*N*,*N*′,*N*′-Tetramethyl-*O*-(*N*-succinimidyl)uronium tetrafluoroborate **(**TSTU) is used as a functional group activator to improve the reactivity of the amine linkage.

3.2.1 Materials, Methodology, and Experimental Investigations

Materials needed include industrial-grade Polylactic Acid (PLA) 4043D obtained from Nature Works, Dichloromethane (DCM) obtained from Cole-Parmer, *N*,*N*,*N*′,*N*′-Tetramethyl-*O*-(*N*-

succinimidyl)uronium tetrafluoroborate **(**TSTU), and amine-terminated Polyethylene Glycol (PEG-NH_2). The reaction described below is modeled after the click chemistry reaction outlined in the article "Amphiphilic phospholipid-iodinated polymer conjugates for bioimaging" [112]

The starting solution prepared according to section 2.3 (41g of PLA dissolved in 800mL of DCM) was used to prepare the appropriate mass concentration of PLA determined for the reaction (i.e., 1.25mg PLA). 0.5mL of this solution contains about $\frac{41.02g}{800mL} * 0.5mL = 25.6$mg of PLA, assuming uniform mixing of the starting solution. To obtain 1.25mg of PLA from the initial solution, the volume of solvent needed to dilute 0.5mL of the starting solution was determined as follows:

$$\left(\frac{25.6mg}{1.25mg} * 0.5mL\right) - 0.5mL = 10.2mL - 0.5mL = \mathbf{9.7mL\ DCM} \quad (1)$$

A solution consisting of 0.5mL DCM containing 1.25mg PLA is prepared from the batch PLA/DCM solution. Adding about 9.7mL of DCM to 0.5mL of the initially prepared PLA/DCM solution should give us an approximately similar mass concentration. TSTU (functional group activator) is slowly added, stirring the reaction mixture for 3 hours. 15.95µL of PEG-NH_2 is added to the solution and stirred at room temperature for 24 hours. The solution is then put into a -20ºC freezer overnight for polymer precipitation.

3.2.2 Results and Conclusions

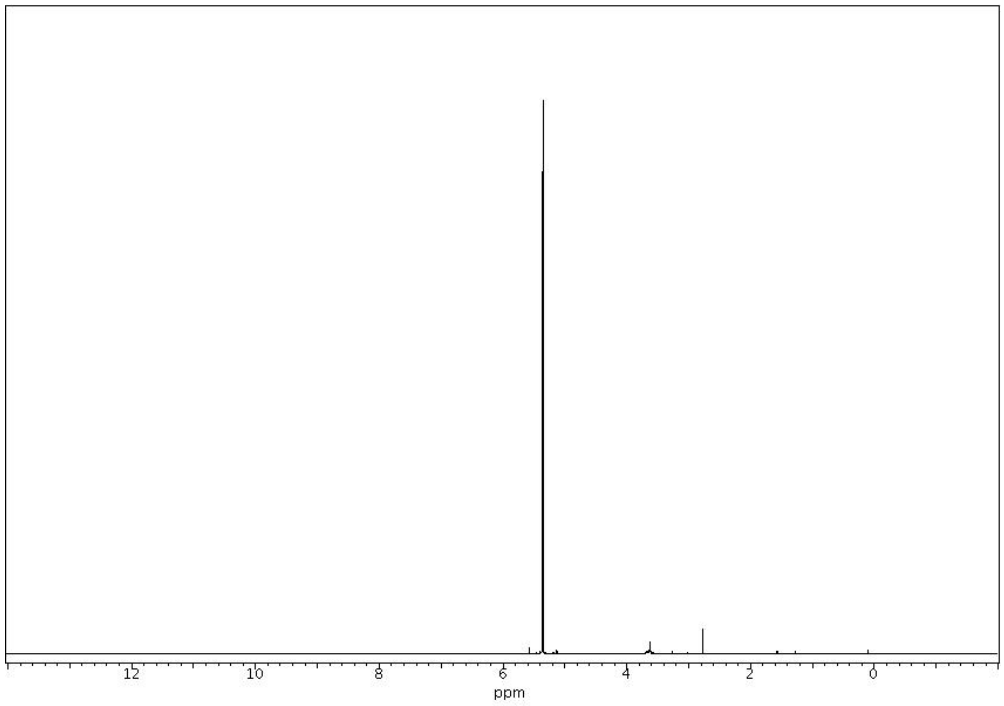

Figure 27. ^{1}H-NMR spectrum of the product resulting from click chemistry reaction between PEG-NH_2 and PLA

Figure 27 shows the proton NMR spectrum of the click chemistry product of the reaction described in section 3.2, with deuterated chloroform as the solvent. The peaks centered about 3.6 and 5.37ppm correspond to the O-CH_2 group in PEG-NH_2 and O-CH group in PLA, respectively [113, 114] indicating the presence of both PEG and PLA blocks present in the product. The intensity of the signal centered on 5.37ppm is indicative of a strong presence of PLA in the sample that was measured in comparison to PEG – NH_2. The spectrum does not, however, show a peak around 1.53, which would correspond to the methyl groups in PLA. If the block copolymer did form, this peak's absence could indicate that the methyl groups are shielded.

The successful PEG – PLA block copolymer synthesis would result in the formation of a peptide bond between the amine end group in PEG and the carboxylic end group in PLA. The

NMR spectrum shown is not sufficient for concluding that the bond formed. In general, for a peak corresponding to the peptide bond to be observed in the NMR spectrum, the relative concentration ratio of reactants must not exceed several orders of magnitude, which is precisely the case with our system. The PLA molecule has a molecular weight of 10^5 g/mol, whereas that of PEG-NH_2 is less than 500g/mol. This disparity in molecular weight, despite a 1:1 mass ratio between the polymers, makes it difficult to observe a representative peak in the NMR spectrum.

It was concluded that a lower molecular weight PLA would be required to establish the peptide linkage. This knowledge about long chain PLA molecules informed the direction of the block polymer synthesis discussed in section 3.3, as lower molecular weight PLA was used in place of a diluted, low mass, high molecular weight PLA.

3.3 Block Copolymerization

This section presents a bulk method to polymerize D, L-lactide in the presence of Methoxy-PEG (mPEG), to form a mPEG-co-PLA Diblock copolymer. mPEG is used to limit polymerization to one side of the homopolymer, to form the diblock copolymer.

3.3.1 Materials, Methodology, and Experimental Investigations

The materials needed to perform the synthesis include methoxy PEG (mPEG) obtained from Sigma Aldrich, a Drying agent, Toluene, Stannous Octoate, dichloromethane, Diethyl Ether, (D, L)- lactide.

Methoxy PEG, mPEG, is initially recrystallized in Toluene two times for about 48 hours prior to the experiment. Toluene is also dried using a drying agent. 0.05% w/w stannous octoate in Toluene solution is prepared. mPEG and DL-lactide are added to a round-bottomed flask. 0.5mL of the stannous octoate/toluene solution is added to this mixture. The content of the flask

is degassed for an hour with a nitrogen flow. The round-bottomed tube is then sealed under static nitrogen and placed inside a silicon oil bath heated to 140ºC and left to stir for 22 hours. The formed polymers are then dissolved in DCM to purify, followed by precipitation using cold diethyl ether.

3.3.2 Results and Conclusions

Figure 28 below shows the TGA data of the synthesized mPEG-PLA block copolymer. The two decomposition regions correspond to the decomposition profiles of the monomer (D, L-Lactide) and homopolymer (mPEG) that participated in the polymerization process.

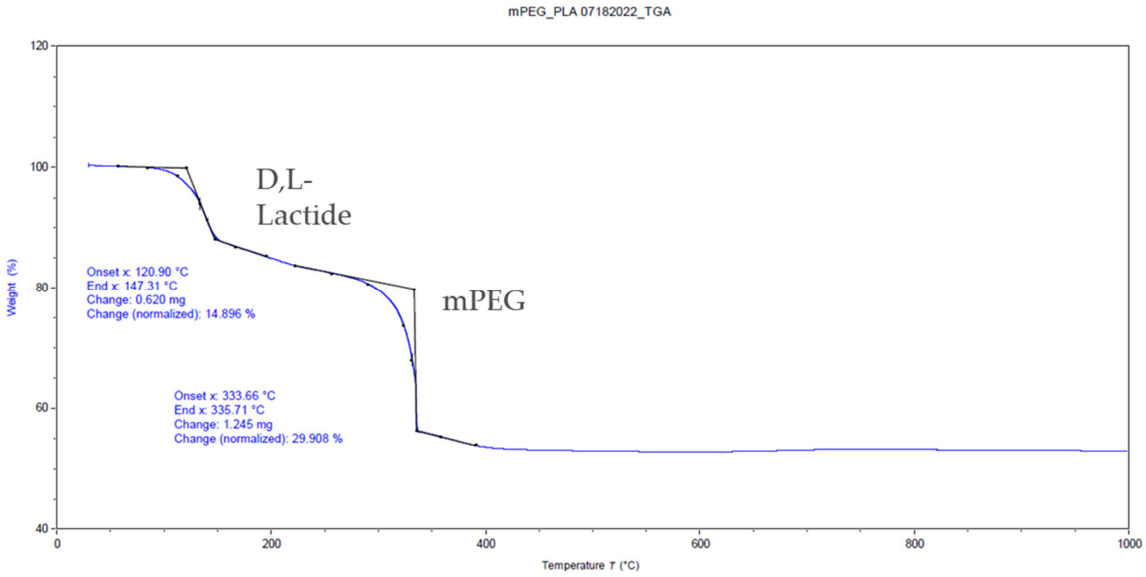

Figure 28. TGA data of the synthesized mPEG-PLAL block copolymer.

Figures 29-31 below show the FTIR spectra of the PLA-PEG block copolymer product, the lactide monomer, and the mPEG homopolymer. The spectrum of the product (Figure 29) shows characteristic peaks for both mPEG (Figure 30) and D,L-lactide (Figure 31), when compared with Figures 30 and 31 respectively. The peaks in the lower wavenumber range for the BCP product comprise an overlap between D, L-Lactide, and mPEG.

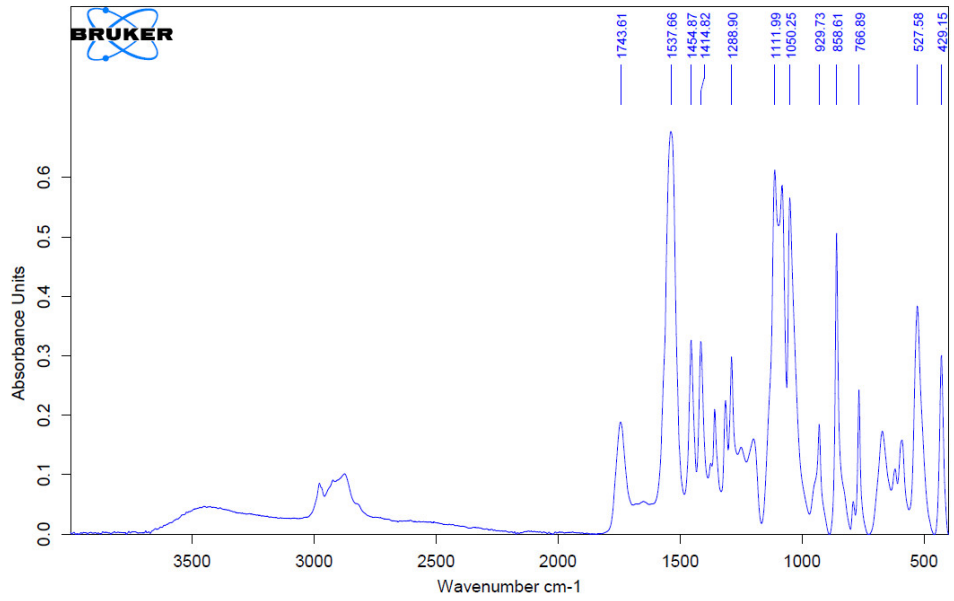

Figure 29. FTIR absorbance spectrum of block copolymerization (BCP) product.

Peaks are observed around 2800 cm^{-1} in all three spectra, and yet, they are all different in nature. These peaks represent the C-H bond stretching, which is present in all molecules. These peaks not being the same could be indicative of the fact that the C-H bonds in all three compounds are all bound to different groups, and as such could serve as corroboratory evidence of block copolymer formation.

In Figures 29 and 31, the peak at 1743 cm^{-1} corresponds to the C=O double bond in both the PLA block of the copolymer and lactide. The signal in Figure 31 is stronger than in Figure 29. Lactide has two C=O double bond units, which explains the intensity of the peak. The lower intensity peak in Figure 31 shows that the C=O bond stretching observed in the block copolymer is not the same as that in D-L lactide, which could be an indication that lactide was ring-opened and copolymerized unto mPEG. This however is not sufficient evidence for the claim.

The weak intensity broad peak observed around 3500 cm^{-1} in Figure 29 is likely from the -OH end group of the unreacted mPEG chains. The formation of the block copolymer is corroborated by an NMR spectrum analysis.

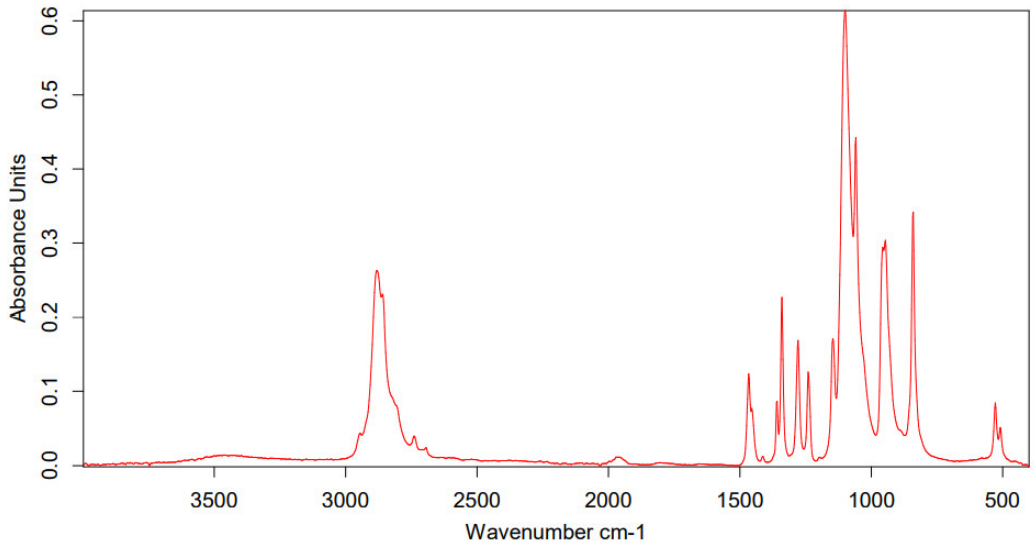

Figure 30. FTIR Absorbance spectrum of mPEG

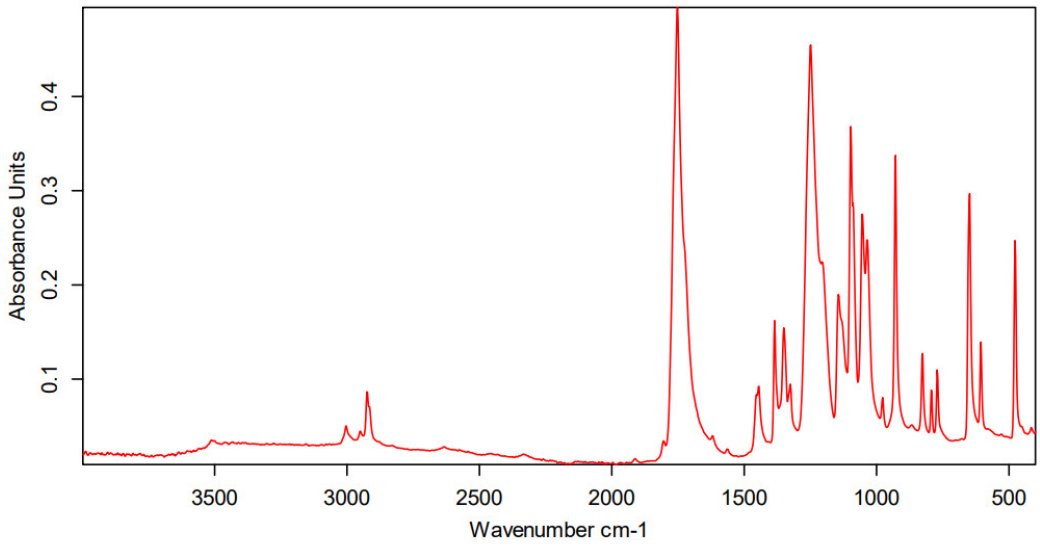

Figure 31. FTIR absorbance spectrum of DL-Lactide

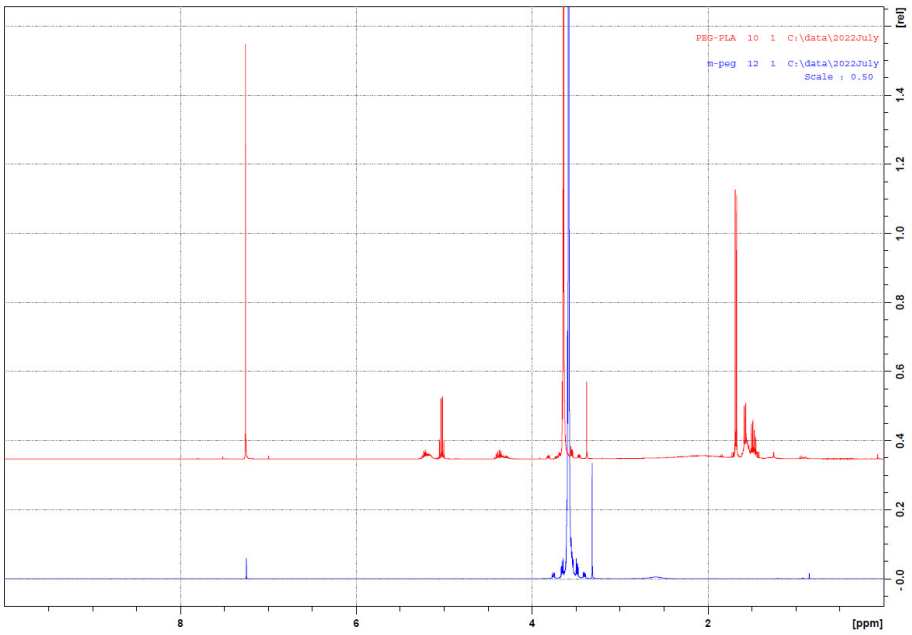

Figure 32. ^{1}H NMR spectra of both the mPEG-PLA block copolymer and mPEG.

Figure 32 shows the NMR spectra of the block copolymer product and mPEG. The NMR data confirm the block copolymer's formation, as noted in the literature. Characteristic peaks at be seen at 5.17ppm and 3.64 ppm correspond to PLA and mPEG, respectively. The peaks between about 1.4 to 1.8ppm correspond to the ester group the block copolymer. The peaks recorded between centered around 3.64 correspond to the O-CH_2- bond in the PEG block of the copolymer, and the characteristic peak at 5.17ppm corresponds to the -O-CH portion of the PLA block [115]The yield recorded for this product was low. Out of the total 20g of reactants used in the process, only about 1g of the reaction product was recovered.

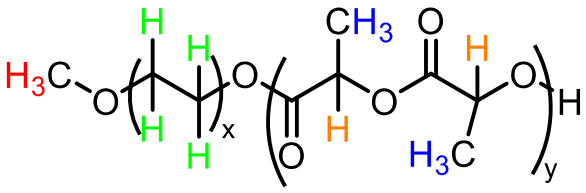

H	Integration	H/unit	Units
H	3	3	1
H	167.9636	4	41.99
H	11.2917+3.4059	2	7.3488
H	37.3899	6	6.23165

Figure 33. Chain length determination of ^{1}H-NMR data for mPEG-PLA Block Copolymer Structure from peak integration

Figure 33 shows the Integration results of the ^{1}H-NMR spectrum for the mPEG-PLA block copolymer product. The analysis of the spectrum is based on the four distinct Hydrogen atoms that found in the structure. The Hydrogen atoms are differentiated based on the type of carbons they are bonded to as well as the block of the copolymer it corresponds to. The elements are color coded in Figure 33 for easy identification. The methoxy end group of mPEG does not participate in the polymerization process, hence the presence of only one unit of that hydrogen. The green hydrogen is characteristic of the PEG block of the copolymer. The mPEG [$CH_3(OCH_2CH_2)_nOH$] used in this synthesis has an average number molecular weight of 2000g/mol. The molecular weight of the mPEG end groups (methane and hydroxyl) subtracted from the molecular weight of the repeat unit is about 44g/mol. To obtain the number of repeat units, we divide (2000-44 = 1956) by 44, which gives about 44.5. In terms of polymer chain

length averages, this number is consistent with the number of units reported in the NMR data analysis for the PEG block shown in Figure 33, which is an indication that mPEG was not altered in the block copolymerization process. The objective of the synthesis was to polymerize D,L-lactide unto mPEG without altering the PEG unit. Thus far, the data suggests that the latter part of the objective was attained. The peaks corresponding to the Hydrogen atoms in the PLA block were also integrated. It is determined from the data that six to seven units of D,L lactide was polymerized unto mPEG. In the synthesis reaction, the reactants were combined in a 1:1 mass ratio. The lactide was as a result the limiting reagent, given its higher number of moles. To extend or reduce the chain length of the copolymer, the amount of lactide added can be adjusted accordingly. If the block copolymer can be converted into microspheres, they can be directly incorporated into a polymer matrix as pore formers. The experiment can be scaled up for industrial production.

Figure 34 shows the DSC profile of the block copolymer sample. A peak temperature is observed at 43.28^{o}C. This temperature is lower than the melting temperature of the PLA microspheres prepared (148.1^{o}C). The block copolymers can be made into microspheres using a melt emulsion process. Figure 35 shows that the particles are not microspheres but appear in the lower micron-size range. This could also mean they might be more easily removable than PLA from a polymer matrix.

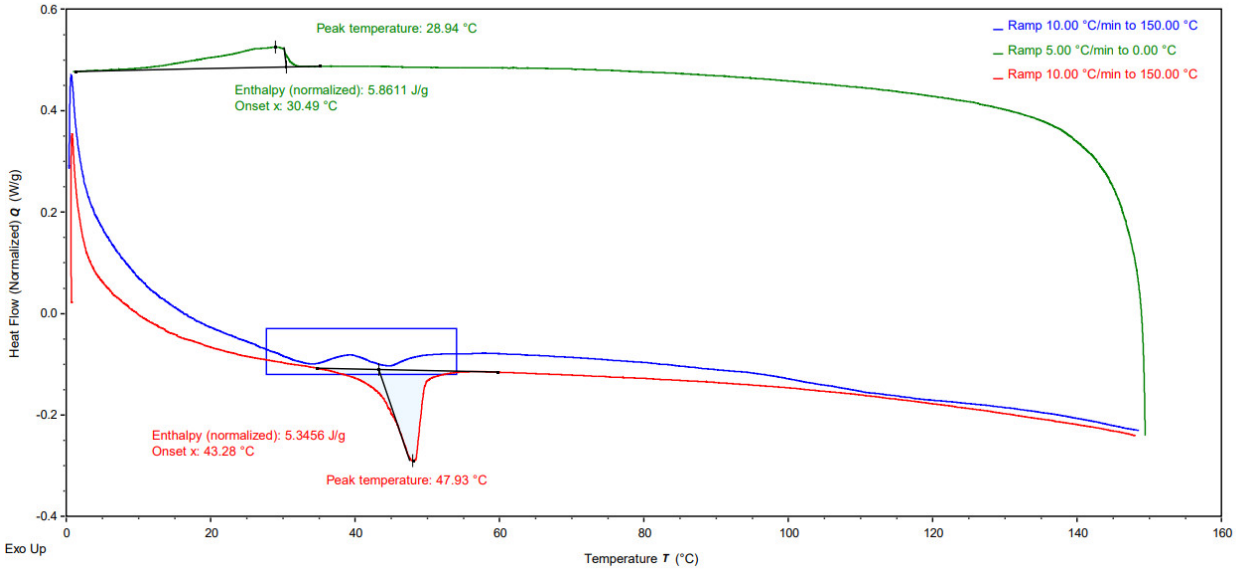

Figure 34. DSC profile of the mPEG-PLA block copolymer.

Figure 35. Microscopic image of mPEG-PLA block copolymerization product.

3.4 Surface Modification

The surface modification allows for the surface properties of polymers to be modified. Polymers may exhibit desired bulk properties but may lack the surface properties that make them an ideal

candidate for a specified application. Surface Modification seeks to change that. Polylactic acid, for example, is a well-known biodegradable, non-toxic polymer used in many biological applications but is hydrophobic. As an ester, polylactic acid has functional groups that make it easy to surface modify and make their surfaces more hydrophilic. In this research, polymer microspheres were surface modified by attaching hydroxyl groups to the surface, making them more reactive in subsequent reactions. We also wanted to understand whether the polymer's bulk properties are affected by surface modification.

3.4.1 Materials, Methodology, and Experimental Investigations

A 0.01M NaOH solution is prepared by dissolving 1g of NaOH in 800mL water. The already-formed microspheres are mixed into the solution and remain in the solution overnight.

3.4.2 Results and Conclusions

Figure 36 shows the zeta potential measurement of PLA microspheres before and after being surface modified with hydroxyl groups, measured in mV. The data shows that the average of the absolute surface charge of the particles decreases with the addition of –OH groups, confirming the successful attachment of the functional group. The lower magnitude of the zeta potential measurements also shows that surface-modified microspheres are less likely to flocculate in solution.

Figure 37 also shows the overlay of the absorption spectra of PLA and surface-modified PLA microspheres. The broad peak centered at the wavenumber 3400 is a characteristic peak of the –OH bond, observed in the surface-modified PLA spectrum and not in the original PLA spectrum.

All other characteristic peaks associated with PLA are aligned in both profiles, indicating that surface modification was achieved.

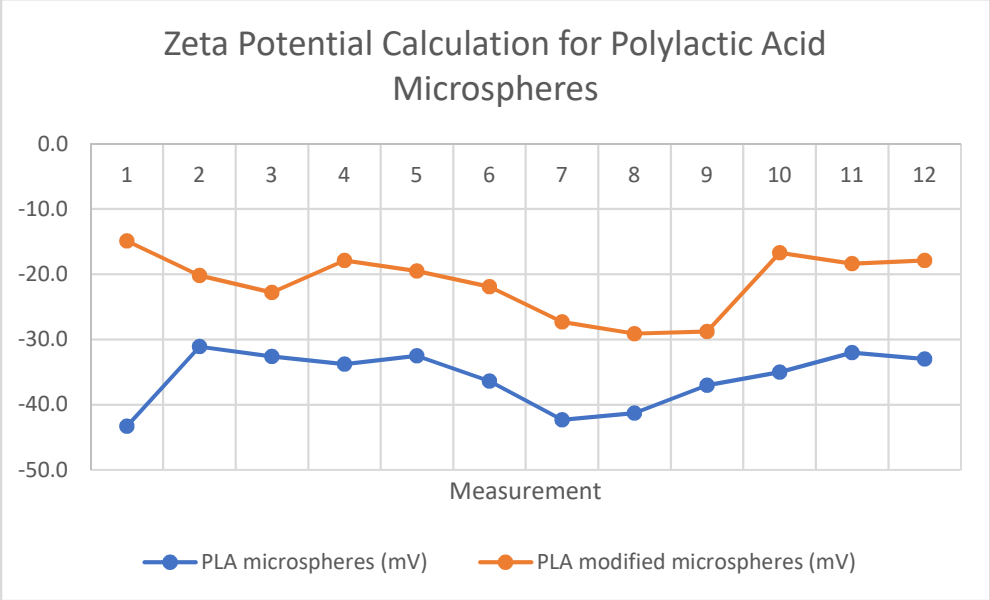

Figure 36. Zeta potential measurements of PLA microspheres before and after surface modification

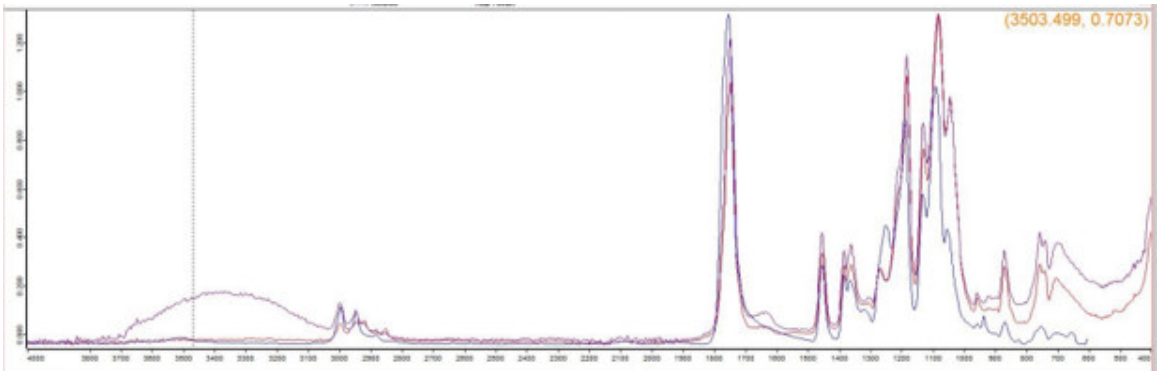

Figure 37. FTIR overlay of PLA and surface-modified PLA microspheres

Surface-modified microspheres were incorporated into a PDMS matrix to investigate the change in the hydrophilicity of PLA microspheres (since PLA is hydrophobic) and their thermal properties. PLA microspheres that had not been surface-modified were also incorporated into a

PDMS matrix as a control. TGA on the cured matrices was performed to investigate these properties, as shown in Figure 38. The TGA showed that neither the thermal properties of the matrix nor the filler material was impacted due to surface modification. The modified PLA microspheres were also immersed in water to dissolve them. The microspheres did not dissolve. This indicates that surface modification only impacts the material's surface properties, not bulk ones.

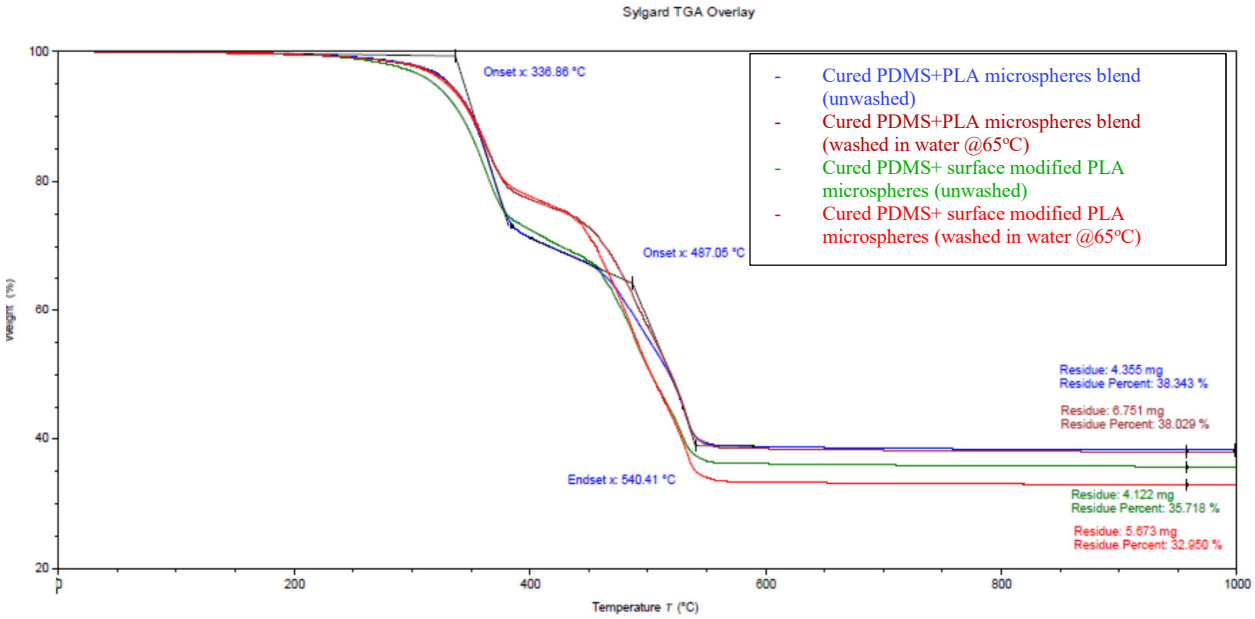

Figure 38. TGA overlay of pure and surface-modified PLA-loaded PDMS (Sylgard 184).

The successful modification of PLA microspheres is helpful for subsequent research. Hydroxyl groups on the surface of microspheres may enhance the formation of core-shell particles, and in the right reaction medium, block copolymers in the solution are formed.

CHAPTER 4

Pore formation: Microsphere Incorporation

4.1 Introduction

The objective of this research remains creating porosity in polymers by embedding pore former materials in the polymer additive manufacturing feedstock. Previous chapters covered different methods for the synthesis and modification of PEG and PLA pore former microspheres. The polymer microspheres are blended into matrices at 10%, 25% and 35% loading rates. PDMS (Sylgard 184) is chosen as the matrix material for all applications in this chapter. Silicone is chosen due to its prevalence in additive manufacturing applications, as well as its elastomeric properties among others. Sylgard 184 is also an RTV silicone, and as such is easy to work with. The rheological properties of the polymer blends are studied. The blended microspheres are then removed from the polymer matrix by solvent extraction and by calcination. The polymer material before and after microsphere removal is studied and characterized by optical imaging, thermogravimetric analysis (TGA), and dynamic mechanical analysis (DMA). The changes in the density and porosity of each polymer blend and each polymer are also investigated.

4.2 Microsphere incorporation into matrices

PLA and PEG microspheres are incorporated into PDMS matrices at different loading percentages. This study is conducted to determine the impact of polymeric pore formers and the porosity they create in matrices on the mechanical properties of the polymer matrix. At each microsphere loading percentage, the pore fillers are introduced into the matrix and mixed using the planetary vacuum mixer under vacuum to facilitate uniform mixing. The matrices are then cured in an oven set at 212ºF for 35 minutes.

Matrix: Sylgard 184 (PLA microspheres before removal)

Microsphere loading	Characterization
10%	TGA DMA Rheology Keyence Mass
25%	TGA DMA Keyence Mass
35%	TGA DMA Keyence Mass

Matrix: Sylgard 184 (neat sylgard before removal)

Microsphere loading	Characterization
0%	TGA DMA Rheology Keyence Mass

Matrix: Sylgard 184. PLA microsphere loading after removal process

Microsphere loading	Core Removal	Characterization
10%	Water extraction	TGA DMA Keyence Mass
	Calcination	TGA DMA Keyence Mass
	DCM Extraction	TGA DMA Keyence Mass
25%	Water extraction	TGA DMA Keyence Mass
	Calcination	TGA DMA Keyence Mass
	DCM Extraction	TGA DMA Keyence Mass
35%	Water extraction	TGA DMA Keyence Mass
	Calcination	TGA DMA Keyence Mass
	DCM Extraction	TGA DMA Keyence Mass

Figure 39. Plan for microsphere incorporation into Sylgard 184 matrix

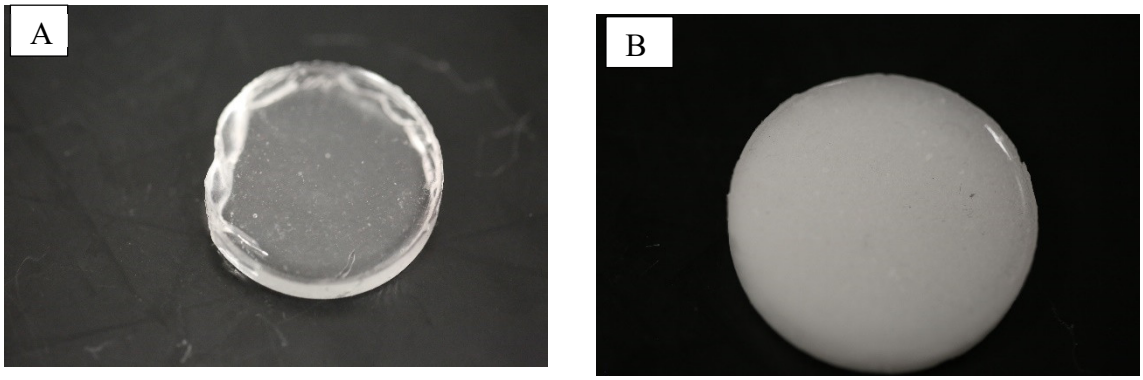

Figure 40. Sylgard 184 matrix loaded with 0% (A) and 10% (B) PLA microspheres

The cured polymer blends are then characterized. PDMS matrices will be loaded at 10, 25, and 35% with PLA, PEG, and modified PLA microspheres created in Chapters 2 and 3. In the case of PEG, liquid PEG 200 was vigorously mixed into PDMS at the same loading percentages with a planetary mixer and immediately cured, converting PEG microdroplets to PEG microspheres. This alternative path was chosen to overcome the challenges associated with producing PEG microspheres using the USP process and the oil-in-water single emulsion process.

4.3 Microsphere removal

Matrices loaded with PLA microspheres were imaged and weighed, then the microspheres were removed. Three removal methods were employed in the removal of microspheres, namely water extraction (leaching), DCM extraction, and calcination (bake-out). In the organic solvent (i.e., DCM) extraction, each sample is wrapped with perforated aluminum foil and suspended in a beaker containing the extraction solvent. Water washing is carried out by suspending samples in water in a centrifuge tube. The tube is then immersed in a water bath sonicator with sonication turned on and the water set to 69ºC. Both leaching methods are carried out overnight. The calcination process is carried out by placing the loaded matrices in an oven set to a temperature that removes the microspheres whiles keeping the matrix material intact for a period.

4.3.1 Organic solvent extraction

Figures 41 and 42 show the images of PDMS-PLA blends before and after removal of PLA from the matrix by organic solvent leaching for 10 wt. % and 25 wt. % PLA respectively. The solvent chosen was dichloromethane (DCM). In each case, a triplicate sample was used, in addition to a neat sample containing no microspheres, to account for repeatability. The figures show that DCM sufficiently leached the microspheres from the polymer blend, based on the translucence of the polymer observed. It appears, however, that some of the microsphere

aggregates trapped in the matrix are not removed. DCM swells PDMS and, as such, leaches the microspheres from the matrix by dissolving it.

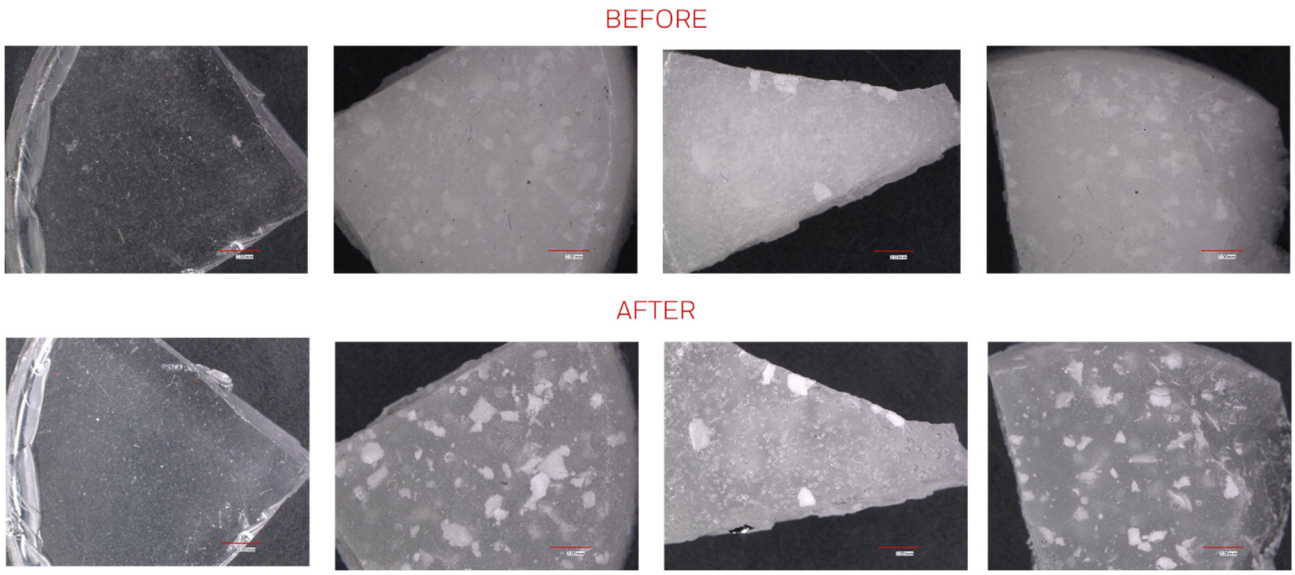

Figure 41. Optical microscope images of matrices before and after DCM extraction – 10% PLA loading

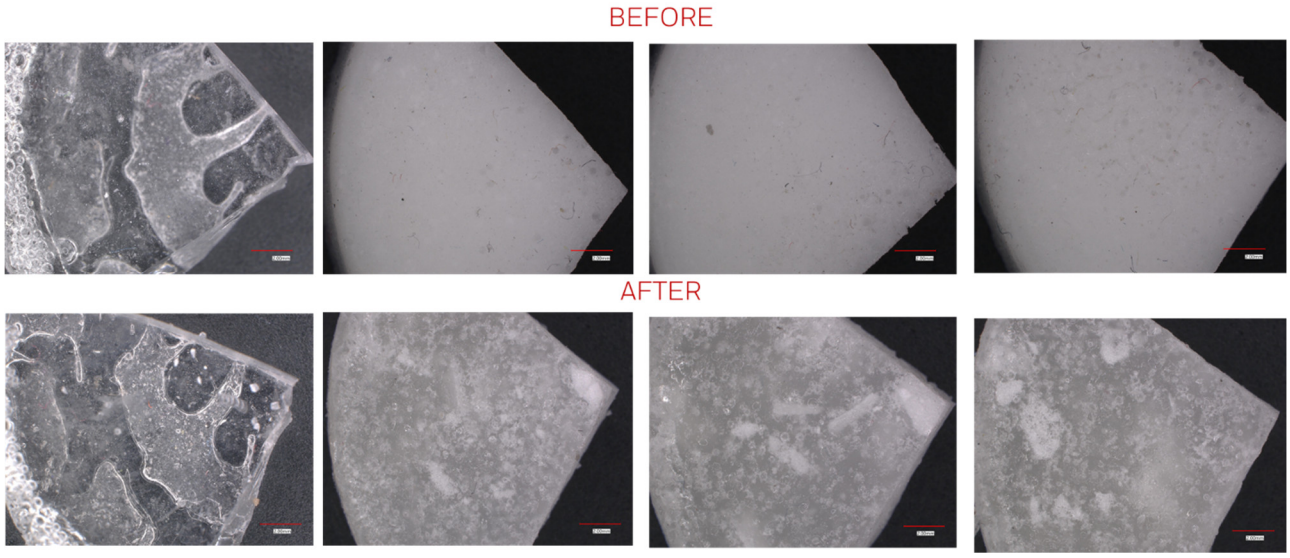

Figure 42. Optical microscope images of matrices before and after DCM extraction - 25% PLA loading

After the extraction process, matrices expand due to swelling but return to their normal size after all the solvent has evaporated. Matrices are placed in a vacuum oven overnight set to 60ºC to remove any remaining DCM. Figures 41 and 42 also show that there are no changes in the volume of the matrices, and therefore, due to proportionality, any change in mass of each matrix can be attributed to a change in density. The polymer blends with 10wt. % loading appear to be more transparent than the 25wt. % blends, owing to more microspheres per cross-sectional area in the case of the 25 wt. % loading of microspheres. In section 4.4, we observe that the increased percentage of microspheres increases the silicone matrix's viscosity, storage, and loss modulus. Tables 4 and 5 show that we cannot remove all the microspheres from the matrix in each case. In the case of the 25% loading, we have a more consistent removal for each sample.

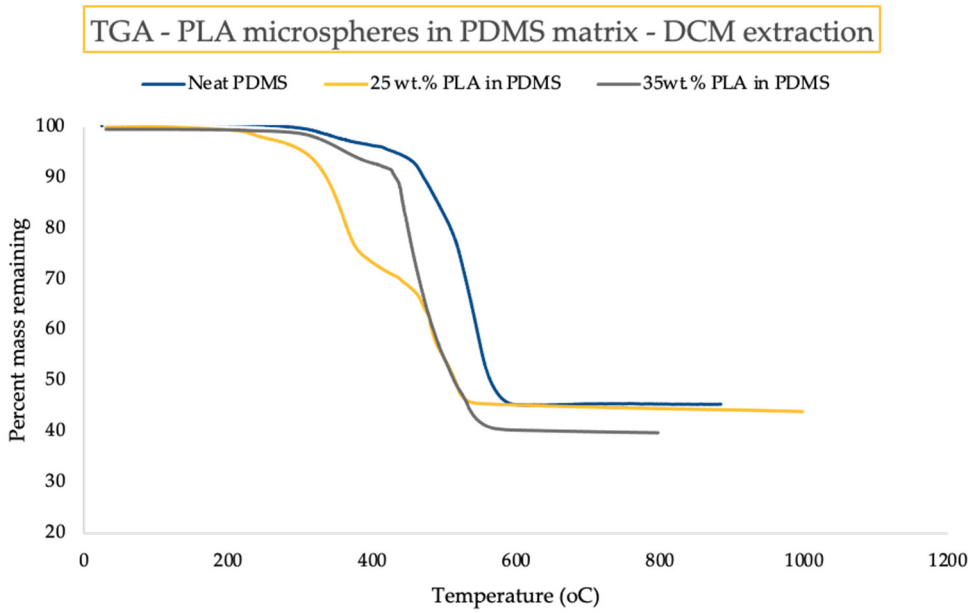

Figure 43. TGA – PLA microspheres in PDMS loaded at 0, 10, and 25wt.% with PLA microspheres.

We also observe that the weight of the neat Sylgard reduces for the 25% PDMS-PLA blend. This weight reduction could be accounted for by the presence of uncured Sylgard 184 still present in

the matrix, which in turn gets dissolved by DCM in the curing process. Figure 43 is the TGA data comparing the degradation rate of PLA-loaded PDMS matrices loaded at 0, 25, and 35 wt.%. If none of the microspheres are removed during solvent extraction without any change to the original mass of the matrix, we should see a weight drop of 25% and 35% in the TGA data corresponding to the removal of the same weight fraction of PLA microspheres. On the other hand, if all the microspheres are removed with no change to the original matrix, we should observe TGA profiles for the loaded matrices congruent to the neat sample. From the optical images shown above, we learn that not all the microspheres are removed from the polymer matrix. The relative degradation observed from the TGA results, in conjunction with the evidence of PLA microspheres still present in the matrix, suggests that a portion of the matrix was uncured, which then was dissolved by the DCM in the swelling process, and this disparity in weight reflects largely as a false negative in the TGA data. This is more prominent in the matrix with the 25 wt.% loading of PLA microspheres. The data in Figure 43 suggests that the fraction of PLA remaining in the matrix is 25%, which does not support the visual evidence of microsphere removal purported by Figure 42. If uncured portions of the matrix were present, then that would imply a reduction of the weight of the matrix, and as such, an increase in the weight fraction of PLA microspheres remaining in the matrix. The data for the 35wt% PLA loading suggests that about 10wt% of PLA remains in the matrix after solvent extraction. This amount may be impacted if a portion of the matrix material was dissolved in DCM as a result of only partially curing.

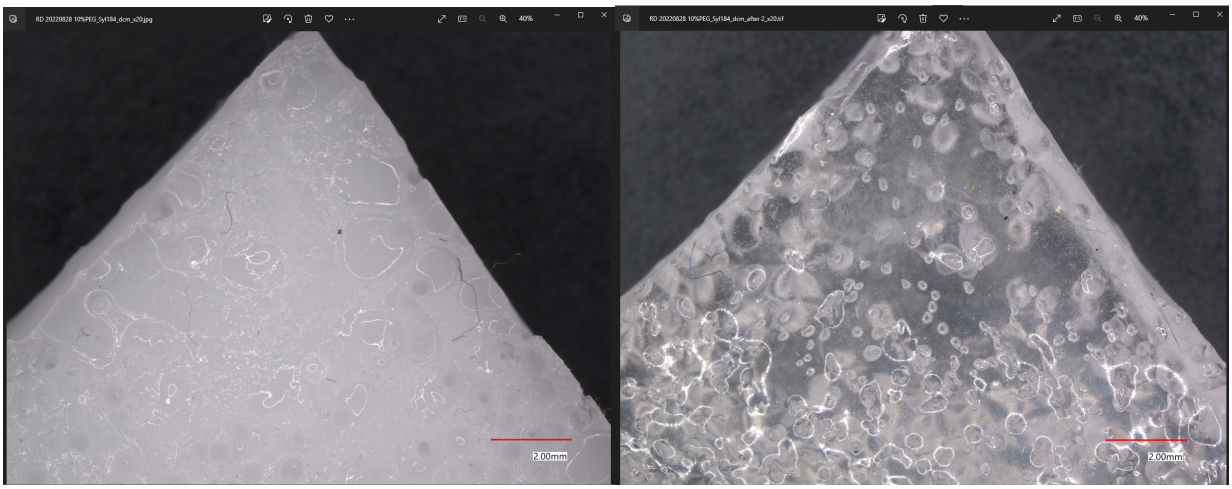

Figure 44. Images of 10wt.% PEG-loaded PDMS matrices before (left) and after (right) the removal of PEG microspheres.

Figure 44 shows the images of PEG-loaded polymer matrices before and after the removal of PEG microspheres at 10wt. % loading of PEG. The difference in translucence between the left and right images provides visual evidence of microsphere removal.

The evasiveness of DCM, combined with its likelihood to dissolve uncured polymers and difficulty removing all traces of it from the polymer matrix, calls for the exploration of other solvent systems that are safer to work with and have the same efficacy as chlorinated organic solvents. For future work, an in-depth solvent study based on the protocol described in Vandenburg et. al [116] will be proposed.

4.3.2 Water extraction

Figure 45 shows the removal process by water extraction for a 10% loading. Samples were suspended in water and placed in a water bath sonicator heated to 69ºC overnight. The image shows little to no change in the dispersion of fillers in the matrices, which is expected, considering PLA does not dissolve in water. This is also observed for a 25% sample loading. Tables 4 and 5 also show no significant change in the mass of the matrix before and after the

removal process, showing that water extraction is not a viable method for microsphere removal. The experiment was repeated for matrix loading with PEG and surface modified PLA microspheres. The added hydrophilicity impacted the PEG microspheres slightly, but not as with the organic solvent leaching, whereas similar results to Figure 45 was observed when the matrices were loaded with surface modified PLA microspheres.

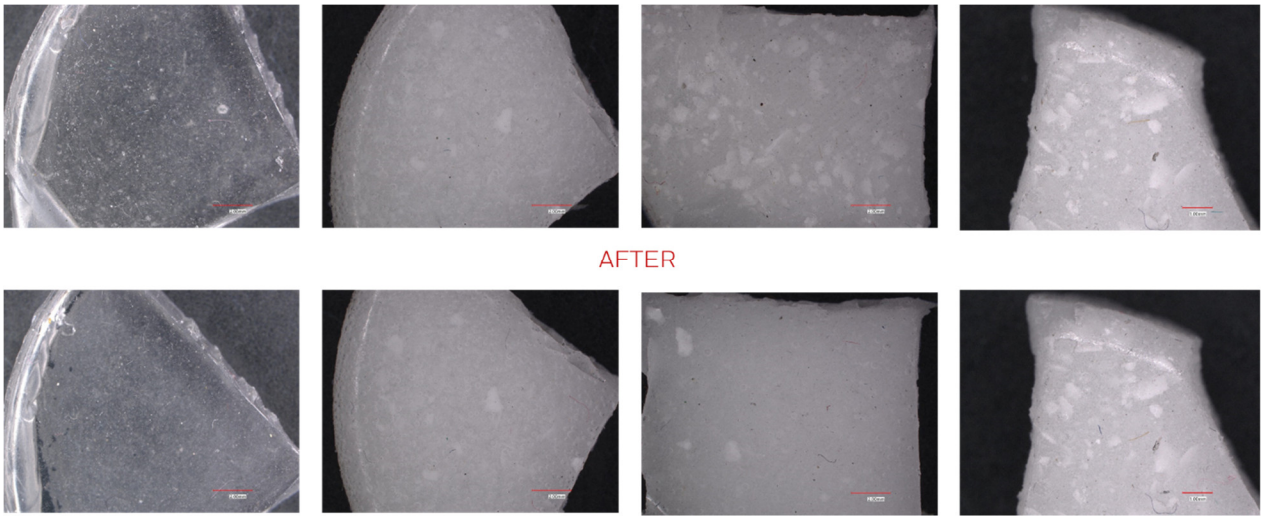

Figure 45. Images of matrices before and after water extraction - 10% PLA loading

4.3.3 Calcination

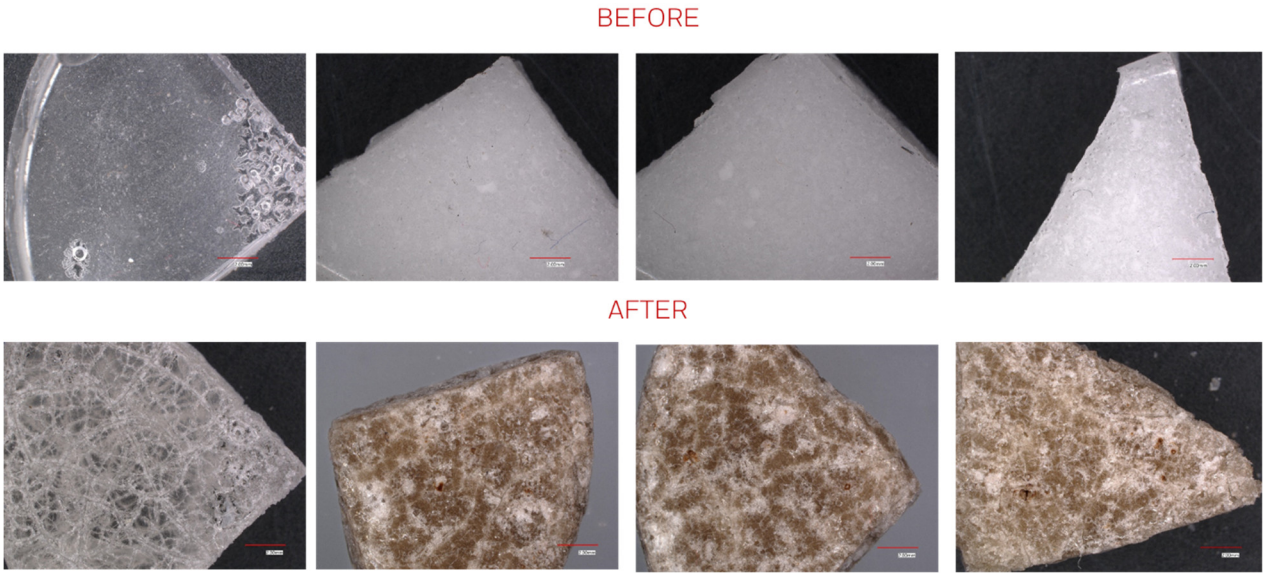

Figure 46. Images of matrices before and after calcination - 10% PLA loading

Samples were placed in an oven set to 572ºF, consistent with the decomposition temperature of PLA, overnight. However, these conditions led to the charring of the matrices, as observed in Figure 46. A further analysis was performed, whereby the oven was set to 500ºF, and the sample was placed in an oven for three hours. This, too, led to the charring of the matrix. As a result, isothermal thermogravimetric analyses were performed for both the PLA microspheres and the PDMS matrix to comprehend better the thermal properties of both filler material and matrix.

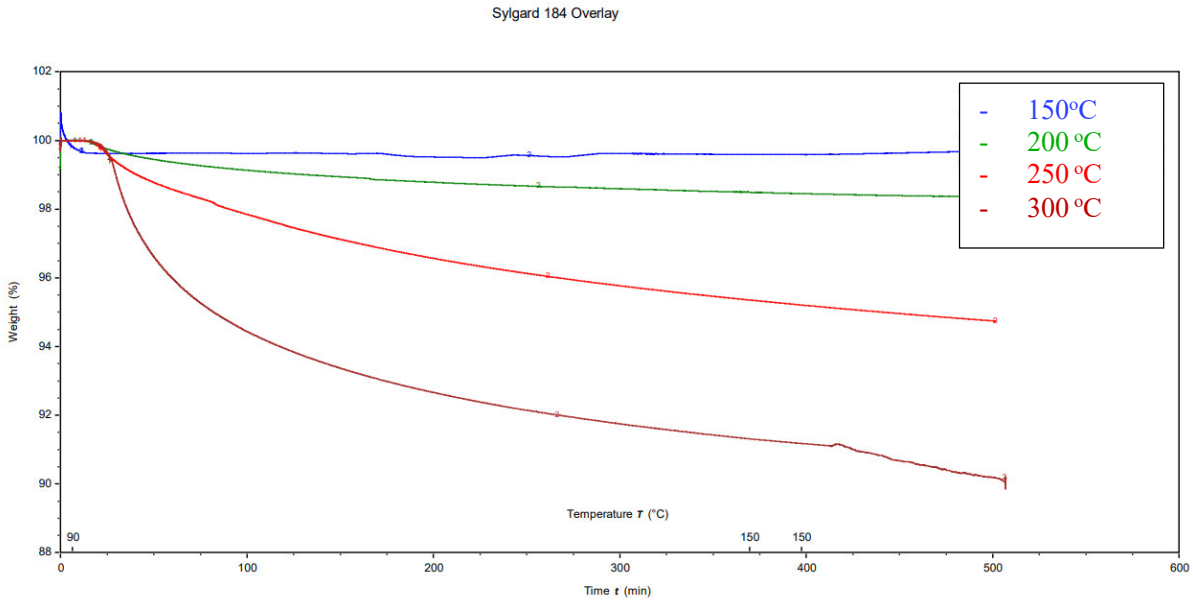

Figure 47. Isothermal TGA data for Sylgard 184 at temperatures 150, 200, 250, and 300ºC over 8 hours.

Temperatures were held at 200, 250, and 300ºC for 8 hours, as reported in Figures 47 and 48. An analysis of the isothermal study shows that the optimal temperature for conducting a calcination experiment for microsphere removal from a PDMS matrix without degradation is at 150ºC, but PLA does not sublime at this temperature. An experiment was conducted for this system whereby PDMS was placed in an oven for three hours at 300ºC. PDMS was observed to be brittle after this. Figure 47 shows that after 3 hours, PDMS undergoes about a 7% degradation of

PDMS. The level of degradation was enough, to change the polymer from being elastomeric to being brittle. It was therefore determined that calcination was not the most effective method for removing PLA from the PDMS matrix.

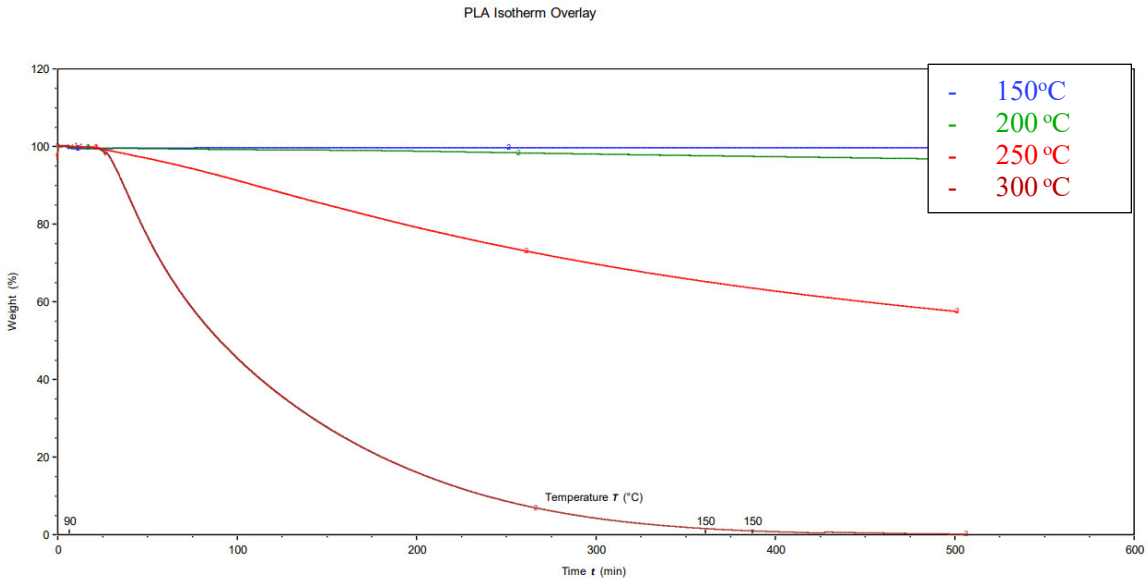

Figure 48. Isothermal TGA data for Polylactic acid at temperatures 150, 200, 250, and 300°C over 8 hours.

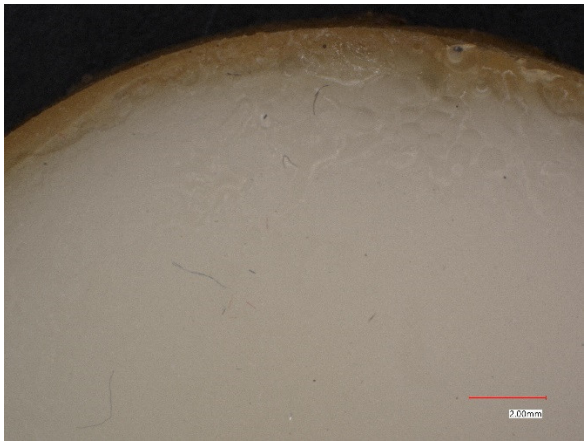

Figure 49. 35 wt.% PEG in PDMS - after calcination

Figure 49 shows the result of calcination of a PDMS matrix loaded with PEG microspheres at a mass fraction of 35 wt.%. The matrix is placed overnight in an oven set to 150°C. The

discoloration observed in Figure 49 may suggest some charring in the matrix material as was observed with, but this is not the case. The polymer matrix maintains its malleability after cure. An isothermal study was performed on PEG 1000, just as it was done for PDMS and PLA.

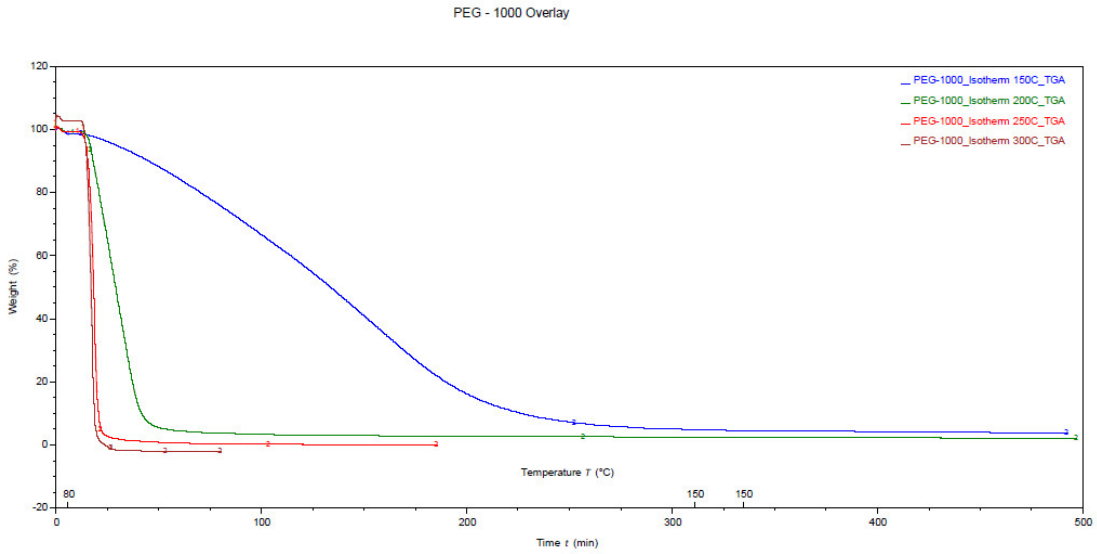

Figure 50. Isothermal Study of PEG 1000 at 150, 200, 250, and 300°C for 8 hours.

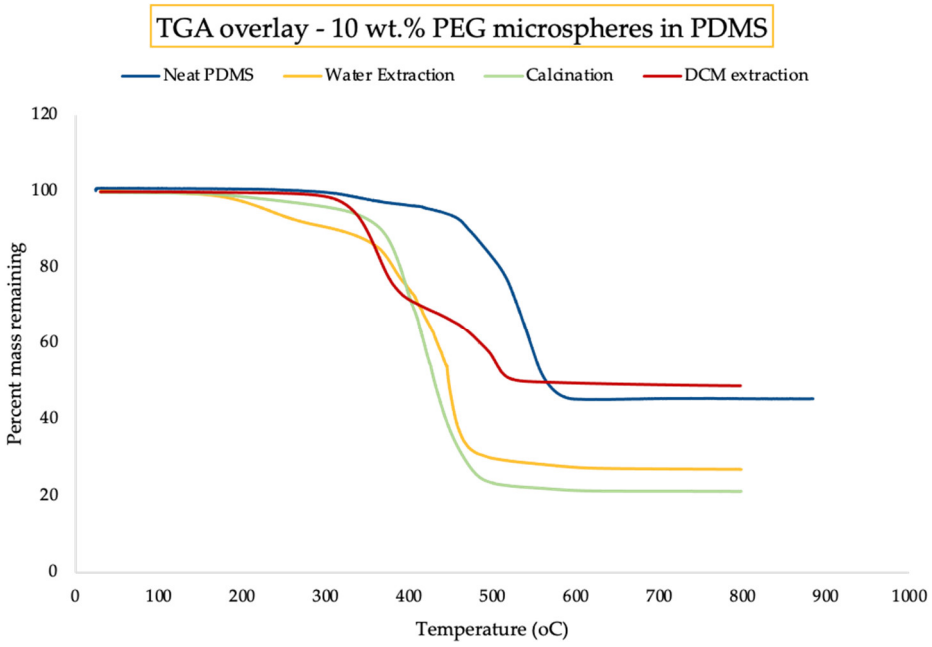

Figure 51. TGA overlay of microsphere removal methods for 10wt.% PEG in PDMS.

Figure 50 shows that at 150ºC, PEG undergoes complete degradation. From Figure 47, PDMS does not undergo any degradation at 150ºC. This implies that in theory, we can completely remove PEG from a PDMS matrix without altering the physical, and likely the mechanical properties of the matrix material.

Figure 51 shows an overlay of TGA microsphere removal data of PDMS matrices loaded with 10wt.% PEG microspheres. Each removal method shown appears to remove PEG from the matrix to a certain degree. Removal by calcination, however, is shown to be the most efficient way for removing PEG from a PDMS matrix.

4.4 Characterization of Sylgard 184 matrix before and after microsphere removal

4.4.1 Rheology

Rheological studies were performed on uncured PDMS and PLA blends. PDMS matrices were loaded with 10, 25, and 35 wt. % PLA microspheres, and the storage modulus, loss modulus, and viscosity were observed. Frequency and Amplitude sweeps were performed on polymer blends at room temperature. PDMS is a transparent polymer, so the translucence should be higher when the microspheres are removed. Figure 52 shows the storage and loss modulus profiles for the various polymer blends in a frequency sweep. Figure 52 shows a steady increase in the loss modulus as the percent of loading increases at a constant rate. The storage modulus, however, does not show a similar trend for each blend. The neat PDMS, 25 wt. % and 35 wt. % loading shows an increasing trend in the storage modulus, just as we observe in the loss modulus.

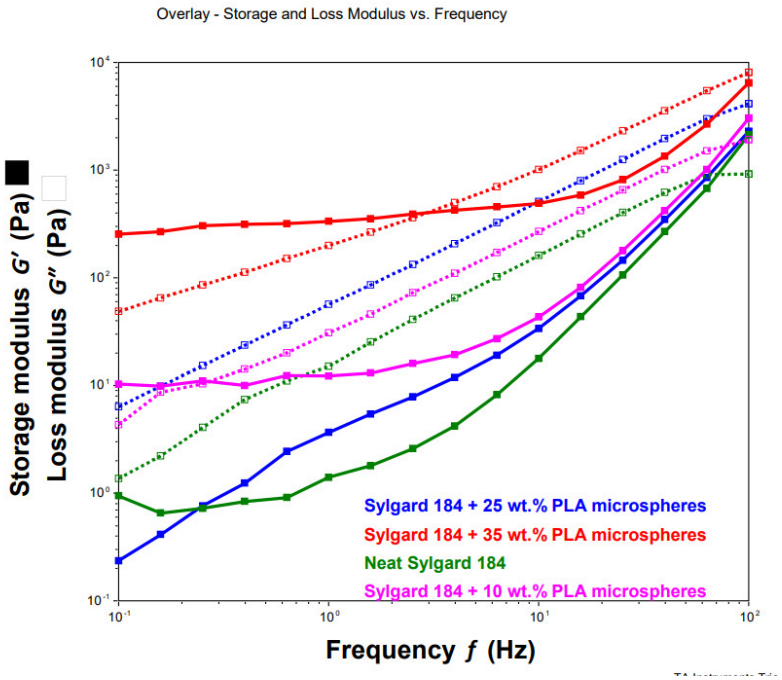

Figure 52. Overlay – Frequency Sweep - Storage and Loss Modulus vs. Frequency

The 10 wt. % loading, however, appears to have a storage modulus higher than neat PDMS and 25 wt. % loaded PDMS, but still significantly lower than the 35 wt. % loading. This could be due to the non-uniform blending of the PLA microspheres into the PDMS matrix. The storage and loss modulus of the 35% loaded matrix is significantly higher than the other instances because it is only a 10% increase from 25%.

Figure 53 shows the viscosity profile of the Sylgard 184 matrix as the concentration of PLA is increased from 10% to 35%. The viscosity increases with an increasing number of microspheres per cross-sectional area due to the higher loading. The viscosity is expected to be constant across time, provided the polymers are uniformly blended into the matrix, in the case of neat PDMS and 25 wt. % loading of the PDMS, this is achieved. In the case of the 10 wt. % and 35 wt. % loadings, the viscosities appear to decrease rapidly before attaining an almost constant viscosity. The experiment was repeated for the 10% loading, and the results remained unchanged.

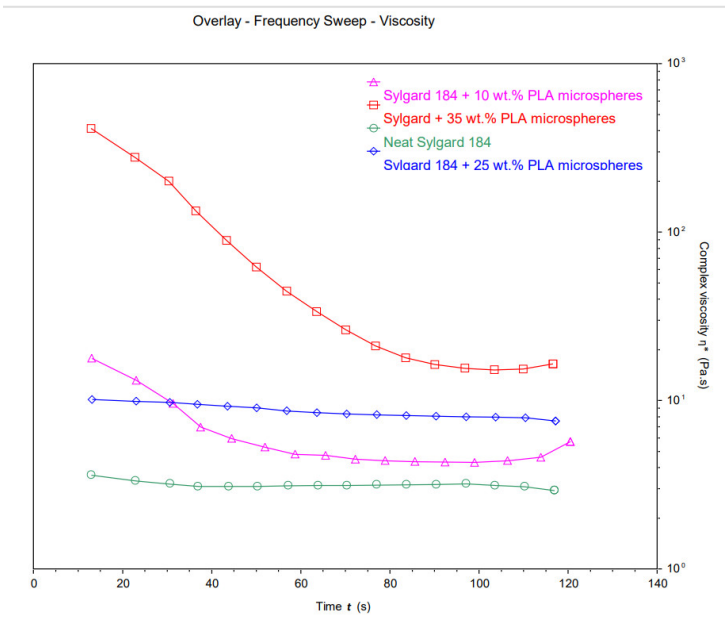

Figure 53. Viscosity of PLA microsphere-loaded Sylgard 184 matrix with respect to time

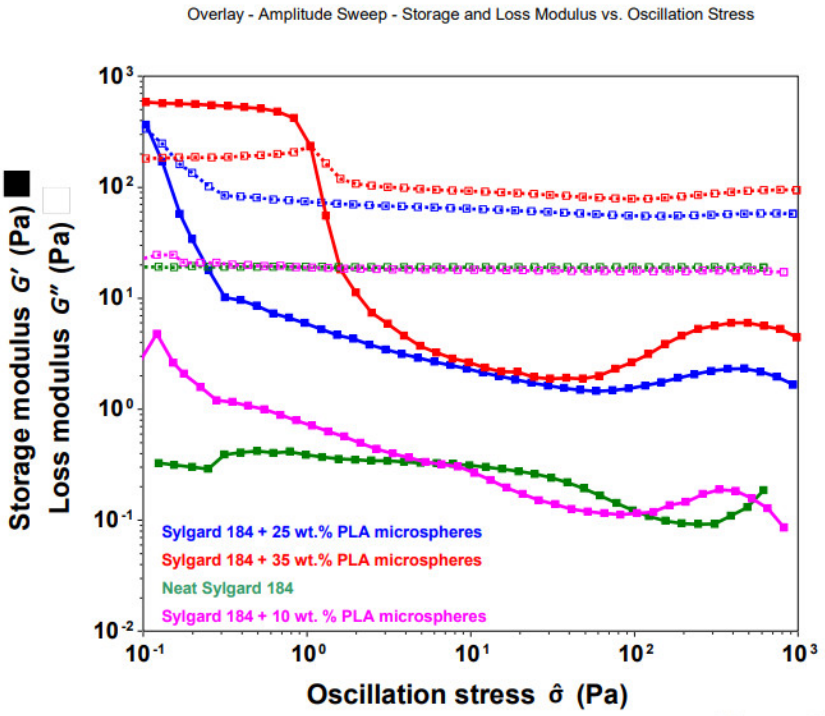

Figure 54. Overlay - Amplitude Sweep - Storage and Loss Modulus vs. Oscillation Stress

The phenomenon observed is referred to as shear thinning, whereby polymer matrices appear to decrease in viscosity over time under a periodic oscillation. This property is desired for 3D direct ink-write applications.

Figure 54 shows the amplitude sweep for the four different loading conditions mentioned earlier, showing the changes in the storage and loss modulus to the oscillation stress. Both storage and loss moduli increase with increasing microsphere loading conditions. For 3-D printing applications, it must be determined whether or not there is an optimal viscosity for extrudability of the microsphere-loaded feedstock.

4.4.2 Density and Porosity

This section analyzes porosity's effect on the PDMS matrix's density. In section 4.3, we observe the changes in the weight of the PDMS matrix due to the removal of loaded microspheres. A change in the mass is directly proportional to the change in density for a given sample volume.

Table 4.

Mass of matrices before and after microsphere removal process: 10 wt.% PLA microsphere loading

Density (g/mL) of Matrices before and after core removal process - 10wt% PLA microsphere loading									
	Water Extraction			**Calcination**			**Solvent Extraction**		
	Before	**After**	**% loss**	**Before**	**After**	**% loss**	**Before**	**After**	**% loss**
Sample 1	0.973	0.985	**-1%**	0.849	0.690	**15.84%**	1.064	0.962	**10%**
Sample 2	0.928	0.928	**0%**	1.030	0.838	**19.24%**	0.634	0.611	**2%**
Sample 3	1.053	1.064	**-1%**	0.905	0.724	**18.11%**	1.290	1.245	**5%**
Neat sample	1.053	1.053	**0%**	1.030	0.962	**6.79%**	1.053	1.053	**0%**

As a result, the percent reduction in mass observed in section 4.3 correspond to the percent reduction of the density.

Table 4 shows the changes in density of PDMS containing 10wt.% PLA microspheres before and after microsphere removal. In theory, we expect to reduce the mass – and subsequently the density – of the matrices by 10% if we selectively remove all the microspheres in each sample. In the water extraction process, there is no evidence of PLA microsphere removal from the matrix. The difference in density for the matrices that went through the calcination process is further evidence of degradation of the matrix as observed in section 4.3.3. DCM extraction appears to be the closest to being successful at removing microspheres. The inconsistencies shown could be attributed to the fraction of uncured PDMS in each matrix, as uncured Sylgard 184 dissolves in DCM. It is therefore likely that Sample 1 has a higher uncured PDMS matrix content than samples 2 and 3. Similar trends are also seen in Table 5, when PDMS is loaded with 25 wt.% of PLA.

Table 5.

Density of matrices before and after microsphere removal process: 25% PLA loading

Density (g/mL) of Matrices before and after core removal process - 25wt% PLA microsphere loading						
	Wash-Out			**Solvent Extraction**		
	Before	**After**	**% loss**	**Before**	**After**	**% loss**
Sample 1	1.086	1.075	1.1%	1.200	1.109	9.1%
Sample 2	0.792	0.792	0.0%	1.154	1.075	7.9%
Sample 3	1.154	1.143	1.1%	1.154	1.075	7.9%
Neat sample	1.268	1.268	0.0%	1.053	0.996	5.7%

Table 6.

Changes in the density of PDMS matrices loaded with PEG microspheres before and after microsphere removal

Density (g/mL) of Matrices before and after core removal process - PEG microsphere loading									
	Water Extraction			Calcination (150 °C overnight)			Solvent Extraction		
	Before	After	% loss	Before	After	% loss	Before	After	% loss
PEG 200 - 25%	1.426	1.381	4.53%	1.160	0.941	21.90%	1.109	0.905	20.37%
PEG 200 - 35%	1.075	1.041	3.40%	1.324	1.036	28.86%	1.222	0.795	42.72%

Table 6 shows the changes in density of PEG-loaded PDMS matrices as different removal methods are applied for 25% and 35 wt.% PEG microspheres. Water extraction appeared to be the least effective method for microsphere removal, even though PEG is a hydrophilic polymer. Solvent extraction of PEG from the PDMS matrix proved to be effective. The 42% loss reported for the 35 wt.% PEG loading is evidence that there remains a fraction of the PDMS that remains uncured and is as such dissolved during the extraction process. Calcination at 150°C overnight appears to be the most effective method for removal of PEG microspheres, with almost all the PEG microspheres being removed in each case. The temperature of calcination chosen was informed by the isothermal study discussed in section 4.3.3.

4.4.3 Dynamic Mechanical Analysis

Figure 55 shows a compression DMA analysis of the PDMS-PLA blends loaded at 10 wt. % for the various pore former removal processes. For this test, the storage modulus was measured as oscillatory stress was applied to each sample. Three porous samples representing two of the three removal methods were used for each test. The graph shows that the mechanical behavior of each

material remains unchanged from one sample to another. A lower storage modulus is recorded for the neat PDMS compared to samples loaded with microspheres.

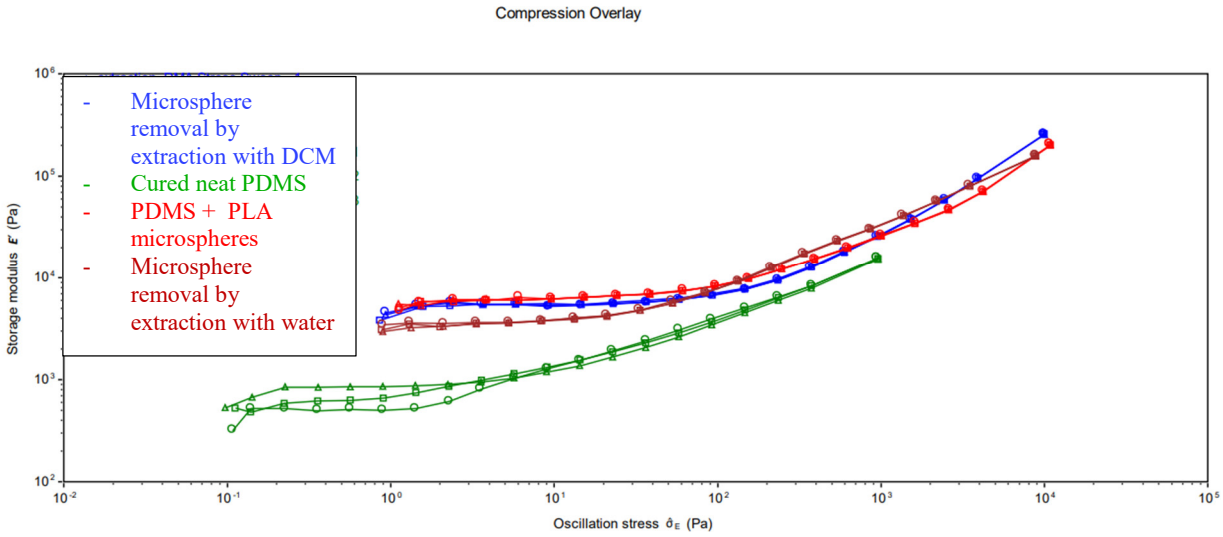

Figure 55. DMA Compression Analysis - Storage Modulus vs. Oscillation Stress for the 10% PLA-in-PDMS microsphere-matrix blend

Figure 56 shows the changes in strain rate with respect to temperature under a constant stress condition. The purpose of this test was to identify whether the resulting porosity changed the elasticity of the matrix material at varying temperatures. In Figure 56, we observe that the result of both solvent extraction techniques does not significantly change the internal structure and properties of the polymer matrix. The glass transition temperatures reported for each test under the same strain are identical. In the case of the calcinated sample, however, it is apparent that the polymer matrix is destroyed in the process of removing the pore materials.

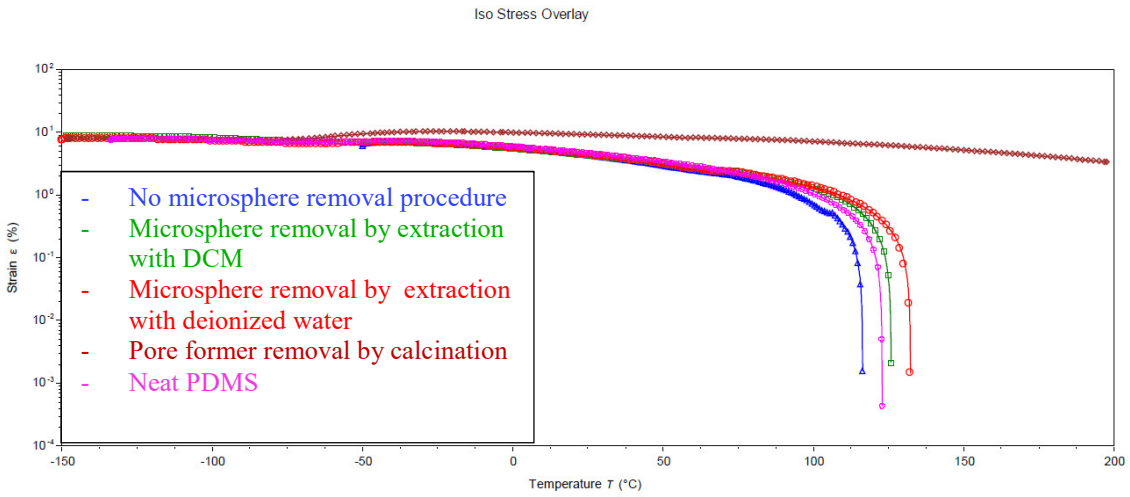

Figure 56. Strain rate vs. temperature under constant stress for 10% PLA-in-PDMS microsphere-matrix blend

The density reduction does not lead to a reduction in the storage modulus of the polymer matrix, as seen in section 4.4.3. We show that we can change the polymer matrix's density without changing the polymer's other physical and mechanical characteristics.

CHAPTER 5

Conclusions

Pore former materials can be used to decrease the density of silicone materials without altering their physical properties. With silicone being a polymer, polymers are an ideal choice of pore formers. The polymer pore former must be chosen so that it can be easily made into microspheres in the 5–100-micron size range and easily removable from a polymer matrix. The matrix material properties and the pore former material properties are variables to consider in pinpointing the ideal pore former removal method. In general, solvent leaching/extraction and calcination/baking out are methods used in removing pore fillers. The polymer primarily used in this work was polydimethylsiloxane (PDMS). Polymers are unique in that for a given compound, the length of the polymer chain directly impacts the material's physical properties. Higher molecular weight polymers of the same material have higher viscosities and, in some cases, exist as a solid under room temperature conditions. For polyethylene glycol (PEG), PEG 200 and PEG 400 exist as liquids, whereas PEG 1000 and PEG 6000 (higher polymer chain length) exist as solids at room temperature. PDMS is an elastomer and increases viscosity as the polymer chain length increases. The silicone elastomer primarily used as a matrix material for this work was SYLGARD^{TM} 184, which is a two-part system mixed in a 10:1 ratio and can be cured under varying conditions. SYLGARD^{TM} 184 has a viscosity of 3500cP and has cure times ranging from 48 hours at room temperature to 10 minutes at 150^{o}C. Polylactic acid (PLA) (Mn: 100,000 g/mol) and PEG 200 (Mn: 200 g/mol) were chosen as the pore former materials. The 4043D PLA is in pellet form and was converted into microspheres using a single oil-in-water emulsion method. The formed microspheres are then blended into the PDMS matrix. The PEG, being a

liquid, was mixed into the SYLGARD™ 184, stirred rigorously and uniformly using a planetary vacuum mixer, and then cured immediately after. PLA and PEG have different physical and thermal properties.

PEG is hydrophilic, whereas PLA is hydrophobic. As such, for a given matrix, the removal methods of the fillers will differ. Leaching the PEG filler out of the matrix material using water is effective due to the hydrophilicity of PEG. In contrast, this process would not work if PLA was the filler material. The solvent chosen for leaching should swell the polymer matrix and selectively dissolve the filler material. Dichloromethane dissolves both PLA and PEG and swells SYLGARD™, making it an ideal solvent for the leaching process. After solvent treatment, the samples are kept in a vacuum oven overnight at 60°C to remove any remaining solvent from the matrix. The bake-out method of pore former removal is effective when the pore former can sublime out of the polymer matrix at a temperature that does not, in turn, degrade the matrix. This method successfully removed low molecular weight PEG from the SYLGARD™ matrix at 100°C overnight. In the case of PLA, however, at 300°C for 3 hours, the PLA was charred in the matrix. The matrix experienced about 3% degradation, causing the material property to change from elastomeric to brittle. In the solvent extraction methods of removing pore formers, the mechanical properties were unaltered, and the density of the polymer matrix was reduced.

A PEG and PLA block copolymer was also synthesized as a possible pore former material. The intent was to synthesize a material with both PEG and PLA properties, intending to make a more easily removable material. The block copolymer formed was, however, insoluble in water and, once blended into the matrix, interfered with the curing process of SYLGARD™ 184. The formed PLA microspheres were also surface modified

by–OH functionalization, aiming to modify the microspheres' chemical and thermal surface properties. This surface modification, however, did not make the PLA microspheres more hydrophilic or change the thermal properties of the microspheres.

Future work will focus on maximizing the removal of pore former materials from the polymer matrix. Chapter 4 of this dissertation shows that even the most effective removal methods do not entirely remove all pore formers. Microspheres will also be incorporated into other PDMS matrices to study their removability using the various pore removal methods. Since the block copolymers have a low melting point, they can potentially be used in a melt emulsion synthesis to create microspheres, which might blend more easily into the polymer matrices, and, subsequently, be more easily removable from the matrix. Work will also be done to increase the yield of polymerization products significantly.

References:

1. Olatunji, O., *Natural polymers: industry techniques and applications*. 2015: Springer.
2. Horn, T.J. and O.L.A. Harrysson, *Overview of Current Additive Manufacturing Technologies and Selected Applications.* Science Progress, 2012. **95**(3): p. 255-282.
3. Panda, A.K., R.K. Singh, and D.K. Mishra, *Thermolysis of waste plastics to liquid fuel: A suitable method for plastic waste management and manufacture of value added products—A world prospective.* Renewable and Sustainable Energy Reviews, 2010. **14**(1): p. 233-248.
4. Hiemenz, P.C. and T.P. Lodge, *Polymer chemistry 2nd edition.* NICE (News & Information for Chemical Engineers), 2007. **25**(4): p. 409-409.
5. Drobny, J.G., *4 - Processing Methods Applicable to Thermoplastic Elastomers*, in *Handbook of Thermoplastic Elastomers (Second Edition)*, J.G. Drobny, Editor. 2014, William Andrew Publishing: Oxford. p. 33-173.
6. Sotoodeh, K., *Analysis and Improvement of Material Selection for Process Piping System in Offshore Industry.* American Journal of Mechanical Engineering, 2018. **6**: p. 17-26.
7. Alison, L., et al., *3D printing of sacrificial templates into hierarchical porous materials.* Scientific Reports, 2019. **9**(1): p. 409.
8. Vesenjak, M., L. Krstulović-Opara, and Z. Ren, *Characterization of irregular open-cell cellular structure with silicone pore filler.* Polymer Testing, 2013. **32**(8): p. 1538-1544.
9. Colombo, P., *Engineering porosity in polymer-derived ceramics.* Journal of the European Ceramic Society, 2008. **28**(7): p. 1389-1395.
10. Bernardo, E., et al., *Porous wollastonite–hydroxyapatite bioceramics from a preceramic polymer and micro- or nano-sized fillers.* Journal of the European Ceramic Society, 2012. **32**(2): p. 399-408.
11. Gambaryan-Roisman, T., et al., *Formation and properties of poly (siloxane) derived ceramic foams.* Ceramics–Processing, Reliability, Tribology and Wear, 2000. **12**: p. 247-251.
12. Calabrese, L., et al., *Morphological and functional aspects of zeolite filled siloxane composite foams.* Journal of Applied Polymer Science, 2018. **135**(2): p. 45683.
13. Wang, X., et al., *3D printing of polymer matrix composites: A review and prospective.* Composites Part B: Engineering, 2017. **110**: p. 442-458.
14. Rankin, J.M., *Silicone microspheres and disposable separation technology for gaseous analytes*, in *Chemistry*. 2015, University of Illinois at Urbana-Champaign.
15. Adams, M.L., A. Lavasanifar, and G.S. Kwon, *Amphiphilic block copolymers for drug delivery.* Journal of Pharmaceutical Sciences, 2003. **92**(7): p. 1343-1355.
16. Lu, F., et al., *The correlation between solvent treatment and the microstructure of PAN-b-PEG copolymer membranes.* Polymer Journal, 2011. **43**(4): p. 378-384.
17. Currie, E.P.K., W. Norde, and M.A. Cohen Stuart, *Tethered polymer chains: surface chemistry and their impact on colloidal and surface properties.* Advances in Colloid and Interface Science, 2003. **100-102**: p. 205-265.
18. Lee, Y.S., *Self-assembly and nanotechnology: a force balance approach*. 2008: John Wiley & Sons.
19. Ruan, G. and S.-S. Feng, *Preparation and characterization of poly(lactic acid)–poly(ethylene glycol)–poly(lactic acid) (PLA–PEG–PLA) microspheres for controlled release of paclitaxel.* Biomaterials, 2003. **24**(27): p. 5037-5044.

20. Gref, R., et al., *Development and characterization of CyA-loaded poly (lactic acid)–poly (ethylene glycol) PEG micro-and nanoparticles. Comparison with conventional PLA particulate carriers.* European Journal of Pharmaceutics and Biopharmaceutics, 2001. **51**(2): p. 111-118.
21. Lassalle, V. and M.L. Ferreira, *PLA nano-and microparticles for drug delivery: an overview of the methods of preparation.* Macromolecular bioscience, 2007. **7**(6): p. 767-783.
22. Xiao, R.Z., et al., *Recent advances in PEG-PLA block copolymer nanoparticles.* International journal of nanomedicine, 2010. **5**: p. 1057-1065.
23. Mattei, M., G.M. Kontogeorgis, and R. Gani, *A comprehensive framework for surfactant selection and design for emulsion based chemical product design.* Fluid Phase Equilibria, 2014. **362**: p. 288-299.
24. Chaisri, W., W.E. Hennink, and S. Okonogi, *Preparation and characterization of cephalexin loaded PLGA microspheres.* Current drug delivery, 2009. **6**(1): p. 69-75.
25. Kim, S. and C.B. Park, *Dopamine-Induced Mineralization of Calcium Carbonate Vaterite Microspheres.* Langmuir, 2010. **26**(18): p. 14730-14736.
26. Rahemi Ardekani, S., et al., *A comprehensive review on ultrasonic spray pyrolysis technique: Mechanism, main parameters and applications in condensed matter.* Journal of Analytical and Applied Pyrolysis, 2019. **141**: p. 104631.
27. Guo, J., *Micro- and nanostructured materials via ultrasonic spray pyrolysis*, in *Chemistry*. 2014, University of Illinois at Urbana-Champaign.
28. Griffin, G.L., *Aerosol Processing of Materials By Toivo T. Kodas and Mark J. Hampden-Smith (Superior Micropowders, Albuquerque, NM). Wiley-VCH: New York. 1999. xxx + 656 pp. $175.00. ISBN 0-471-24669-7.* Journal of the American Chemical Society, 2000. **122**(14): p. 3565-3565.
29. Tsai, S.C., et al., *Ultrasonic spray pyrolysis for nanoparticles synthesis.* Journal of Materials Science, 2004. **39**(11): p. 3647-3657.
30. Košević MG, Z.M., Stopić SR, Stevanović JS, Weirich TE, Friedrich BG, Panić VV, *Structural and Electrochemical Properties of Nesting and Core/Shell Pt/TiO2 Spherical Particles Synthesized by Ultrasonic Spray Pyrolysis.* Metals, 2020. **10**: p. 1-11.
31. Stopic, S., et al., *Synthesis of TiO2 core/RuO2 shell particles using multistep ultrasonic spray pyrolysis.* Materials Research Bulletin, 2013. **48**(9): p. 3633-3635.
32. Chen, M., et al., *Self-assembled composite matrix in a hierarchical 3-D scaffold for bone tissue engineering.* Acta Biomaterialia, 2011. **7**(5): p. 2244-2255.
33. Tao, S.L. and T.A. Desai, *Microfabricated drug delivery systems: from particles to pores.* Advanced Drug Delivery Reviews, 2003. **55**(3): p. 315-328.
34. Tham, C.Y., Hamid, Z. A. A., Ahmad, Z. A., & Ismail, H. , *Surface Engineered Poly(lactic acid) (PLA) Microspheres by Chemical Treatment for Drug Delivery System.* Key Engineering Materials, 2013: p. 214-218.
35. Chen, J.-P. and C.-H. Su, *Surface modification of electrospun PLLA nanofibers by plasma treatment and cationized gelatin immobilization for cartilage tissue engineering.* Acta Biomaterialia, 2011. **7**(1): p. 234-243.
36. Wu, W., Q. He, and C. Jiang, *Magnetic Iron Oxide Nanoparticles: Synthesis and Surface Functionalization Strategies.* Nanoscale Research Letters, 2008. **3**(11): p. 397.
37. Yi, S., et al., *A reverse micelle strategy for fabricating magnetic lipase-immobilized nanoparticles with robust enzymatic activity.* Scientific Reports, 2017. **7**(1): p. 9806.

38. McKeen, L.W., *Chapter 1 - Introduction to Plastics and Elastomers*, in *The Effect of Creep and Other Time Related Factors on Plastics and Elastomers (Second Edition)*, L.W. McKeen, Editor. 2009, William Andrew Publishing: Boston. p. 1-31.
39. McKeen, L.W., *11 - Fluoropolymers*, in *The Effect of UV Light and Weather on Plastics and Elastomers (Fourth Edition)*, L.W. McKeen, Editor. 2019, William Andrew Publishing. p. 361-391.
40. Shrivastava, A., *2 - Polymerization*, in *Introduction to Plastics Engineering*, A. Shrivastava, Editor. 2018, William Andrew Publishing. p. 17-48.
41. Wang, Y. and F. Li, *An Emerging Pore-Making Strategy: Confined Swelling-Induced Pore Generation in Block Copolymer Materials.* Advanced Materials, 2011. **23**(19): p. 2134-2148.
42. Hillmyer, M., *Block copolymer synthesis.* Current Opinion in Solid State and Materials Science, 1999. **4**(6): p. 559-564.
43. Tian, H., et al., *Biodegradable cationic PEG–PEI–PBLG hyperbranched block copolymer: synthesis and micelle characterization.* Biomaterials, 2005. **26**(20): p. 4209-4217.
44. Zhang, X., et al., *Synthesis and characterization of the paclitaxel/MPEG-PLA block copolymer conjugate.* Biomaterials, 2005. **26**(14): p. 2121-8.
45. Kricheldorf, H.R., H. Hachmann-Thiessen, and G. Schwarz, *Telechelic and Star-Shaped Poly(l-lactide)s by Means of Bismuth(III) Acetate as Initiator.* Biomacromolecules, 2004. **5**(2): p. 492-496.
46. Otsuka, H., Y. Nagasaki, and K. Kataoka, *Surface Characterization of Functionalized Polylactide through the Coating with Heterobifunctional Poly(ethylene glycol)/Polylactide Block Copolymers.* Biomacromolecules, 2000. **1**(1): p. 39-48.
47. Hiki, S. and K. Kataoka, *A Facile Synthesis of Azido-Terminated Heterobifunctional Poly(ethylene glycol)s for "Click" Conjugation.* Bioconjugate Chemistry, 2007. **18**(6): p. 2191-2196.
48. Hiki, S. and K. Kataoka, *Versatile and Selective Synthesis of "Click Chemistry" Compatible Heterobifunctional Poly(ethylene glycol)s Possessing Azide and Alkyne Functionalities.* Bioconjugate Chemistry, 2010. **21**(2): p. 248-254.
49. Kou, L., H. He, and C. Gao, *Click chemistry approach to functionalize two-dimensional macromolecules of graphene oxide nanosheets.* Nano-Micro Letters, 2010. **2**(3): p. 177-183.
50. Wang, D.K., et al., *The influence of composition on the physical properties of PLA-PEG-PLA-co-Boltorn based polyester hydrogels and their biological performance.* Journal of Materials Chemistry, 2012. **22**(14): p. 6994-7004.
51. Sim, T., et al., *Development of a docetaxel micellar formulation using poly (ethylene glycol)–polylactide–poly (ethylene glycol)(PEG–PLA–PEG) with successful reconstitution for tumor targeted drug delivery.* Drug delivery, 2018. **25**(1): p. 1362-1371.
52. Liu, X., et al., *Adenosine-functionalized biodegradable PLA-b-PEG nanoparticles ameliorate osteoarthritis in rats.* Scientific reports, 2019. **9**(1): p. 1-14.
53. Chow, T., *Miscible blends and block copolymers. Crystallization, melting, and interaction.* Macromolecules, 1990. **23**(1): p. 333-337.
54. Coleman, D., *Block copolymers: Copolymerization of ethylene terephthalate and polyoxyethylene glycols.* Journal of Polymer Science, 1954. **14**(73): p. 15-28.

55. Mohapatra, A.K., S. Mohanty, and S. Nayak, *Effect of PEG on PLA/PEG blend and its nanocomposites: A study of thermo-mechanical and morphological characterization.* Polymer composites, 2014. **35**(2): p. 283-293.
56. Kent, K., et al., *Controlling the porosity and density of silicone rubber prosthetic materials.* Journal of Prosthetic Dentistry, 1983. **50**(2): p. 230-236.
57. Abshirini, M., et al., *Synthesis and characterization of porous polydimethylsiloxane structures with adjustable porosity and pore morphology using emulsion templating technique.* Polymer Engineering & Science, 2021. **61**(7): p. 1943-1955.
58. Zhang, L., et al., *Paraffin oil based soft-template approach to fabricate reusable porous pdms sponge for effective oil/water separation.* Langmuir, 2019. **35**(34): p. 11123-11131.
59. Yu, C., et al., *Facile preparation of the porous PDMS oil-absorbent for oil/water separation.* Advanced Materials Interfaces, 2017. **4**(3): p. 1600862.
60. Turco, A., et al., *An innovative, fast and facile soft-template approach for the fabrication of porous PDMS for oil–water separation.* Journal of Materials Chemistry A, 2017. **5**(45): p. 23785-23793.
61. Thurgood, P., et al., *Porous PDMS structures for the storage and release of aqueous solutions into fluidic environments.* Lab on a Chip, 2017. **17**(14): p. 2517-2527.
62. Cha, K.J. and D.S. Kim, *A portable pressure pump for microfluidic lab-on-a-chip systems using a porous polydimethylsiloxane (PDMS) sponge.* Biomedical microdevices, 2011. **13**(5): p. 877-883.
63. Rutz, B.H. and J.C. Berg, *A review of the feasibility of lightening structural polymeric composites with voids without compromising mechanical properties.* Advances in Colloid and Interface Science, 2010. **160**(1): p. 56-75.
64. Feng, J. and Y. Yin, *Self-templating approaches to hollow nanostructures.* Advanced Materials, 2019. **31**(38): p. 1802349.
65. Stephen W. Paddock, T.J.F., Michael W. Davidson. *Introductory Confocal Concepts*
66. Azad MOHAMMED, A.A., *SCANNING ELECTRON MICROSCOPY (SEM): A REVIEW.* International Conference on Hydraulics and Pneumatics - HERVEX, 2018(ISSN 1454 - 8003).
67. Zaefferer, S., *A critical review of orientation microscopy in SEM and TEM.* Crystal Research and Technology, 2011. **46**(6): p. 607-628.
68. Berthomieu, C. and R. Hienerwadel, *Fourier transform infrared (FTIR) spectroscopy.* Photosynthesis research, 2009. **101**(2): p. 157-170.
69. Scientific, T. *Introduction to FTIR spectroscopy*.
70. Sindhu, R., P. Binod, and A. Pandey, *Chapter 17 - Microbial Poly-3-Hydroxybutyrate and Related Copolymers*, in *Industrial Biorefineries & White Biotechnology*, A. Pandey, et al., Editors. 2015, Elsevier: Amsterdam. p. 575-605.
71. Tissue, B.M. *Nuclear Magnetic Resonance (NMR) Spectroscopy*. 1996 9/12/1996.
72. Coats, A. and J. Redfern, *Thermogravimetric analysis. A review.* Analyst, 1963. **88**(1053): p. 906-924.
73. Inan, T.Y., *2 - Thermoplastic-based nanoblends: Preparation and characterizations*, in *Recent Developments in Polymer Macro, Micro and Nano Blends*, P.M. Visakh, G. Markovic, and D. Pasquini, Editors. 2017, Woodhead Publishing. p. 17-56.
74. Sturtevant, J.M., *Biochemical applications of differential scanning calorimetry.* Annual review of physical chemistry, 1987. **38**(1): p. 463-488.

75. Freire, E., *Differential scanning calorimetry.* Protein stability and folding, 1995: p. 191-218.
76. Zhong, Q. and C.R. Daubert, *Chapter 15 - Food Rheology*, in *Handbook of Farm, Dairy and Food Machinery Engineering (Second Edition)*, M. Kutz, Editor. 2013, Academic Press: San Diego. p. 403-426.
77. Faustino, C. and L. Pinheiro, *Analytical Rheology of Honey: A State-of-the-Art Review.* Foods, 2021. **10**(8).
78. Ferraris, C.F. and N.S. Martys, *3 - Concrete rheometers*, in *Understanding the Rheology of Concrete*, N. Roussel, Editor. 2012, Woodhead Publishing. p. 63-82.
79. Groenewoud, W.M., *CHAPTER 4 - DYNAMIC MECHANICAL ANALYSIS*, in *Characterisation of Polymers by Thermal Analysis*, W.M. Groenewoud, Editor. 2001, Elsevier Science B.V.: Amsterdam. p. 94-122.
80. *Mastersizer 3000 - Delivering the data you need for outcomes you can trust*. 2023 [cited 2023 March 6th]; Available from: https://www.malvernpanalytical.com/en/products/product-range/mastersizer-range/mastersizer-3000?campaignid=32743320&adgroupid=2289135180&creative=317614278903&keyword=malvern%20mastersizer%203000&matchtype=p&network=g&device=c&pk_campaign=32743320&pk_adgroupid=2289135180&pk_kwd=malvern%20mastersizer%203000&pk_source=google&pk_medium=cpc&pk_content=317614278903&gclid=CjwKCAiAjPyfBhBMEiwAB2CCIu3z51uwc3uHiJocfD2NWipVfYsnAFe-xqMqvJ-hlDFse5ukH0jI_xoCTdgQAvD_BwE.
81. Kawaguchi, H., *Functional polymer microspheres.* Progress in Polymer Science, 2000. **25**(8): p. 1171-1210.
82. Davachi, S.M. and B. Kaffashi, *Polylactic Acid in Medicine.* Polymer-Plastics Technology and Engineering, 2015. **54**(9): p. 944-967.
83. Ebadi-Dehaghani, H., et al., *On O2 gas permeability of PP/PLA/clay nanocomposites: A molecular dynamic simulation approach.* Polymer Testing, 2015. **45**: p. 139-151.
84. Bao, L., et al., *Gas permeation properties of poly(lactic acid) revisited.* Journal of Membrane Science, 2006. **285**(1-2): p. 166-172.
85. Deng, H. and Z. Lei, *Preparation and characterization of hollow Fe3O4/SiO2@PEG–PLA nanoparticles for drug delivery.* Composites Part B: Engineering, 2013. **54**: p. 194-199.
86. Brzeziński, M., et al., *Stereocomplexed PLA microspheres: Control over morphology, drug encapsulation and anticancer activity.* Colloids and Surfaces B: Biointerfaces, 2019. **184**: p. 110544.
87. Avérous, L., *Chapter 21 - Polylactic Acid: Synthesis, Properties and Applications*, in *Monomers, Polymers and Composites from Renewable Resources*, M.N. Belgacem and A. Gandini, Editors. 2008, Elsevier: Amsterdam. p. 433-450.
88. Raquez, J.-M., et al., *Polylactide (PLA)-based nanocomposites.* Progress in Polymer Science, 2013. **38**(10): p. 1504-1542.
89. Tobío, M., et al., *Stealth PLA-PEG Nanoparticles as Protein Carriers for Nasal Administration.* Pharmaceutical Research, 1998. **15**(2): p. 270-275.
90. Wang, H., et al., *Preparation and degradability of poly(lactic acid)–poly(ethylene glycol)–poly(lactic acid)/SiO2 hybrid material.* Journal of Applied Polymer Science, 2008. **110**(6): p. 3985-3989.

91. Gorrasi, G. and R. Pantani, *Effect of PLA grades and morphologies on hydrolytic degradation at composting temperature: Assessment of structural modification and kinetic parameters.* Polymer Degradation and Stability, 2013. **98**(5): p. 1006-1014.
92. Tyler, B., et al., *Polylactic acid (PLA) controlled delivery carriers for biomedical applications.* Advanced Drug Delivery Reviews, 2016. **107**: p. 163-175.
93. Brzeziński, M. and T. Biela, *Stereocomplexed Polylactides*, in *Encyclopedia of Polymeric Nanomaterials*, S. Kobayashi and K. Müllen, Editors. 2015, Springer Berlin Heidelberg: Berlin, Heidelberg. p. 2274-2281.
94. Sin, L.T., A.R. Rahmat, and W.A.W.A. Rahman, *Polylactic acid : PLA biopolymer technology and applications*. First edition. ed. Plastics design library. 2013, Amsterdam ; Boston: Elsevier, WA. xiii, 341 pages.
95. Jain, J.P. and N. Kumar, *Self Assembly of Amphiphilic (PEG)3-PLA Copolymer as Polymersomes: Preparation, Characterization, and Their Evaluation As Drug Carrier.* Biomacromolecules, 2010. **11**(4): p. 1027-1035.
96. Wei, Y., et al., *Microcosmic Mechanisms for Protein Incomplete Release and Stability of Various Amphiphilic mPEG-PLA Microspheres.* Langmuir, 2012. **28**(39): p. 13984-13992.
97. Vouyiouka, S.N. and C.D. Papaspyrides, *4.34 - Mechanistic Aspects of Solid-State Polycondensation*, in *Polymer Science: A Comprehensive Reference*, K. Matyjaszewski and M. Möller, Editors. 2012, Elsevier: Amsterdam. p. 857-874.
98. Ainali, N.M., et al., *Thermal Stability and Decomposition Mechanism of PLA Nanocomposites with Kraft Lignin and Tannin.* Polymers, 2021. **13**(16): p. 2818.
99. Persson, A., *Identification of Alternative Solvents to DCM for Dissolving PLA*. 2018.
100. Cheng, Y., et al., *Polylactic acid (PLA) synthesis and modifications: a review.* Frontiers of Chemistry in China, 2009. **4**(3): p. 259-264.
101. Wang, Y., S. Zhang, and D.S.W. Benoit, *Degradable poly(ethylene glycol) (PEG)-based hydrogels for spatiotemporal control of siRNA/nanoparticle delivery.* J Control Release, 2018. **287**: p. 58-66.
102. Alper, A. and D.S. Pashankar, *Polyethylene Glycol: A Game-Changer Laxative for Children.* Journal of Pediatric Gastroenterology and Nutrition, 2013. **57**(2): p. 134-140.
103. Zheng, C.Y., G. Ma, and Z. Su, *Native PAGE eliminates the problem of PEG–SDS interaction in SDS-PAGE and provides an alternative to HPLC in characterization of protein PEGylation.* Electrophoresis, 2007. **28**(16): p. 2801-2807.
104. Wang, J., et al., *Hyperbranched-star PEI-g-PEG as a nonviral vector with efficient uptake and hypotoxicity for retinoblastoma gene therapy application.* Colloid and Interface Science Communications, 2022. **50**: p. 100647.
105. Matsumura, S., et al., *Prevention of Carbon Nanohorn Agglomeration Using a Conjugate Composed of Comb-Shaped Polyethylene Glycol and a Peptide Aptamer.* Molecular Pharmaceutics, 2009. **6**(2): p. 441-447.
106. Hossain, M.N., S.-J. Lee, and C.-L. Kim, *Fabrication of TiO2 ̶ KH550 ̶ PEG Super-Hydrophilic Coating on Glass Surface without UV/Plasma Treatment for Self-Cleaning and Anti-Fogging Applications.* Materials, 2022. **15**(9): p. 3292.
107. Ghasemi, R., et al., *mPEG-PLA and PLA-PEG-PLA nanoparticles as new carriers for delivery of recombinant human Growth Hormone (rhGH).* Scientific Reports, 2018. **8**(1): p. 9854.

108. Liu, H., et al., *Three-Component Dynamic Covalent Chemistry: From Janus Small Molecules to Functional Polymers.* Journal of the American Chemical Society, 2021. **143**(49): p. 20735-20746.
109. Li, S., et al., *SuFExable polymers with helical structures derived from thionyl tetrafluoride.* Nature Chemistry, 2021. **13**(9): p. 858-867.
110. Wu, P., *The Nobel Prize in Chemistry 2022: Fulfilling Demanding Applications with Simple Reactions*. 2022, ACS Publications.
111. Kolb, H.C., M.G. Finn, and K.B. Sharpless, *Click Chemistry: Diverse Chemical Function from a Few Good Reactions.* Angewandte Chemie International Edition, 2001. **40**(11): p. 2004-2021.
112. Djorgbenoo, R., et al., *Amphiphilic phospholipid–iodinated polymer conjugates for bioimaging.* Biomaterials Science, 2021. **9**(14): p. 5045-5056.
113. Heald, C.R., et al., *Poly(lactic acid)−Poly(ethylene oxide) (PLA−PEG) Nanoparticles: NMR Studies of the Central Solidlike PLA Core and the Liquid PEG Corona.* Langmuir, 2002. **18**(9): p. 3669-3675.
114. Slivniak, R. and A.J. Domb, *Lactic acid and ricinoleic acid based copolyesters.* Macromolecules, 2005. **38**(13): p. 5545-5553.
115. Wang, C., et al., *Dual-purpose magnetic micelles for MRI and gene delivery.* Journal of Controlled Release, 2012. **163**(1): p. 82-92.
116. Vandenburg, H.J., et al., *A simple solvent selection method for accelerated solvent extraction of additives from polymers.* Analyst, 1999. **124**: p. 1707-1710.